

Microwave Measurements Laboratory  
for Accelerators

John Byrd, Stefano De Santis Derun Li,  
Bob Rimmer  
USPAS  
June 2003  
Santa Barbara

# Table of Contents

|   |           |
|---|-----------|
| <b>TABLE OF CONTENTS</b>                | <b>2</b>  |
| <b>MICROWAVES AND BEAM INTERACTIONS</b> | <b>4</b>  |
| SOME DEFINITIONS AND MAXWELL EQUATIONS  | 4         |
| THE WAVE EQUATION                       | 6         |
| TEM MODES                               | 11        |
| TM MODES                                | 13        |
| TE MODES                                | 18        |
| STANDING WAVES                          | 22        |
| <b>SIGNAL ANALYSIS</b>                  | <b>41</b> |
| TIME AND FREQUENCY DOMAIN               | 42        |
| USEFUL PROPERTIES OF FOURIER TRANSFORMS | 42        |
| SIGNAL BANDWIDTH AND TIME RESPONSE      | 43        |
| IMPULSE RESPONSE AND TRANSFER FUNCTION  | 44        |
| LAPLACE TRANSFORM                       | 46        |
| OTHER TRANSFORMS                        | 47        |
| AMPLITUDE MODULATION/DEMODULATION       | 48        |
| PHASE AND FREQUENCY MODULATION          | 49        |
| AM/PM CONVERSION                        | 51        |
| NOISE                                   | 52        |
| <b>MICROWAVE INSTRUMENTS</b>            | <b>53</b> |
| SPECTRUM ANALYZERS                      | 53        |
| NETWORK ANALYZERS                       | 61        |
| SAMPLING OSCILLOSCOPES                  | 66        |
| <b>MICROWAVE DEVICES AND COMPONENTS</b> | <b>72</b> |
| TRANSMISSION LINES                      | 72        |
| FILTERS                                 | 77        |
| POWER DIVIDERS, POWER COUPLERS          | 80        |
| DIODE DETECTORS                         | 93        |
| MIXERS                                  | 95        |
| <b>BEAM SIGNALS</b>                     | <b>98</b> |

|   |            |
|---|------------|
| <b>GENERAL APPROACH</b>   | <b>98</b>  |
| <b>SINGLE PARTICLE CURRENT</b>                                  | <b>99</b>  |
| <b>SINGLE PARTICLE DIPOLE SIGNAL</b>                            | <b>101</b> |
| <b>BEAM INDUCED SIGNALS</b>                                     | <b>107</b> |
| <b>COUPLED BUNCH OSCILLATIONS</b>                               | <b>108</b> |
| <b>SINGLE BUNCH SPECTRA</b>                                     | <b>111</b> |
| <b>SINGLE BUNCH OSCILLATIONS</b>                                | <b>112</b> |
| <b>HEAD TAIL OSCILLATIONS</b>                                   | <b>114</b> |
| <b>BEAM TRANSFER FUNCTIONS</b>                                  | <b>119</b> |
| <br>  |            |
| <b>RF CAVITIES</b>  | <b>122</b> |
| <hr/>   |            |
| <b>INTRODUCTION:</b>  | <b>122</b> |
| <b>SIMPLE EQUIVALENT CIRCUIT, TRANSMISSION-LINE ANALOGY:</b>    | <b>122</b> |
| <b>PROPERTIES OF PARALLEL RESONANT CIRCUIT AND REAL CAVITY:</b> | <b>124</b> |
| <b>REAL CAVITIES:</b>   | <b>136</b> |
| <b>FIELD MEASUREMENT</b>  | <b>137</b> |
| <br>  |            |
| <b>PICKUPS AND KICKERS</b>                                      | <b>140</b> |
| <hr/>   |            |
| <b>PICKUP RESPONSE FUNCTIONS</b>                                | <b>142</b> |
| <b>KICKER RESPONSE FUNCTIONS</b>                                | <b>142</b> |
| <b>RECIPROCITY</b>  | <b>144</b> |
| <b>RELATIONS BETWEEN PICKUP AND KICKER CHARACTERISTICS</b>      | <b>148</b> |
| <b>TYPES OF PICKUPS</b>   | <b>152</b> |

# Microwaves and beam interactions

## *Some definitions and Maxwell equations*

The sources of electromagnetic fields are charge and current, and we usually use the charge and current densities when describing their effects:

$$\rho = \frac{dq}{dV}$$

$$\mathbf{J} = \frac{d\mathbf{I}}{dS}$$

$$\mathbf{J} = \sigma\mathbf{E} \quad \text{conduction current}$$

$$\mathbf{J} = \rho\mathbf{v} \quad \text{free charge current}$$

These obey the continuity equation:

$$\nabla \cdot \mathbf{J} + \frac{\partial \rho}{\partial t} = 0$$

The Maxwell equations in differential form are

$$\nabla \cdot \mathbf{D} = \rho$$

$$\nabla \times \mathbf{E} = - \frac{\partial \mathbf{B}}{\partial t}$$

$$\nabla \cdot \mathbf{B} = 0$$

$$\nabla \times \mathbf{H} = \mathbf{J} + \frac{\partial \mathbf{D}}{\partial t}$$

Where  $\mathbf{E}$  is the electric field strength,  $\mathbf{B}$  is the magnetic flux density,  $\mathbf{D}$  is the electric displacement or electric flux density,  $\mathbf{H}$  is the magnetic field intensity

$$\mathbf{B} = \mu\mathbf{H} = \mu_r\mu_0\mathbf{H}$$

$$\mathbf{D} = \epsilon\mathbf{E} = \epsilon_r\epsilon_0\mathbf{E}$$

The Maxwell equations in integral form are

$$\int_s \mathbf{D} \cdot d\mathbf{S} = \int_v \rho \, dV \quad \text{Gauss law}$$

$$\int_s \mathbf{B} \cdot d\mathbf{S} = 0$$

$$\int \mathbf{E} \cdot d\mathbf{l} = - \frac{\partial}{\partial t} \int_s \mathbf{B} \cdot d\mathbf{S} \quad \text{Faraday law}$$

$$\int \mathbf{H} \cdot d\mathbf{l} = \int_s \mathbf{J} \cdot d\mathbf{S} + \frac{\partial}{\partial t} \int_s \mathbf{D} \cdot d\mathbf{S} \quad \text{Ampere law}$$

The energy densities in the fields are:

$$\frac{dU_E}{dV} = \frac{1}{2} \epsilon |\mathbf{E}|^2$$

$$\frac{dU_M}{dV} = \frac{1}{2} \mu |\mathbf{H}|^2$$

## *The wave equation*

take the curl of one of the Maxwell equations in a charge-free, homogenous, linear, and isotropic medium:

$$\nabla \times \nabla \times \mathbf{E} = - \frac{\partial}{\partial t} (\nabla \times \mathbf{B})$$

$$-\nabla^2 \mathbf{E} + \nabla (\nabla \cdot \mathbf{E}) = - \frac{\partial}{\partial t} \left( \mu \mathbf{J} + \mu \epsilon \frac{\partial \mathbf{E}}{\partial t} \right)$$

$$\nabla^2 \mathbf{E} - \nabla \left( \frac{\rho}{\epsilon} \right) = \mu \sigma \frac{\partial \mathbf{E}}{\partial t} + \mu \epsilon \frac{\partial^2 \mathbf{E}}{\partial t^2}$$

then for regions with no free charge or conduction current

$$\nabla^2 \mathbf{E} - \mu \epsilon \frac{\partial^2 \mathbf{E}}{\partial t^2} = 0$$

This is the homogeneous wave equation, and a similar equation can be derived for  $\mathbf{B}$ .

Solutions of the wave equation demonstrate propagation of the function with a velocity

$$v = \frac{1}{\sqrt{\mu \epsilon}}$$

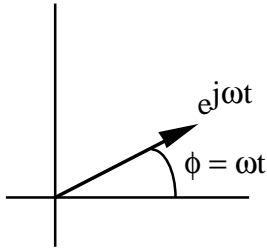
The energy flow associated with the wave is given by the Poynting vector:

$$\frac{d \mathbf{P}}{dS} = \frac{d}{dt} \frac{dU}{dS} = \mathbf{E} \times \mathbf{H}$$

## Phasor notation

We may use the convention that sinusoidally time-varying vectors may be written with the time-varying factor  $e^{j\omega t}$  suppressed:

$$\mathbf{E}(x,y,z,t) = \text{Re}[\mathbf{E}(x,y,z)e^{j\omega t}]$$



$\text{Re}(e^{j\omega t}) = \text{in-phase component}$

$\text{Im}(e^{j\omega t}) = (90^\circ) \text{ out-of-phase component}$

$$v(t) = v_0 e^{j\omega t}$$

$$\frac{dv}{dt} = j\omega v$$

e.g. for a series LRC circuit we have

$$L \frac{d I_L(t)}{dt} + R I_R(t) + \frac{1}{C} \int I_C(t) dt = V \cos(\omega t)$$

in phasor notation (and in frequency domain) this becomes:

$$j\omega L I_L(\omega) + R I_R(\omega) + \frac{I_C(\omega)}{j\omega C} = V(\omega)$$

In phasor notation then, the Maxwell equations are easily written as:

$$\nabla \cdot \mathbf{D} = \rho$$

$$\nabla \times \mathbf{E} = -j\omega\mathbf{B}$$

$$\nabla \cdot \mathbf{B} = 0$$

$$\nabla \times \mathbf{H} = \mathbf{J} + j\omega\mathbf{D}$$

and the average power is given again by the Poynting vector as:

$$\mathbf{P} = \frac{1}{2} \operatorname{Re}(\mathbf{E} \times \mathbf{H}^*)$$

The wave equation in phasor notation becomes the three-dimensional Helmholtz equation:

and

$$\nabla^2 \mathbf{E} = -\omega^2 \mu \epsilon \mathbf{E} = -k^2 \mathbf{E}$$

$$\nabla^2 \mathbf{B} = -\omega^2 \mu \epsilon \mathbf{B} = -k^2 \mathbf{B}$$

where

$$k^2 = \omega^2 \mu \epsilon$$



Now break the equation into parts using:

$$\nabla^2 \mathbf{E} = \nabla_t^2 \mathbf{E} + \frac{\partial^2 \mathbf{E}}{\partial z^2}$$

And consider a time- harmonic wave with time and distance variations described by  $e^{j(\omega t - \beta z)}$ , (propagation in the z direction with velocity  $v_z$ ) we have

$$\frac{\partial^2 \mathbf{E}}{\partial z^2} = -\beta^2 \mathbf{E}$$

and

$$\nabla_t^2 \mathbf{E} = (\beta^2 - k^2) \mathbf{E}$$

where  $\beta$  is the propagation constant

$$\beta = \frac{\omega}{v_z}$$

$k$  is the wavenumber

$$k = \frac{\omega}{v} = \omega \sqrt{\epsilon \mu}$$

We commonly classify the solutions to the wave equation in the following types:

- 1) TEM modes  
Waves that contain neither electric nor magnetic field in the direction of propagation. The name transverse electromagnetic mode arises from the fact that all of the fields lie entirely in the transverse plane. They are the usual transmission line waves along a multiconductor guide.
- 2) TM modes  
Waves that contain electric field but no magnetic field in the direction of propagation. Also known as E, or electric, waves.
- 3) TE modes  
Waves that contain magnetic field but no electric field in the direction of propagation. Also known as H, or magnetic, waves.
- 4) Hybrid modes  
Boundary conditions require all field components, may often be considered a coupling of TE and TM modes by the boundary conditions. Common in structures with "complex" 3-dimensional geometry.

## ***TEM modes***

Re-write the three-dimensional curl equations explicitly:

$$\nabla \times \mathbf{E} = -j\omega\mu\mathbf{H}$$

$$\nabla \times \mathbf{H} = j\omega\epsilon\mathbf{E}$$

$$\frac{\partial E_z}{\partial y} + j\beta E_y = -j\omega\mu H_x$$

$$\frac{\partial H_z}{\partial y} + j\beta H_y = -j\omega\epsilon E_x$$

$$-\frac{\partial E_z}{\partial x} - j\beta E_x = -j\omega\mu H_y$$

$$-\frac{\partial H_z}{\partial x} - j\beta H_x = j\omega\epsilon E_y$$

$$\frac{\partial E_y}{\partial x} - \frac{\partial E_x}{\partial y} = -j\omega\mu H_z$$

$$\frac{\partial H_y}{\partial x} - \frac{\partial H_x}{\partial y} = j\omega\epsilon E_z$$

and with  $E_z = H_z = 0$  we can find

$$\beta = \omega\sqrt{\epsilon\mu} = k$$

From the Helmholtz equation for  $E_x$

$$\left(\frac{\partial^2}{\partial x^2} + \frac{\partial^2}{\partial y^2} + \frac{\partial^2}{\partial z^2}\right) E_x = -k^2 E_x$$

substituting for  $e^{-j\beta z}$  dependence

$$\frac{\partial^2}{\partial z^2} E_x = -\beta^2 E_x = -k^2 E_x$$

then

$$\left(\frac{\partial^2}{\partial x^2} + \frac{\partial^2}{\partial y^2}\right) E_x = 0$$

similarly for  $E_y$ , and we find

A similar equation may be derived for  $\mathbf{H}$ , and we find that the electric field can be expressed as the gradient of a scalar potential, as in the electrostatic case

$\nabla_t^2 \Phi_t = 0$  derived for  $\mathbf{H}$ , and we find that expressed as the gradient of a

$$\mathbf{E}_t = -\nabla_t \Phi_t$$

The propagation constant for TEM modes  $\beta_{\text{TEM}}$  must be

$$\beta_{\text{TEM}} = \pm jk$$

and in a vacuum the wave travels at the speed of light

$$c = \frac{1}{\sqrt{\epsilon_0 \mu_0}}$$

$$H_y = \pm \sqrt{\frac{\epsilon}{\mu}} E_x$$

$$B_y = \pm \frac{E_x}{c}$$

TEM modes are the transmission mode of choice when sending information, since there is no frequency cut-off in their operation, and all frequencies travel at the same speed, the speed of light.

Examples:

- Plane light
- Radio waves
- Coaxial lines
- Striplines

## ***TM modes***

First solve for the field components, given the curl relationships shown in the section on TEM modes

$$E_x = - \frac{1}{k^2 - \beta^2} \left( j\beta \frac{\partial E_z}{\partial x} + j\omega\mu \frac{\partial H_z}{\partial y} \right)$$

$$E_y = \frac{1}{k^2 - \beta^2} \left( -j\beta \frac{\partial E_z}{\partial y} + j\omega\mu \frac{\partial H_z}{\partial x} \right)$$

$$H_x = \frac{1}{k^2 - \beta^2} \left( j\omega\epsilon \frac{\partial E_z}{\partial y} - j\beta \frac{\partial H_z}{\partial x} \right)$$

$$H_y = - \frac{1}{k^2 - \beta^2} \left( j\omega\epsilon \frac{\partial E_z}{\partial x} + j\beta \frac{\partial H_z}{\partial y} \right)$$

and with  $(k^2 - \beta^2) = k_c^2$ ,  $E_z \neq 0$ ,  $H_z = 0$  we can find

$$E_y = - \frac{j}{k^2} \beta \frac{\partial E_z}{\partial y}$$

$$E_x = - \frac{j}{k^2} \beta \frac{\partial E_z}{\partial x}$$

$$H_x = \frac{1}{k^2} j\omega\epsilon \frac{\partial E_z}{\partial y}$$

$$H_y = - \frac{1}{k^2} j\omega\epsilon \frac{\partial E_z}{\partial x}$$

From the Helmholtz equation for  $E_z$

$$\left( \frac{\partial^2}{\partial x^2} + \frac{\partial^2}{\partial y^2} + \frac{\partial^2}{\partial z^2} \right) E_z = -k^2 E_z$$

and again substituting for  $e^{-j\beta z}$  dependence

then 
$$\frac{\partial^2}{\partial z^2} E_z = -\beta^2 E_z$$

$$\left( \frac{\partial^2}{\partial x^2} + \frac{\partial^2}{\partial y^2} + k^2 - \beta^2 \right) E_z = 0$$

or

$$\nabla_t^2 E_z + (k^2 - \beta^2) E_z = 0$$

We write

$$(k^2 - \beta^2) = k_c^2$$

then

$$\nabla_t^2 E_z + k_c^2 E_z = 0$$

and the eigenvalue  $k_c$  determines the cut-off frequency ( $\omega_c = k_c/\sqrt{\mu\epsilon}$ ) below which the mode cannot propagate.

The axial propagation number  $\beta$  is generally combined into a complex number  $\gamma$  which allows attenuation constant  $\alpha$ :

$$\gamma = \alpha + j\beta$$

In this discussion, we have set  $\alpha = 0$ .

The phase velocity for each mode is

$$v_z = \frac{\omega}{\sqrt{k^2 - k_c^2}} = \frac{c}{\sqrt{1 - \left(\frac{\omega_c}{\omega}\right)^2}}$$

The equation

$$\nabla_t^2 E_z + k_c^2 E_z = 0$$

has general solutions

$$E_z = (A' \sin k_x x + B' \cos k_x x)(C' \sin k_y y + D' \cos k_y y)$$

where

$$k_x^2 + k_y^2 = k_c^2$$

This must be solved subject to the boundary conditions of the specific problem. Let's look at a rectangular waveguide as an example. A perfectly conducting boundary at  $x=0$  and  $y=0$  requires  $B' = 0$  and  $D' = 0$ . We write  $A'C' = A$ , and have:

$$E_z = A \sin k_x x \sin k_y y$$

Boundary conditions of  $E_z = 0$  at  $x = a$  and  $y = b$  result in the requirement

$$k_x a = m\pi$$

$$k_y b = n\pi$$

where  $m, n = 1, 2, 3, \dots$

From  $k_x^2 + k_y^2 = k_c^2$

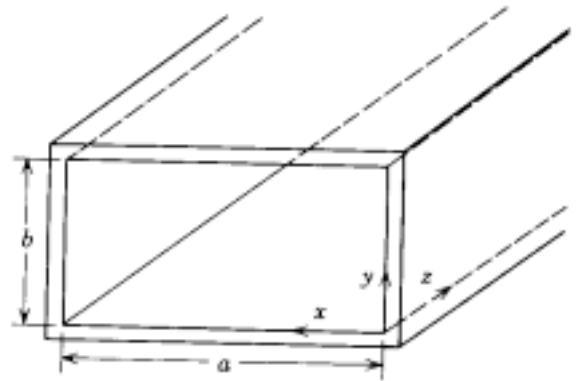
$$\omega_{c_{m,n}} = \frac{k_{c_{m,n}}}{\sqrt{\mu\epsilon}} = \frac{1}{\sqrt{\mu\epsilon}} \sqrt{\left(\frac{m\pi}{a}\right)^2 + \left(\frac{n\pi}{b}\right)^2}$$

and this gives us our attenuation constant below cut-off frequency, and propagation constant above cut-off:

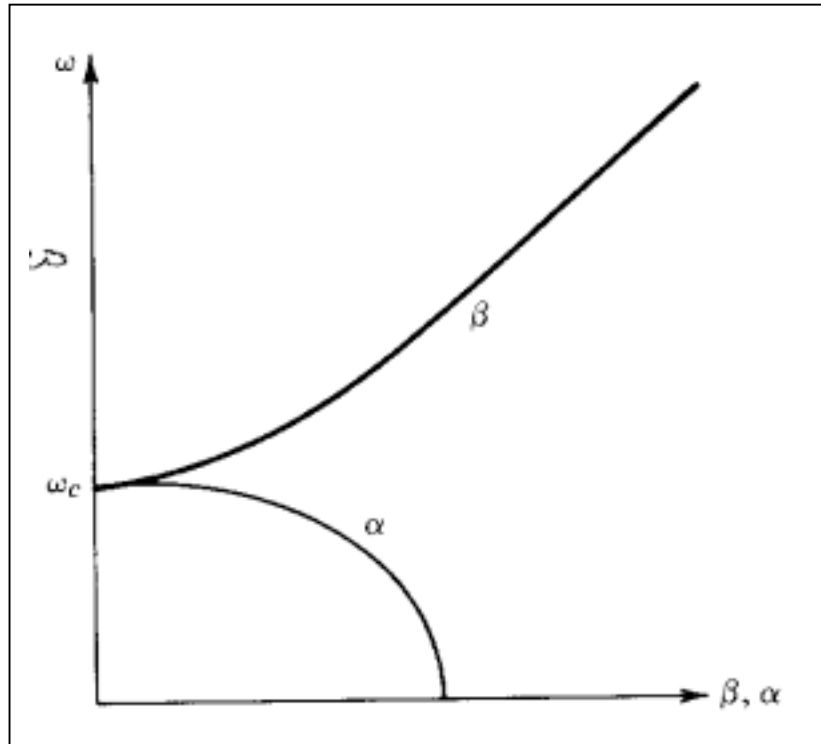
$$\alpha = k_{c_{m,n}} \sqrt{1 - \left(\frac{\omega}{\omega_{c_{m,n}}}\right)^2} \quad \omega < \omega_{c_{m,n}}$$

$$\beta = k \sqrt{1 - \left(\frac{\omega_{c_{m,n}}}{\omega}\right)^2} \quad \omega > \omega_{c_{m,n}}$$

$$v_p = \frac{\omega}{\beta} = \frac{\omega}{\sqrt{k^2 - k_c^2}} = \frac{c}{\sqrt{1 - \left(\frac{\omega_c}{\omega}\right)^2}}$$



Phase velocity



Group velocity 
$$v_g = \frac{d\omega}{d\beta} = c \sqrt{1 - \left(\frac{\omega_c}{\omega}\right)^2}$$

Energy propagates at the group velocity, and signals become distorted when  $v_g$  is not constant over the frequency band of the signal. This effect is known as dispersion.



The other field components are derived by substitution of  $E_z$  into previous equations, e.g.

$$E_y = -\frac{j}{k^2} \beta \frac{\partial E_z}{\partial y} \quad \text{gives} \quad E_x = -\frac{j\beta k_x}{k_{c_{m,n}}^2} A \cos k_x x \sin k_y y$$

similarly

$$E_y = -\frac{j\beta k_y}{k_{c_{m,n}}^2} A \sin k_x x \cos k_y y$$

$$H_x = \frac{j\omega\epsilon k_y}{k_{c_{m,n}}^2} A \sin k_x x \cos k_y y$$

$$H_y = -\frac{j\omega\epsilon k_x}{k_{c_{m,n}}^2} A \cos k_x x \sin k_y y$$

## ***TE modes***

The roles of **E** and **H** interchange in relation to the TM case, but with a different boundary condition at the conducting wall

$$\mathbf{n} \cdot \nabla_t H_z = 0$$

The transverse fields are described by:

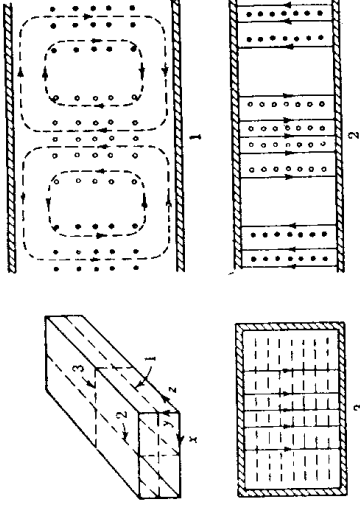
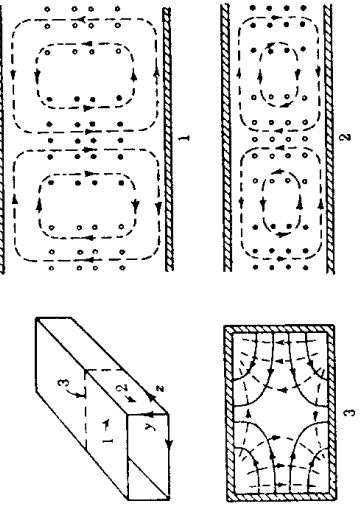
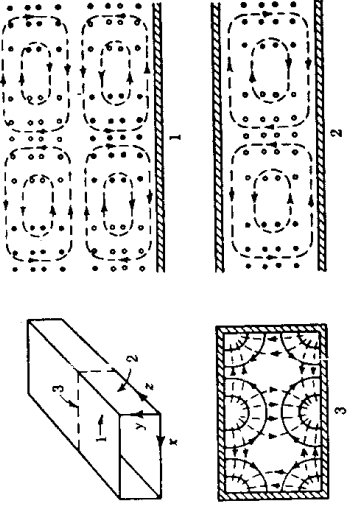
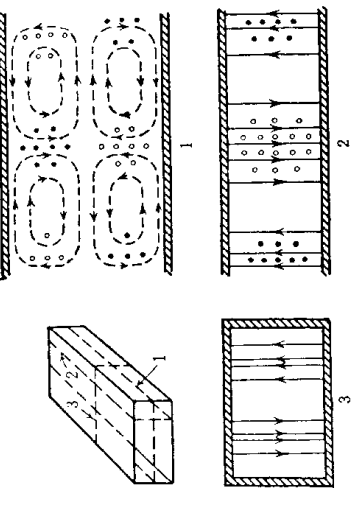
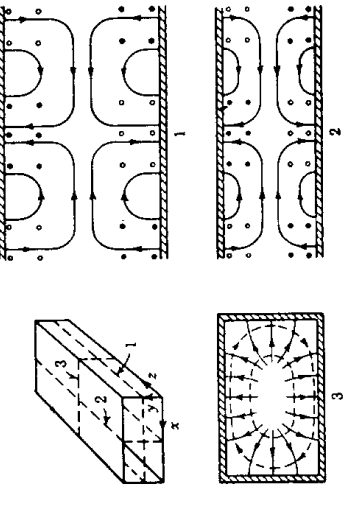
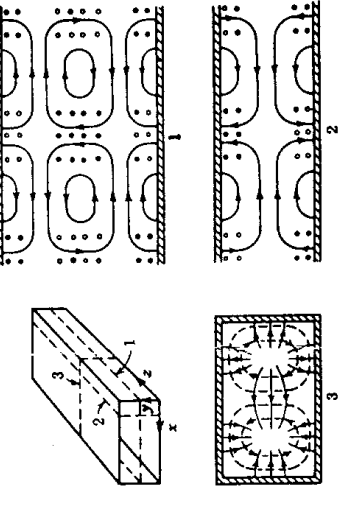
$$\begin{aligned} \mathbf{H}_t e^{\pm j\beta z} &= -j \frac{\beta}{k^2} \nabla_t H_z e^{\pm j\beta z} \\ \mathbf{E}_t e^{\pm j\beta z} &= \pm \sqrt{\frac{\epsilon_0}{\mu_0}} \frac{k}{k^2} \mathbf{z} \times \mathbf{H}_t e^{\pm j\beta z} \end{aligned}$$

Again the solution for a given case is found by applying the appropriate boundary conditions, and for the rectangular waveguide we find:

$$\begin{aligned} H_z &= H_0 \cos \frac{n\pi x}{a} \cos \frac{m\pi x}{a} e^{\pm j\beta z} \\ k_c &= \pi \left[ \left( \frac{n}{a} \right)^2 + \left( \frac{m}{b} \right)^2 \right] \end{aligned}$$

The TE mode is most commonly used for low-loss power transmission. Waveguide is quite dispersive, resulting in signal degradation over long lengths. At frequencies substantially above the cut-off of the TE mode (say a factor of two higher), other modes may propagate in the waveguide, with different group velocities and coupling to input/output systems, causing more severe signal degradation.

Summary of wave types for rectangular guides<sup>a</sup>

|  |   |  |
|--|---|--|
| <p><math>TE_{10}</math></p>   | <p><math>TE_{11}</math></p>   | <p><math>TE_{21}</math></p>   |
| <p><math>TE_{20}</math></p>  | <p><math>TM_{11}</math></p>  | <p><math>TM_{21}</math></p>  |

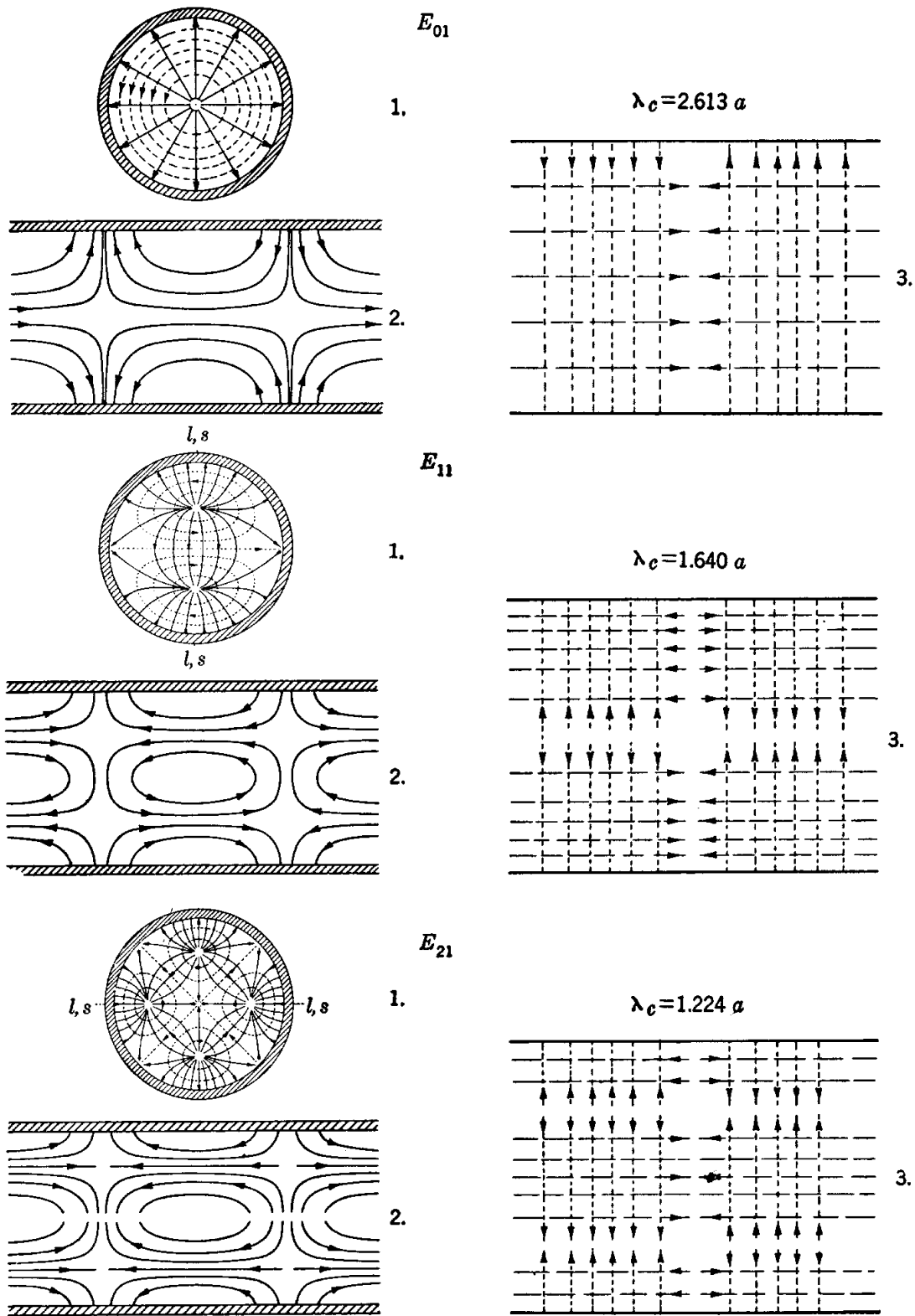


FIG. 2-5.—Field distribution for  $E$ -modes in circular waveguide.

1. Cross-sectional view
2. Longitudinal view through plane  $l-l$
3. Surface view from  $s-s$

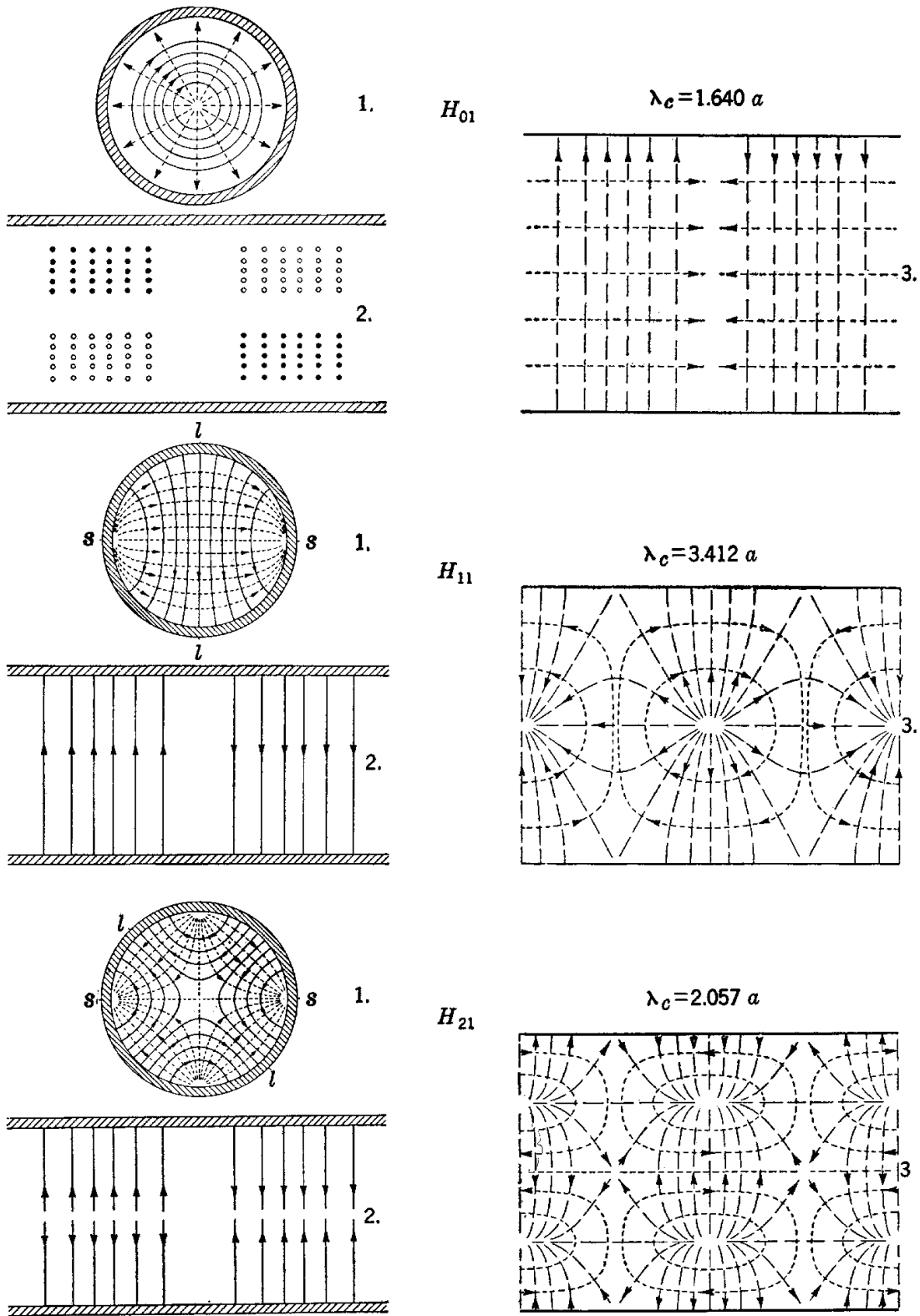
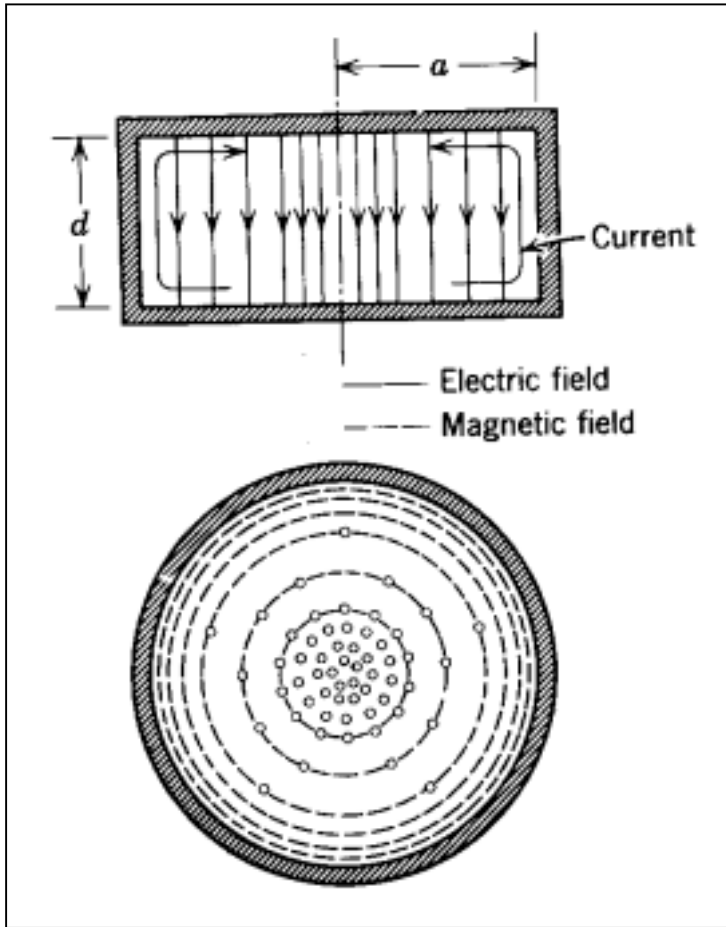


FIG. 2-6.—Field distribution for  $H$ -modes in circular waveguide.

1. Cross-sectional view
2. Longitudinal view through plane  $l-l$
3. Surface view from  $s-s$

## Standing waves

Counter-propagating waves of equal amplitude combine to give a standing pattern with  $\mathbf{E}$  and  $\mathbf{H}$  in both time-quadrature and spatial-quadrature. A useful application is in resonant fields in cavities.



Consider the cylindrical cavity shown. The mode may be considered a  $TM_{01}$  wave in circular waveguide at the cut-off frequency.

Our Helmholtz equation

$$\nabla_t^2 E_z + (k^2 - \beta^2) E_z = 0$$

in polar coordinates (appropriate for a cylindrical system) becomes:

$$\frac{1}{r} \frac{\partial}{\partial r} r \frac{\partial E_z}{\partial r} + \frac{1}{r^2} \frac{\partial^2 E_z}{\partial \phi^2} + k_c^2 E_z = 0$$

with solution:

$$E_z = E_0 J_n(k_c r) e^{j(n\phi \pm k_z z)}$$

The boundary condition  $E_z = 0$  at  $r=a$  requires

$$J_n(k_c a) = 0$$

then

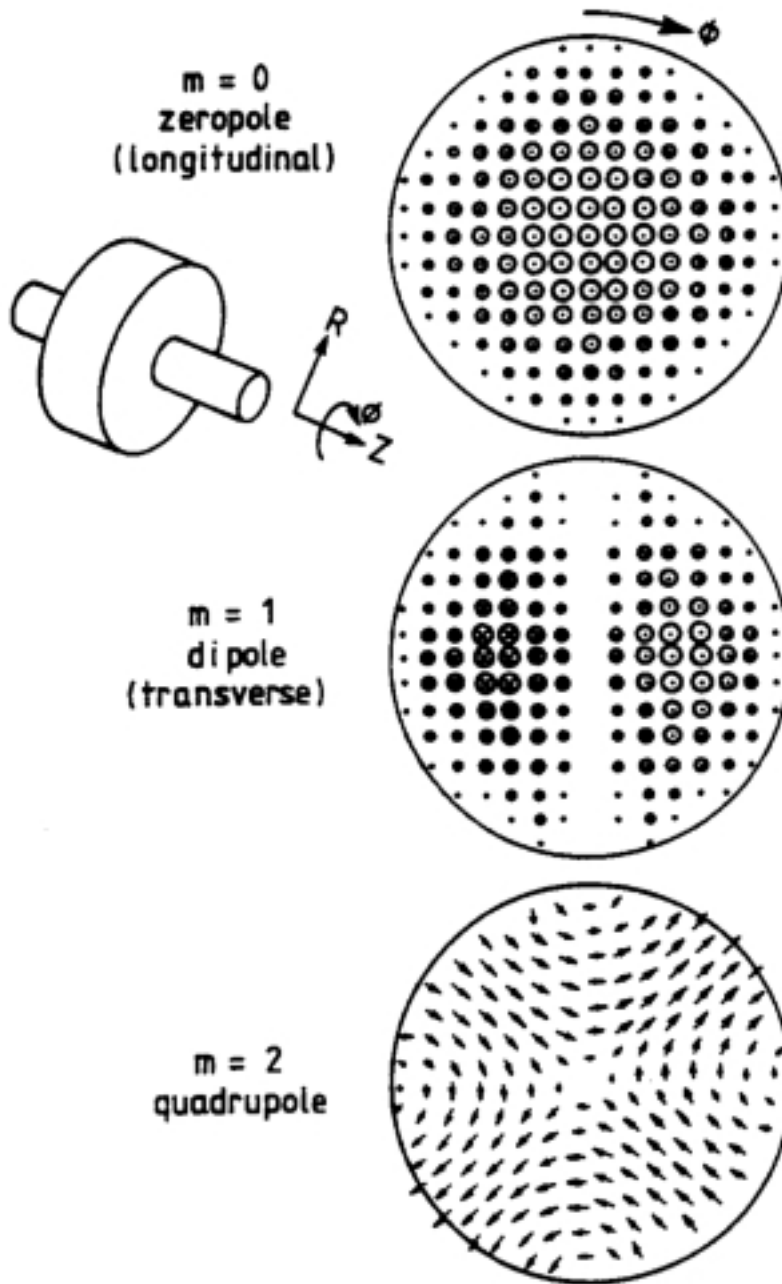
$$k_c a = \rho_{n,m} = m^{\text{th}} \text{ zero of } J_n$$

The field components are simple:

$$E_r = \pm \frac{\beta}{k} \sqrt{\frac{\epsilon_0}{\mu_0}} H_\phi = -j E_0 \frac{\beta}{k_c} J_n'(k_c r) e^{j(n\phi \pm \beta z)}$$

$$E_\phi = \pm \frac{\beta}{k} \sqrt{\frac{\epsilon_0}{\mu_0}} H_r = E_0 \frac{\beta}{k^2} \frac{n}{r} J_n(k_c r) e^{j(n\phi \pm \beta z)}$$

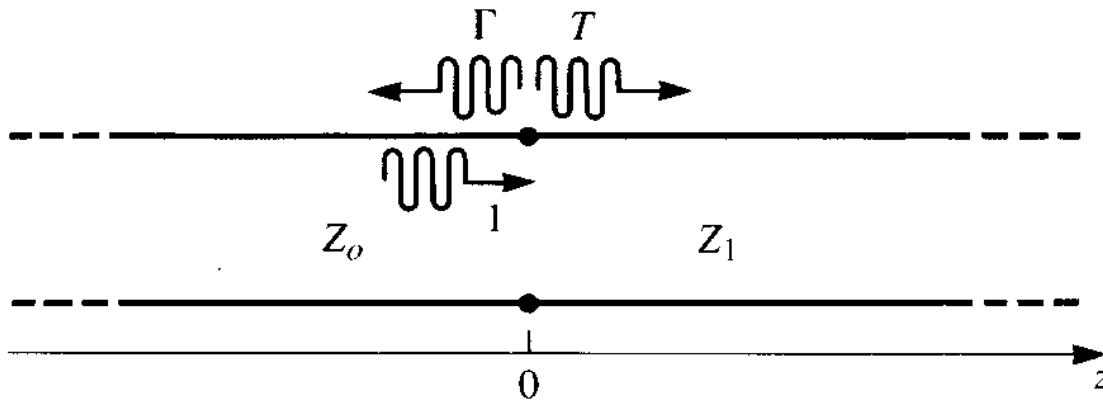
where  
 $k_c = \rho_{01} = 2.405$



Since the energy flowing into a resonator reflects from a boundary, forming a standing wave, we can picture how power builds up in the cavity from multiple reflections. Input power is dissipated in the cavity walls, and in any external "load" that is coupled to the cavity. The ratio of the stored energy to the dissipated power gives the "Q":

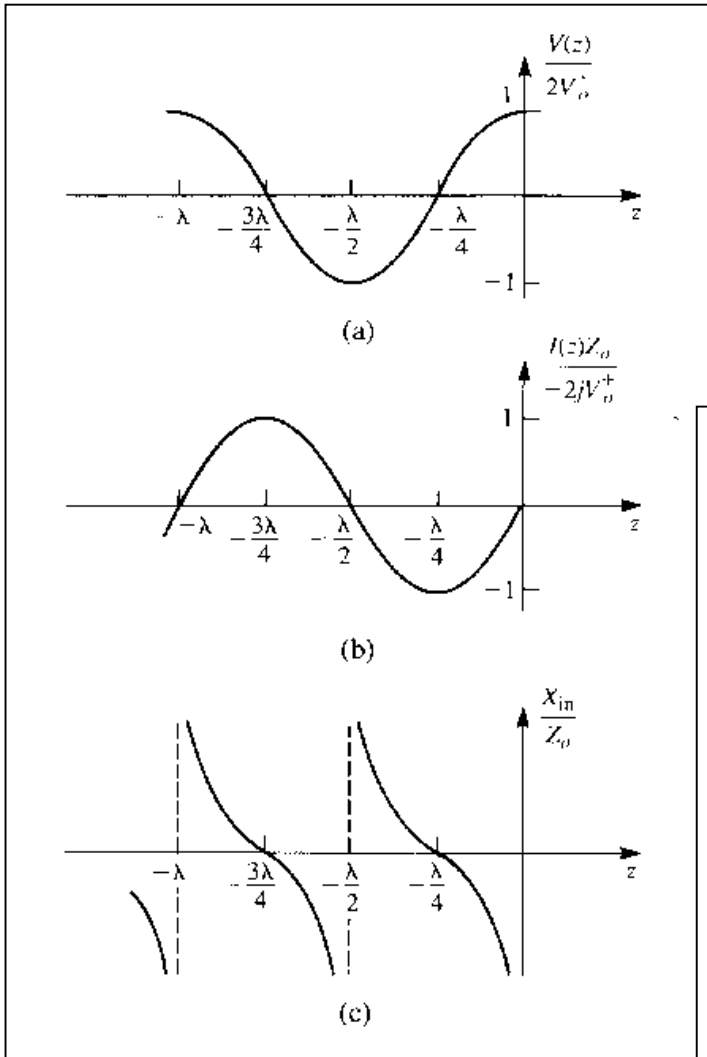
$$Q = \frac{\omega U}{P}$$

Standing waves may also form on transmission lines, as a result of waves reflecting at discontinuities in the line - i.e. a change in line impedance. Such standing waves may lead to nodes where the voltage / current is large / small.

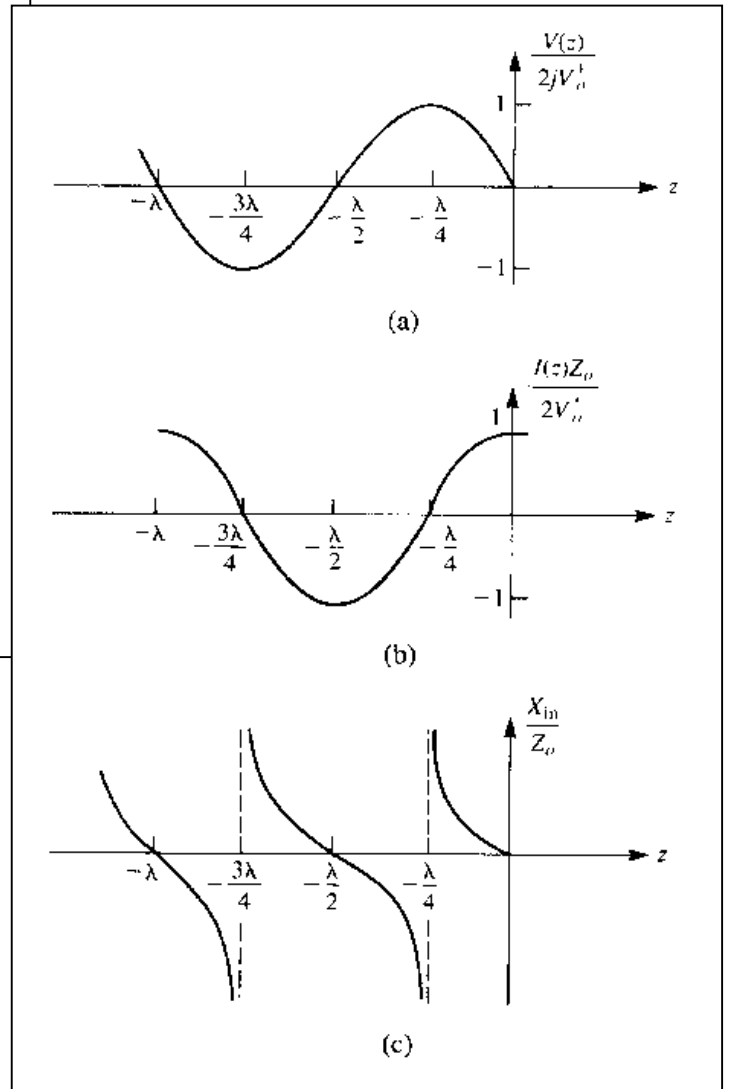




### Open circuit



### Short circuit



## Charged particle beams

### Relativistic kinematics

$$\gamma_{\text{relativistic}} = \frac{1}{\sqrt{1 - \beta^2}} \qquad \beta_{\text{relativistic}} = \frac{v}{c}$$

In the classical limit,  $\beta \ll 1$  and  $\gamma \rightarrow 1$

In the relativistic limit,  $\beta \rightarrow 1$  and  $\gamma$  is proportional to energy

| Quantity   | Non-relativistic    | Relativistic                      |
|------------|---------------------|-----------------------------------|
| Energy E   | $1/2 mv^2 + m_0c^2$ | $\gamma m_0c^2$                   |
| Momentum p | $mv$                | $\gamma m_0v = \gamma m_0\beta c$ |
| Force F    | $m dv/dt = ma$      | $m/\beta d\gamma/dt$              |

It proves convenient to use units of

|          |                     |
|----------|---------------------|
| energy   | MeV                 |
| momentum | MeV/ c              |
| mass     | MeV/ c <sup>2</sup> |

then the kinematic equations may be written without factors of "c":

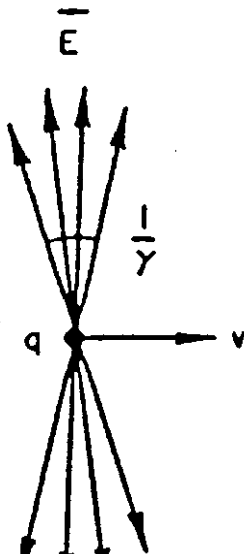
$$E = \sqrt{p^2 + m^2} = \gamma m_0$$

$$E = \text{K.E.} + m$$

$$\text{K.E.} = E - m_0 = m_0(\gamma - 1)$$

$$p = \gamma m_0 v$$

$$v = \frac{p}{E} = \frac{p}{\sqrt{p^2 + m^2}}$$



The fields of ultra-relativistic particles resemble plane waves -  $\mathbf{E}$  and  $\mathbf{B}$  are transverse to each other and lie in a disk transverse to the particle velocity.

The opening angle of the radial E-field is of the order  $1/\gamma$ .

We have only radial E field and azimuthal H field, confined to a disk perpendicular to the direction of motion of the charge, producing a  $\delta$ -function distribution in the direction of motion.

The situation remains the same for charges moving along the axis of an infinitely conducting smooth cylindrical pipe. The electric field lines are then terminated with surface charges on the inside wall.

For non-relativistic particles the situation is more complex. For low- $\gamma$  beams the space-charge force which cancels out with the magnetic forces of ultra-relativistic charges cannot be neglected, and the fields associated with a charge are not so well confined to a disk around the charge.

Here, we will deal mainly with the simpler case of ultra-relativistic charges, and ignore these latter complications.

- § Charged particle beams may be sensed via the electromagnetic fields they create.
- § They may respond to external electric and magnetic fields.
- § They can also interact with the fields they create.

## Time domain and frequency domain

We have a tendency to experience events as they happen in time, but we are also sensitive to identifying in frequency, for example the color of objects.

In electrodynamics we measure and understand signals and behavior in two dominant modes, time-domain and frequency-domain.

Time domain signals may be, for example, the measured current induced by a passing electric charge. We may see an impulse as the charge passes, then another as the next charge passes, and so on. Understanding signals in this way is very important.

Sometimes the time-domain information does not clearly explain all behavior, and we find that looking at the frequency spectrum of a signal can give a more complete understanding and insight into a problem.

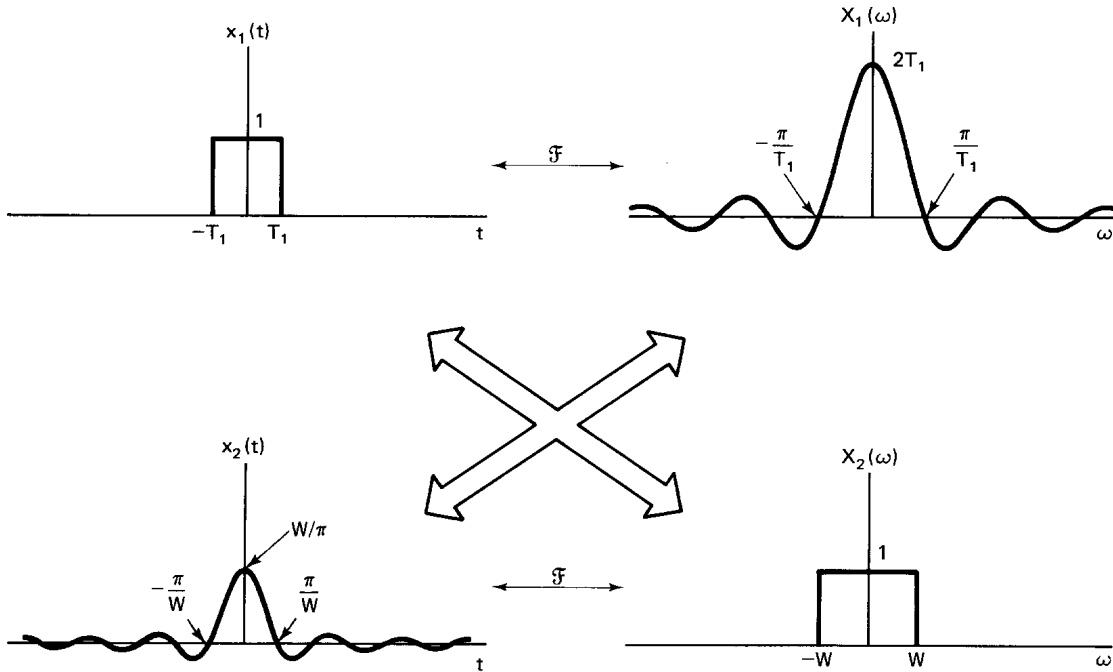
Some problems are best analyzed in time-domain, others in frequency-domain.

| <b>Frequency Domain appropriate when:</b>   | <b>Time Domain appropriate when:</b>  |
|---|---|
| Periodic processes  | Single shot   |
| High Q, low bandwidth   | Low Q, high bandwidth   |
| Frequency-dependent parameters <ul style="list-style-type: none"><li>• Complex impedances</li><li>• Filter response</li></ul> | Amplitude-dependent parameters, e.g. limits of linear range of components <ul style="list-style-type: none"><li>• Saturation (<math>P_{1dB}</math>)</li><li>• Slew rates</li><li>• Damage thresholds (<math>V_{max}</math>)</li></ul> |
| Linear phenomena  | Non-linear phenomena <ul style="list-style-type: none"><li>• mixers</li><li>• diodes</li></ul>  |
| Discrete frequency phenomena <ul style="list-style-type: none"><li>• oscillators</li></ul>                                    | Discrete-time operations <ul style="list-style-type: none"><li>• Sample &amp; Hold</li><li>• Digitization</li></ul>   |

To convert signals from one domain to the other, we use the Fourier transform:

$$x(t) = \frac{1}{2\pi} \int_{-\infty}^{\infty} X(\omega) e^{j\omega t} d\omega$$

$$X(\omega) = \int_{-\infty}^{\infty} x(t) e^{-j\omega t} dt$$



## Beam signals

For real beams we may have  $10^9$  or more particles in a bunch, and the bunch has some longitudinal profile, often Gaussian. For such a Gaussian distribution, the wall currents induced by the passage of an ultra-relativistic beam may be written:

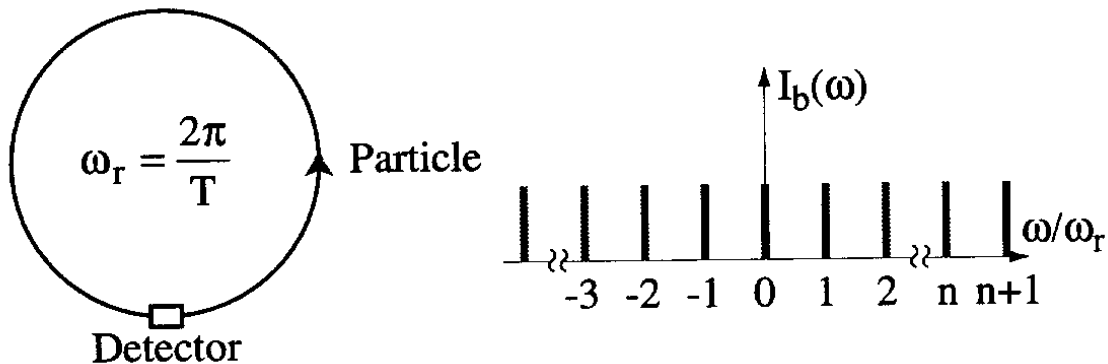
$$i(t) = \frac{q}{\sqrt{2\pi} \sigma} e^{-\left(\frac{t}{\sqrt{2} \sigma}\right)^2} * \sum_{n=-\infty}^{\infty} \delta(t - n\tau)$$

where  $\sigma$  is the bunch length,  $q$  the charge, and bunches are spaced by time interval  $\tau$ .

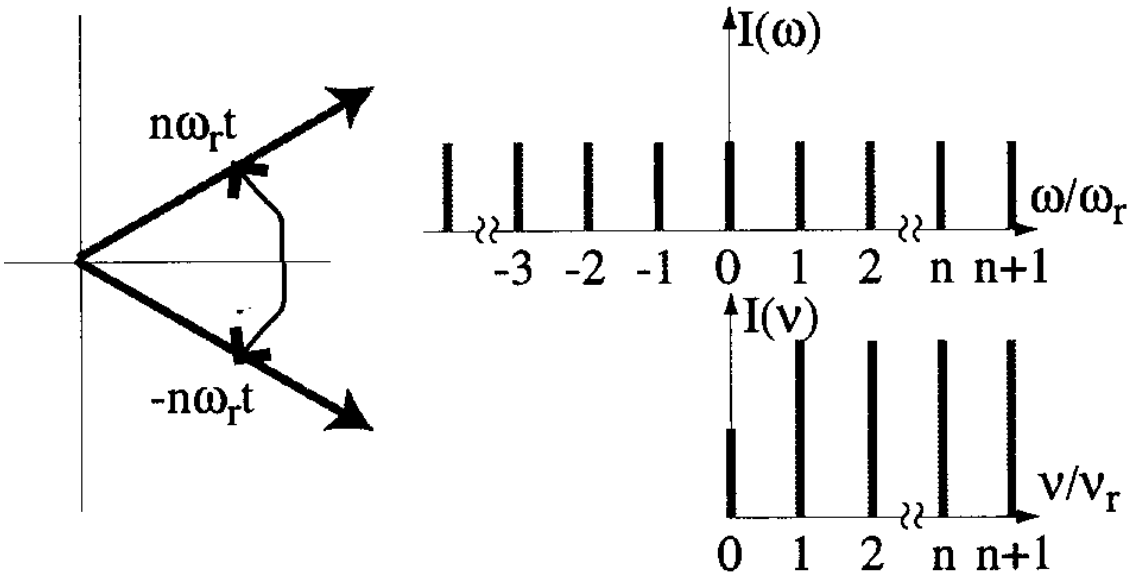
In frequency domain, the spectrum is

$$I(f) = I_0 e^{-(\sqrt{2} \pi \sigma f)^2} \sum_{n=-\infty}^{\infty} \delta(f - n f_0)$$

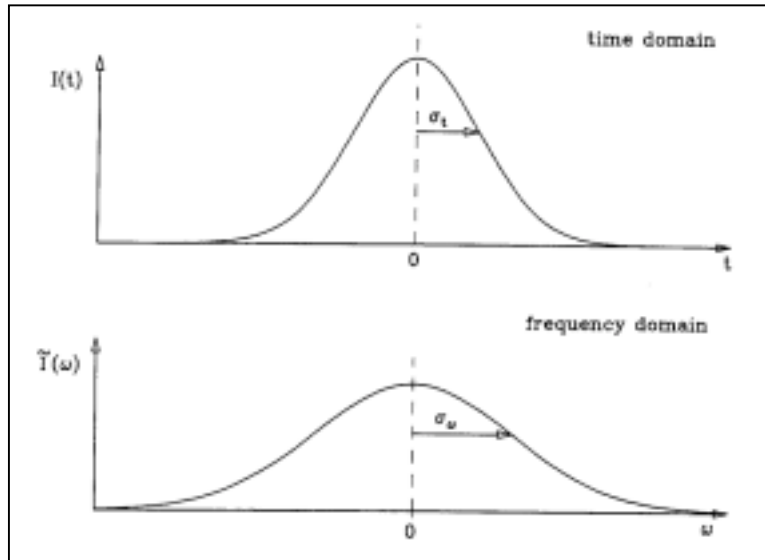
In this expression there are positive and negative frequency components:



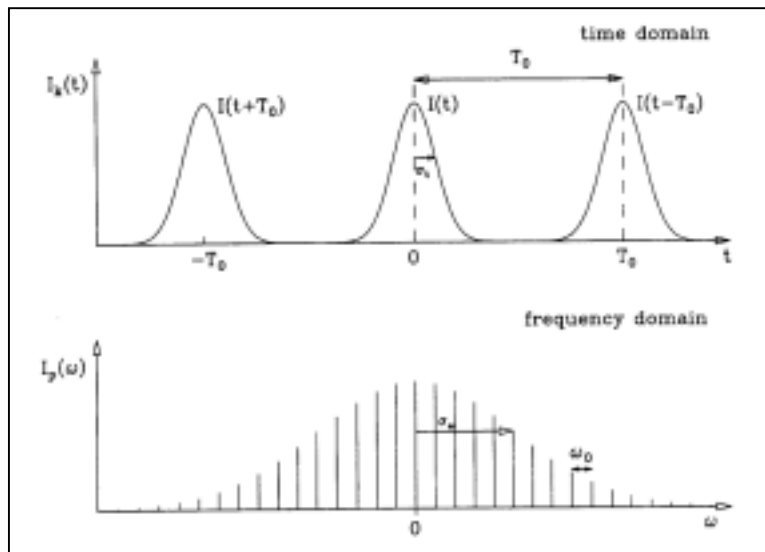
A spectrum analyzer shows positive components, with the negative part "folded" over at d.c. :



## Single-passage



## Repetitive-passages





For a 500 MHz RF system, typical values might be

$$\sigma \approx 10 \text{ ps}$$

$$\tau \approx 2 \text{ ns}$$

then we can see that the beam current spectrum e-folding frequency is  $1/\sqrt{2}\pi\sigma$  or about 20 GHz.

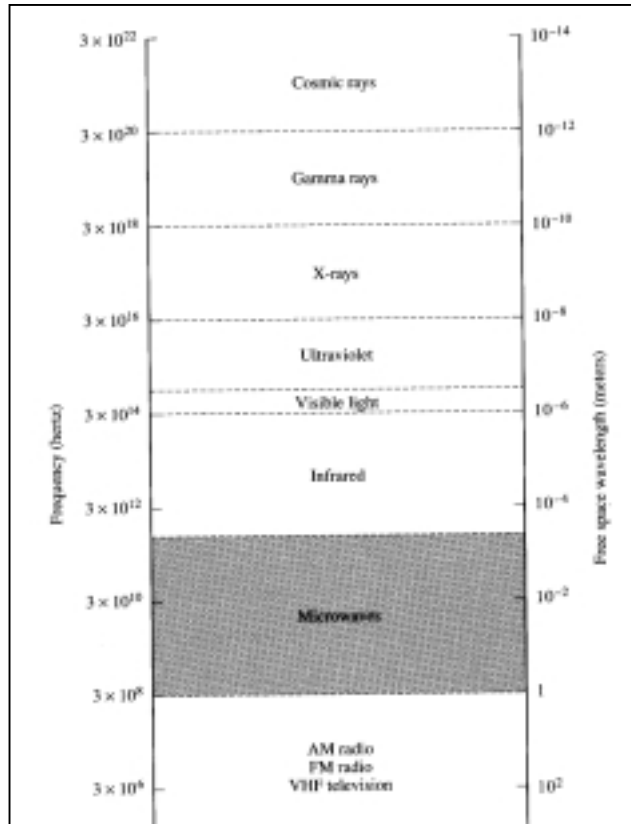
If we wish to perturb a single bunch, we must have a system that will generate fields before the arrival of the bunch and dissipate them afterwards, such that no other bunches experience the fields. This gives a bandwidth requirement of the order of 500 MHz in this case.

Much information on beam parameters may be gained by measuring electromagnetic signals in the RF to microwave ranges for typical beams.

Higher frequencies and larger bandwidths are required to "see" more detail and shorter timescales.

Similarly, to operate on typical beams requires devices and power sources with RF to  $\mu$ wave frequency response.

In the future, for very compact beams with femtosecond timescales, lasers may replace microwave systems for diagnostics and manipulation of beams.



| Component             | Frequency range |
|-----------------------|-----------------|
| AM radio              | 535–1605 kHz    |
| Shortwave radio       | 3–30 MHz        |
| FM radio              | 88–108 MHz      |
| Commercial television |                 |
| Channels 2–4          | 54–72 MHz       |
| Channels 5–6          | 76–88 MHz       |
| Channels 7–13         | 174–216 MHz     |
| Channels 14–83        | 470–890 MHz     |
| Microwave ovens       | 2.45 GHz        |

| Commonly used letter designation | Frequency range | Wavelength range |
|----------------------------------|-----------------|------------------|
| L-band                           | 1–2 GHz         | 30–15 cm         |
| S-band                           | 2–4 GHz         | 15–7.5 cm        |
| C-band                           | 4–8 GHz         | 7.5–3.75 cm      |
| X-band                           | 8–12 GHz        | 3.75–2.5 cm      |
| K <sub>u</sub> -band             | 12–18 GHz       | 2.5–1.67 cm      |
| K-band                           | 18–27 GHz       | 1.67–1.11 cm     |
| K <sub>a</sub> -band             | 27–40 GHz       | 1.11–0.75 cm     |
| U-band                           | 40–60 GHz       | 7.5–5 mm         |
| V-band                           | 60–80 GHz       | 5–3.75 mm        |
| W-band                           | 80–100 GHz      | 3.75–3 mm        |

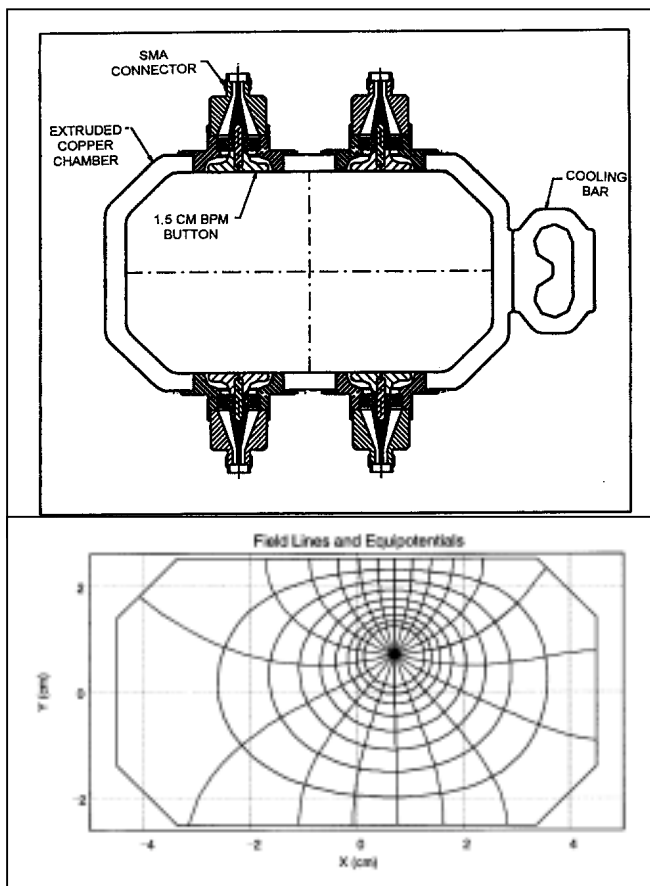
## Image current

The beam induces in the enclosing vacuum chamber walls an equal and opposite *image current* in order to match the boundary conditions at the walls. The beam may be considered a perfect current source for most calculations.

$$i_{\text{wall}}(t) = - i_{\text{beam}}(t)$$

$$I_{\text{wall}}(\omega) = - I_{\text{beam}}(\omega)$$

This wall current may be sensed by electrodes mounted inside the vacuum chamber, and signals derived from the beam-induced wall current provide valuable information on beam properties, for example beam position:



## Interaction of beams with electromagnetic fields

The force on a particle of charge  $q$  in an electromagnetic field is

$$\mathbf{f} = q[\mathbf{E} + \mathbf{v} \times \mathbf{B}]$$

A charged particle passing from point  $a$  to point  $b$  with velocity  $\mathbf{v} = \beta \mathbf{c}$  will receive a momentum change (kick):

$$\Delta \mathbf{p} = q \int_{a, t_a}^{b, t_b} [\mathbf{E} + \mathbf{v} \times \mathbf{B}] dt$$

The longitudinal  
energy change

electric field gives an

$$\Delta U = q \int_{a, t_a}^{b, t_b} \mathbf{E} \cdot d\mathbf{s}$$

For ultra-relativistic particles  $\beta \approx 1$  and

then

$$ds = dz = \beta c dt$$

$$\Delta U = \Delta \mathbf{p} \cdot \beta \mathbf{c}$$

## The beam voltage

The energy change is often expressed as the beam voltage:

$$V_b = \frac{\Delta U}{q} = \int_{a, t_a}^{b, t_b} \mathbf{E}(s, t) \cdot d\mathbf{s}$$

In phasor notation,  $E_s(s, t) = E_s(s) e^{j\omega t}$ , and with  $t = s/v$  we have:

$$V_b = \int_a^b E_s e^{jk_b s} ds$$

where  $k_b$  is the *beam* wavenumber. The factor  $e^{jk_b s}$  leads us to the transit-time factor T:

$$V_b = T \int_a^b E_s ds$$

or

$$T = \int_a^b e^{jk_b s} ds$$

For resonant cavities, we often find symmetry in the longitudinal direction, and a cosine or sine term will apply here for the transit time, depending on the symmetry of the mode about its center point.

The variation of the beam voltage with transverse position is not an arbitrary function, and one can show that  $V_b$  is a two-dimensional scalar solution of the Laplace equation for highly relativistic particles:

$$\nabla_t^2 V_b + \frac{1}{(\beta\gamma c)^2} \frac{\partial^2 V_b}{\partial t^2} = 0$$

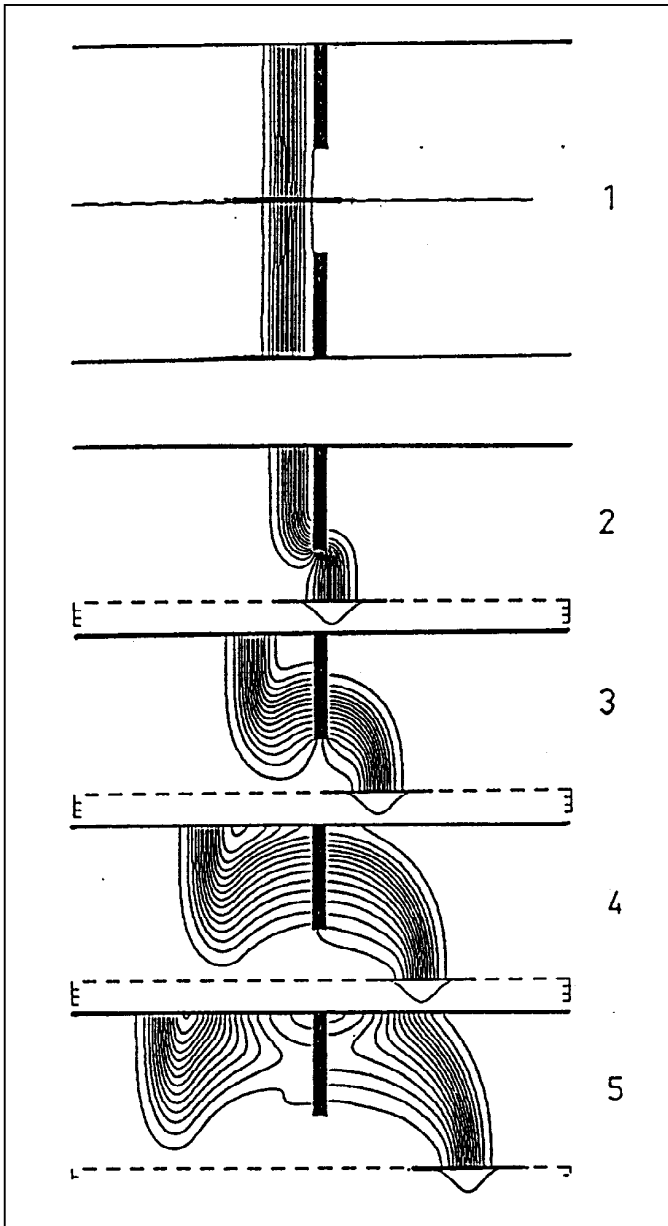
or in phasor notation:

$$\nabla_t^2 V_b + \frac{k_b^2}{\gamma^2} V_b = 0$$

- § Solving for  $V_b$  reduces to a simple electrostatics problem
- § The problem of calculating the spatial variation of a device's effect across its aperture can be reduced to a two-dimensional boundary-value problem

## Beam impedance

The various accelerator components, such as RF cavities, bellows, injection septa, dielectric walls, and even a smooth pipe of finite conductivity result in scattering or trapping of the beam-induced fields. These fields can last for long enough to be experienced by a charge following the exciting charge, causing perturbations to the energy or angle of the following particle's orbit.



In the time-domain the beam-induced electromagnetic field in an accelerator component may be described by *wake function*; in the frequency-domain by the *beam impedance* (sometimes known as the *coupling impedance*).

The beam impedance is a complex quantity: the real part is associated with extraction of energy from the beam; the imaginary part with deformation of the beam profile.

The wake function and impedance are equivalent, in the sense that the impedance is the Fourier transform of the wake function.

### Computer modeling

We have seen here analytical expressions for

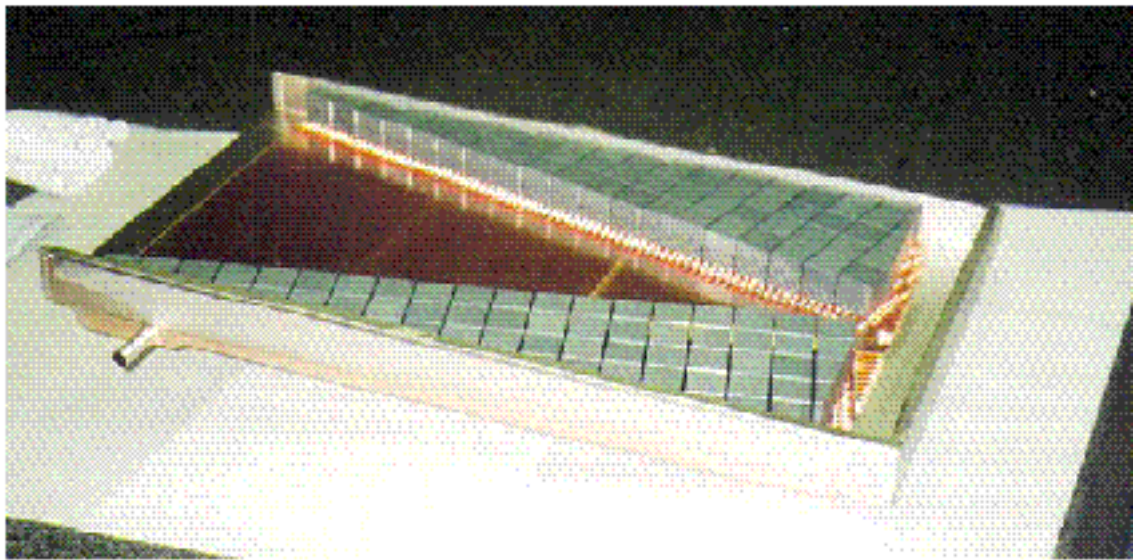
electrodynamic parameters for charged particle beams in electromagnetic fields. Many components in particle accelerators are too complex and/or

devoid of symmetry to allow simple calculation, and we resort to computer modeling.

Many techniques exist for calculation of electrodynamic quantities, e.g.

- Finite element
- Finite difference
- Boundary element
- Mode matching
- etc...

One example is the MAFIA code which uses a finite difference technique to rigorously solve the Maxwell equations on a rectangular grid. Models may be created in full 3-D, and solved in time-domain and/or frequency-domain.



Waveguide load



# Signal Analysis

- Time and Frequency description of signals.
  - Fourier transform
  - Laplace transform
  - Discrete Fourier and Z transforms and aliasing
  - impulse response and transfer function
- Modulation/Demodulation.
  - AM
  - FM and PM
  - Transmission through linear system (AM/PM conversion)
- Noise Considerations
  - noise sources
  - thermal noise
  - signal/noise ratio

## ***Time and Frequency Domain***

Any time domain signal can be expressed as a sum of sinewaves. This is known as a Fourier transform.

$$f(t) = \frac{1}{2\pi} \int_{-\infty}^{+\infty} F(\omega) e^{j\omega t} d\omega$$

The Fourier transform is defined here as (caution: some texts use different definitions.)

$$F(\omega) = \int_{-\infty}^{+\infty} f(t) e^{-j\omega t} dt$$

For periodic signals

$$V(t) = \frac{a_0}{2} + \sum_{n=1}^{\infty} a_n \cos(n\omega_0 t) + b_n \sin(n\omega_0 t)$$

where the coefficients  $a_n$  are given by

$$a_n = \frac{2}{T_0} \int_{T_0} V(t) \cos(n\omega_0 t) dt$$

$$b_n = \frac{2}{T_0} \int_{T_0} V(t) \sin(n\omega_0 t) dt$$

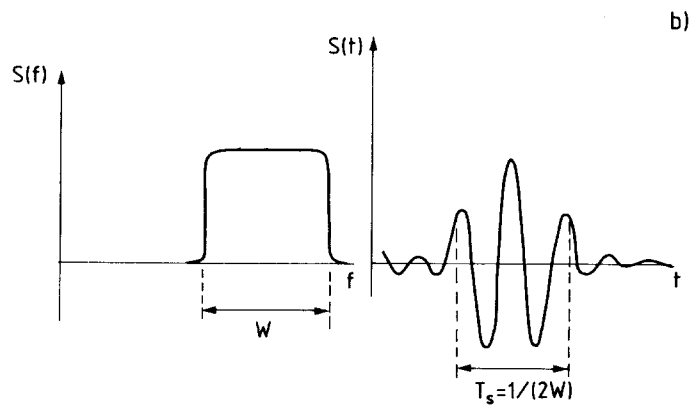
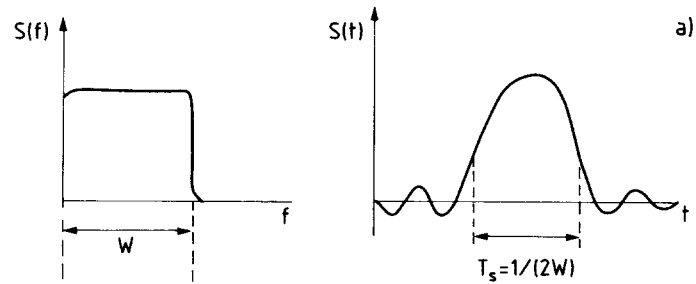
This known as a Fourier series

## ***Useful Properties of Fourier Transforms***

|   |                          |
|---|--------------------------|
| $ax_1(t) + bx_2(t) \Leftrightarrow aX_1(\omega) + bX_2(\omega)$   | Linearity                |
| $x(t-t_0) \Leftrightarrow e^{-j\omega t_0} X(\omega)$   | Time shifting            |
| $\frac{dx(t)}{dt} \Leftrightarrow j\omega X(\omega)$  | Differentiation          |
| $\int_{-\infty}^{\tau} x(t) dt \Leftrightarrow \frac{1}{j\omega} X(\omega) + \pi X(0) \delta(\omega)$                 | Integration              |
| $x(at) \Leftrightarrow \frac{1}{ a } X\left(\frac{\omega}{a}\right)$  | Time scaling             |
| $\int_{-\infty}^{+\infty}  f(t) ^2 dt = \frac{1}{2\pi} \int_{-\infty}^{+\infty}  F(\omega) ^2 d\omega$                | Parseval's Thm           |
| $\text{Im}(X(\omega)) = \frac{1}{\pi} \int_{\infty}^{\omega} d\omega' \frac{\text{Re}(X(\omega'))}{\omega' - \omega}$ | for $x(t)=0$ for $t < 0$ |

## Signal Bandwidth and Time Response

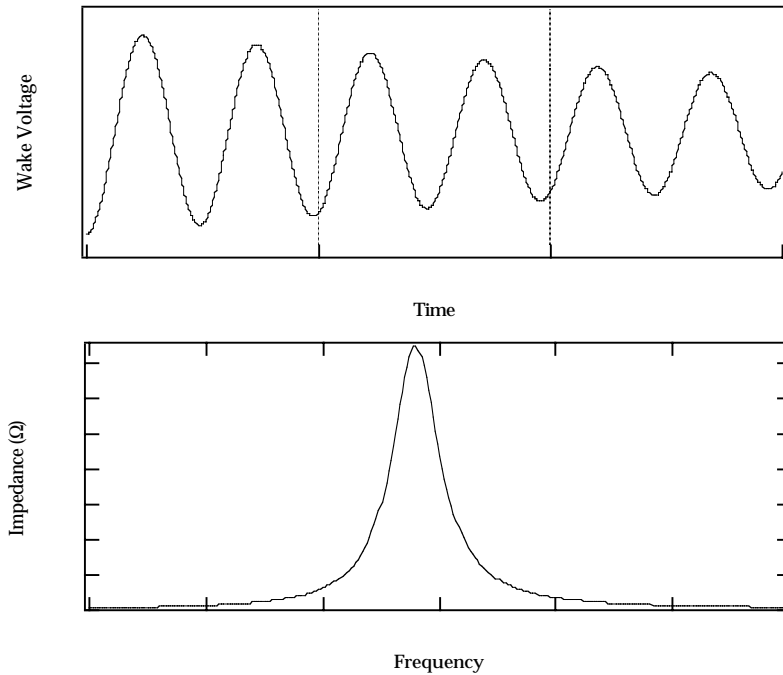
For signals with time length  $T$ , the frequency bandwidth is  $BW \sim 1/2T$ . This is independent of the frequency of the signal.



## *Impulse Response and Transfer Function*

Consider a system with a response to an impulse given by  $h(t)$ .  
The FT of the impulse response is defined as the transfer function  $H(\omega)$ .

A common application of this in accelerators is wakefields and impedance. Consider a point charge passing through an RF cavity. It excites a wakefield (e.g. on axis) that decays with some time constant.



Often it is more practical or relevant to measure the step response of a system. The step response of a system is just the integral of the impulse response. Therefore a one can get the impulse response from the derivative of the step response measurement.

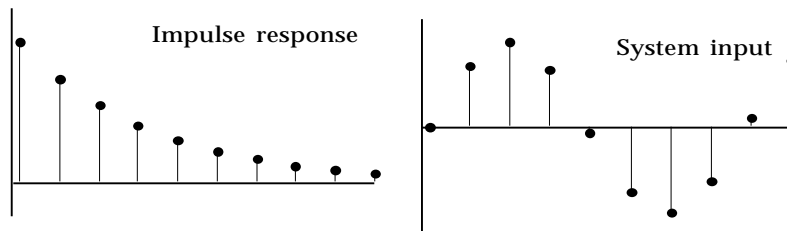
# Convolutions

The response of a system to an arbitrary input is given by the convolution of the input with the response of the system.

$$y(t) = \int_{-\infty}^{+\infty} x(\tau)h(t-\tau)d\tau$$

where  $x(t)$  is the input to the system,  $h(t)$  is the impulse response, and  $y(t)$  is the output.

Convolutions can be thought of as summing up the impulse response from a series of delta functions of varying amplitude.



Convolutions are most easily evaluated in the frequency domain. The FT of a convolution is just the product of the FT of  $x(t)$  and  $h(t)$

$$Y(\omega) = X(\omega)H(\omega)$$

Once the FT transform of the output is found, the result can be FT'ed back to the time domain.

A common occurrence of convolutions in accelerators is the response of an RF cavity to an arbitrary drive (such as beam current). In this case, the voltage is given by

$$V(t) = \int_{-\infty}^{+\infty} i(\tau)W_{||}(t-\tau)d\tau$$

where  $W_{||}(t)$  is the wake voltage (i.e. impulse response) of the RF cavity and  $i(t)$  is the driving beam current. The voltage in the frequency domain is

$$V(\omega) = I(\omega)Z_{||}(\omega)$$

where  $Z_{||}(\omega)$  is the impedance.

## Laplace Transform

We can generalize the FT to a class of signals with complex frequency  $s=\sigma+j\omega$ . This form of transform is called the Laplace Transform and is defined by

$$F(s)=\int_{-\infty}^{+\infty} f(t)e^{-st}dt$$

The inverse LT is given by

$$f(t)=\frac{1}{2\pi j}\int_{-\infty}^{+\infty} F(s)e^{st}ds$$

The LT is useful for analyzing linear systems (particularly linear systems with feedback) because it reduces differential equations to algebraic equations.

Example: Consider a simple L-R circuit. The differential equation for the current is given by

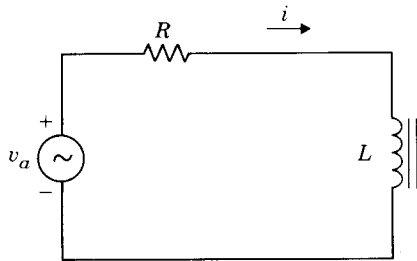
$$L\frac{di}{dt}+Ri=V(t)$$

where  $V(t)$  is an arbitrary input voltage to the circuit. Taking the LT of both sides yields

$$sI(s)+(1/\tau)I(s)=V(s)/L$$

Solving for  $I(s)$

$$I(s)=\frac{V(s)}{s+1/\tau}$$



If we know the LT for  $V(t)$  we can find  $i(t)$ .

## *Other Transforms*

Discrete time signals have transforms which are very similar to those of continuous signals called discrete Fourier transforms (DFTs). These signals are most commonly encountered in systems with digital sampling.

$$x[n] = \sum_{k=1}^N a_k e^{jk(2\pi/N)n}$$

where

$$a_k = \frac{1}{N} \sum_{n=1}^{\infty} x[n] e^{-jk((2\pi/N)n)}$$

The most common form of the DFT is the fast Fourier transform (FFT) which is a common algorithm for finding the DFT of  $2^n$  points. The DFT is also useful in describing bunched beam signals since they often are periodic pulses.

For discrete time data, the equivalent to the Laplace transform is the Z-transform given by

$$X(z) = \sum_{n=-\infty}^{\infty} x[n] z^{-n}$$

The inverse ZT is

$$x[n] = \frac{1}{2\pi j} \oint X(z) z^{n-1} dz$$

Hilbert Transforms

$$H(t) = \frac{1}{\pi} \int_{-\infty}^{\infty} \frac{f(\tau)}{t-\tau} d\tau$$

Used for analyzing transmission through linear systems. Generates only positive frequency signals.

## Amplitude Modulation/Demodulation

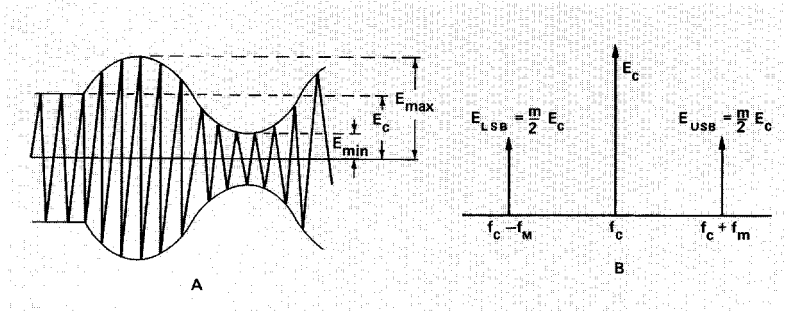
Simple amplitude modulation can be written mathematically as

$$\begin{aligned} V_s(t) &= V_m \cos(\omega_m t + \phi_m) V_c \cos(\omega_c t + \phi_c) \\ &= \frac{V_m V_c}{2} (\cos((\omega_m - \omega_c)t + (\phi_m - \phi_c)) + \cos((\omega_m + \omega_c)t + (\phi_m + \phi_c))) \end{aligned}$$

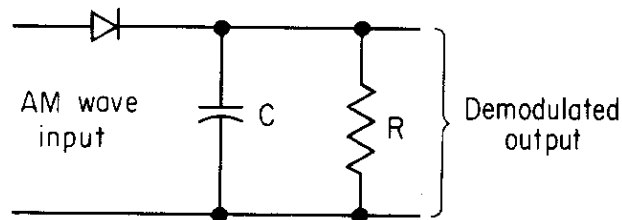
AM modulation including the carrier is usually written as

$$V_s(t) = V_c \cos(\omega_c t + \phi_c) (1 + m \cos(\omega_m t + \phi_m))$$

The ratio of the sideband to the carrier is  $ism/2$ .



Consider the above case where a signal has been modulated onto a carrier. How do we demodulate the the result in order to recover the original modulation signal? One technique is to multiply the signal by the carrier resulting in two sets of frequencies,  $\omega_m$  and  $2*\omega_c \pm \omega_m$ . If the signal is low-pass filtered, we can recover the original modulation. This is sometimes referred to as demodulating or mixing a signal down to baseband. Another common technique illustrated below is a diode or envelope detector.





## ***Phase and Frequency Modulation***

The phase of a signal can also be modulated

$$V_s(t) = V_c \cos(\phi(t))$$

where

$$\phi(t) = \omega_c t + \hat{\phi} \sin(\omega_m t)$$

Frequency modulation is just a special case of phase modulation. The instantaneous angular frequency is given by

$$\omega(t) = \frac{d\phi}{dt} = \omega_c + \hat{\phi} \omega_m \cos(\omega_m t) = \omega_c + 2\pi \Delta f \cos(\omega_m t)$$

where  $\Delta f$  is the peak frequency deviation from the carrier. The peak phase deviation and frequency deviation are related by

$$\hat{\phi} = \frac{\Delta f}{f_m}$$

Using the Fourier expansions

$$\cos(x \sin \theta) = J_0(x) + 2J_2(x) \cos 2\theta + 2J_4(x) \cos 4\theta + \dots$$

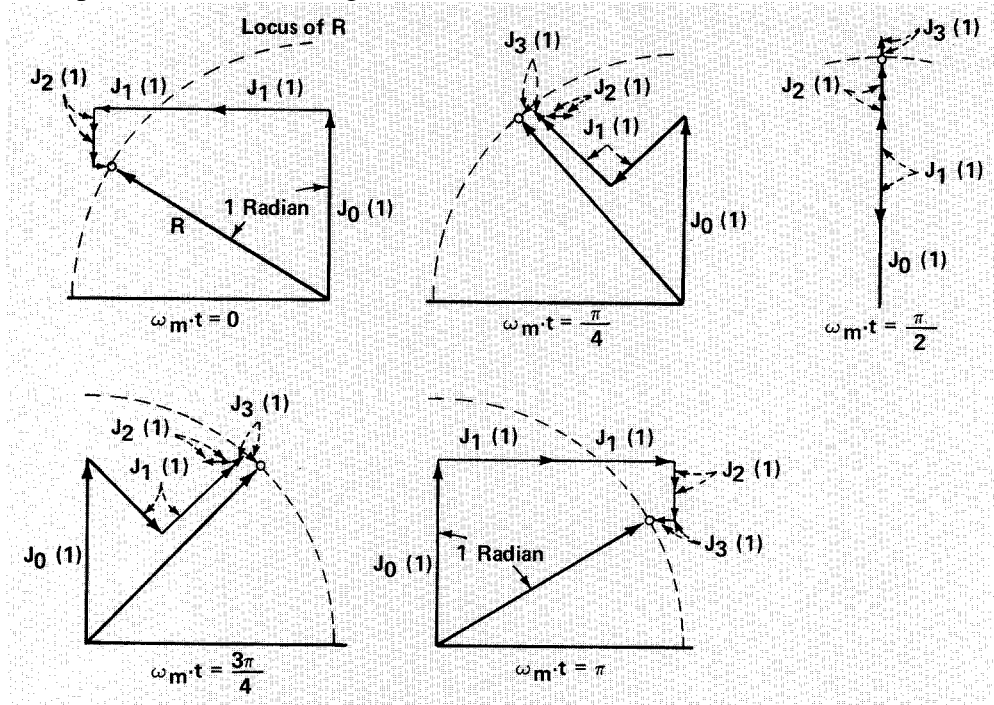
$$\sin(x \sin \theta) = 2J_1(x) \cos \theta + 2J_3(x) \cos 3\theta + \dots$$

where  $J_n$  are the Bessel functions, the PM signal can be written as

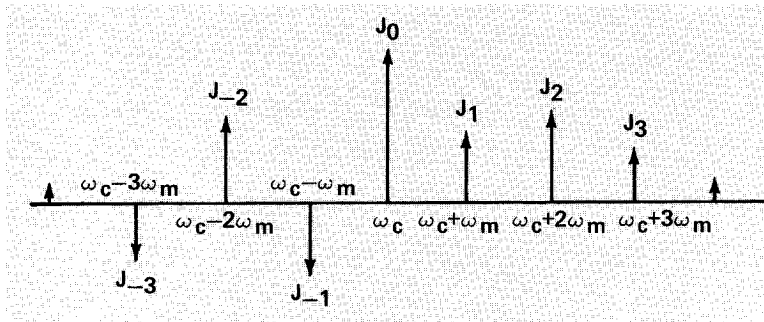
$$\begin{aligned} V_s(t) = & J_0(\hat{\phi}) \cos(\omega_c t) - J_1(\hat{\phi}) (\cos(\omega_c - \omega_m)t - \cos(\omega_c + \omega_m)t) \\ & + J_2(\hat{\phi}) (\cos(\omega_c - 2\omega_m)t + \cos(\omega_c + 2\omega_m)t) \\ & - J_3(\hat{\phi}) (\cos(\omega_c - 3\omega_m)t - \cos(\omega_c + 3\omega_m)t) \\ & + \dots \end{aligned}$$

The signal becomes an infinite sum of harmonics of the modulation frequency, each proportional to the Bessel function corresponding to that harmonic.

A phasor representation of the signal is shown below.



The frequency spectrum is shown below. Note that the relative phase of the upper and lower sidebands is different. The relative phase does not appear on the spectrum analyzer because phase information is lost.



## AM/PM Conversion

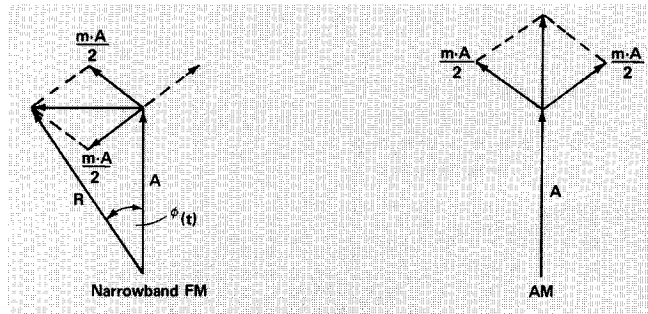
Consider a modulated signal

$$V(t) = \text{Re}\{V (1 + \hat{a}\cos(\omega_m t)) e^{j(\omega_c t + \hat{\phi}\sin(\omega_{pm}t))}\}$$

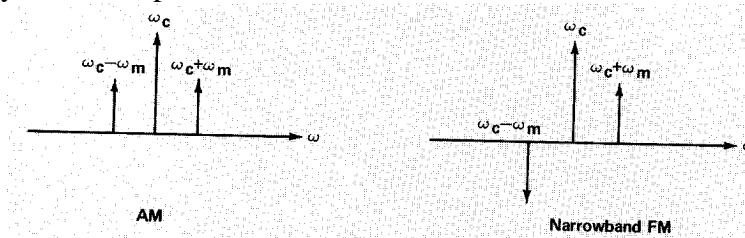
For small amplitude modulations this can be written as

$$V(t) \approx V_c \text{Re}\left\{ e^{j\omega_c t} \left[ 1 + \frac{\hat{a}}{2} (e^{j\omega_{am}t} + e^{-j\omega_{am}t}) + \frac{\hat{\phi}}{2} (e^{j\omega_{am}t} - e^{-j\omega_{am}t}) \right] \right\}$$

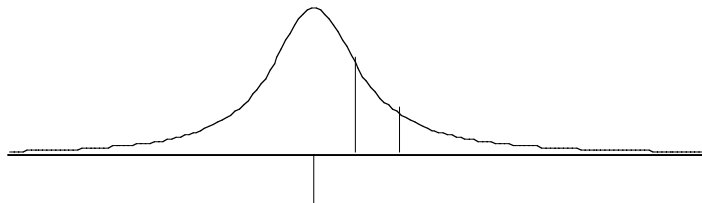
We can compare amplitude and frequency modulation using a phasor representation shown below.



In the frequency domain representation is shown below.



When the modulated signal passes through a filter (e.g. an RF cavity), AM can become FM and vice versa. Shown below is an FM signal. When the cavity is tuned to the carrier, the upper and lower sidebands have the same response. When tuned away, the asymmetry in the response doesn't allow cancellation of the FM phasors and an AM



occurs.

## Noise

External to detector

- environmental noise (i.e. EMI,atmospheric, etc.)
- beam noise (Schottky noise)
- propagating modes in the vacuum chamber

Internal to detector

- magnetic noise (Barkhausen effect)
- shot noise (quantized electron current flow)
- 1/f noise (flicker noise)
- thermal electronic noise (Johnson noise)

$$\begin{aligned}\langle V_n^2 \rangle &= 4kT \int_{f_1}^{f_2} R(f) df \\ &= 4kTR\Delta f\end{aligned}$$

where

k=Boltzmann's constant= $1.38 \times 10^{-23}$  Joules/deg-K

T=absolute temperature of source resistance R in degrees-K

$\Delta f$ =system bandwidth in Hz

R=source resistance in  $\Omega$

(note that this is an approximation valid up to  $\sim 1 \times 10^{13}$  Hz.)

If a matched load is connected to the noise source (i.e. load impedance=R), the maximum power transferred to the load is

$$P_n = kT\Delta f$$

The noise power density is just kT.

Signal/noise ratio is defined either as the ratio of the signal power to the noise power or signal voltage to noise voltage.

The noise figure of a device is defined to the ratio of the S/N at the device input to the S/N at the output. This can be written as

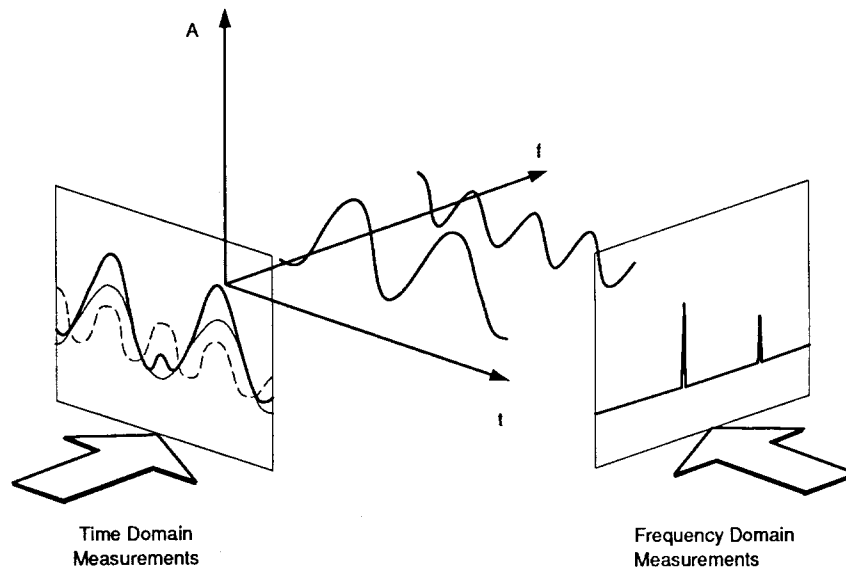
$$F = \frac{N_{DUT} + kT\Delta f G_{DUT}}{kT\Delta f G_{DUT}}$$

where  $G_{DUT}$  and  $N_{DUT}$  are the gain and noise of the device under test. The noise figure of an a device is usually defined at room temperature (290 K).

# Microwave Instruments

## *Spectrum analyzers*

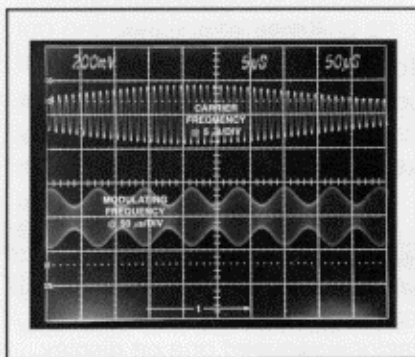
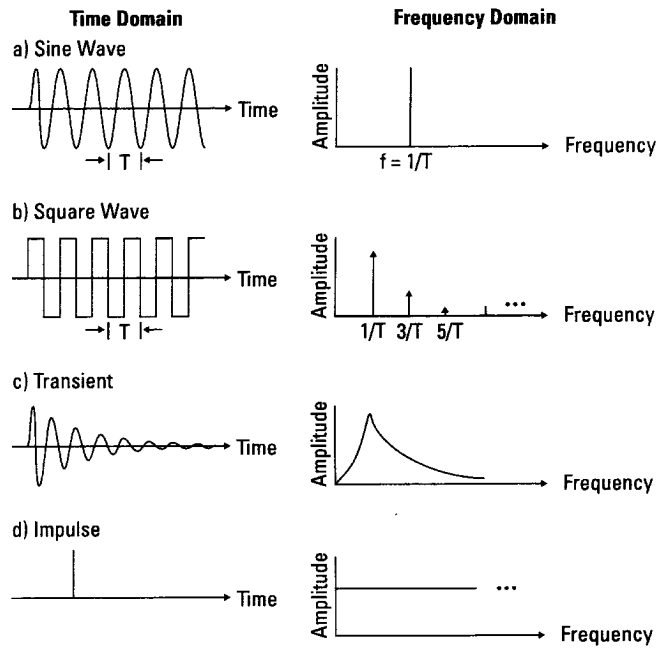
Spectrum analyzers allow us to examine signals in the frequency domain, that is, to determine the frequency spectrum of signals that in everyday life are experienced as time-varying phenomena that can be viewed for example on an oscilloscope. From Fourier analysis we know that a time-varying signal may be constructed from a collection of sine waves of different frequencies and amplitudes. A spectrum analyzer will allow measurement of the sinusoidal frequency components of a time varying input signal. The spectrum is a graphical display of the amplitude and frequency of a signal's sine wave components.



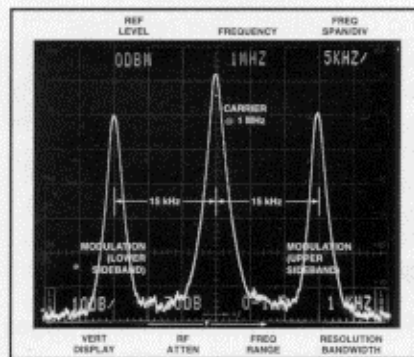
The need for spectral analysis of signals arises in many applications, where a frequency domain approach is more instructive than analyzing complex time-domain waveforms. With an analyzer it is possible to observe:

- an oscillator frequency
- carrier frequency
- amount and frequency of amplitude and frequency modulation
- unexpected modulation

...



Oscilloscope Waveform: Modulated Carrier at 1 MHz, 15 kHz Modulation

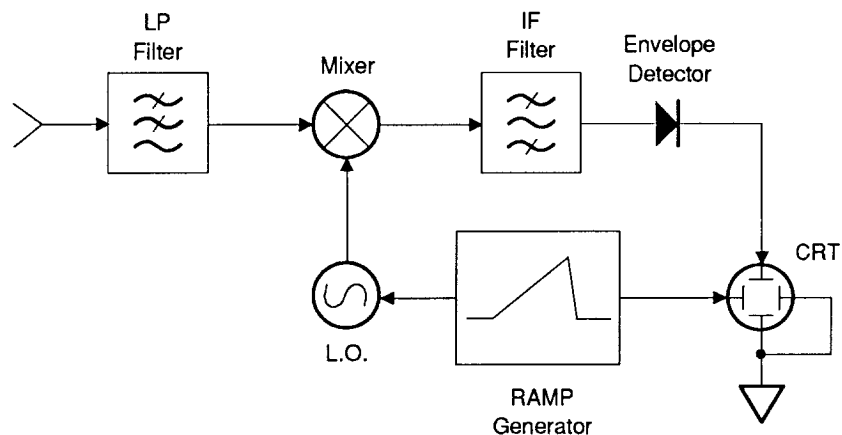


Spectrum Analyzer Waveform: Modulated Carrier at 1 MHz, 15 kHz Modulation

Spectrum analyzers fall into two categories: (a) sweeping or superheterodyne analyzers, and (b) fast Fourier transform (FFT) or dynamic signal analyzers. FFT analyzers measure signals in the time domain and apply a Fast Fourier Transform to obtain frequency domain information on the stored signal. Spectrum analyzers may also be equipped with tracking generators, and signal analyzers are often equipped with noise generators, allowing the measurement of frequency response of devices such as filters, amplifiers, and particle beams. Although signal analyzers have advantages in some measurement applications, current technology limits the frequency range, sensitivity, and dynamic range of FFT analyzers, and we will discuss the sweeping analyzer here.

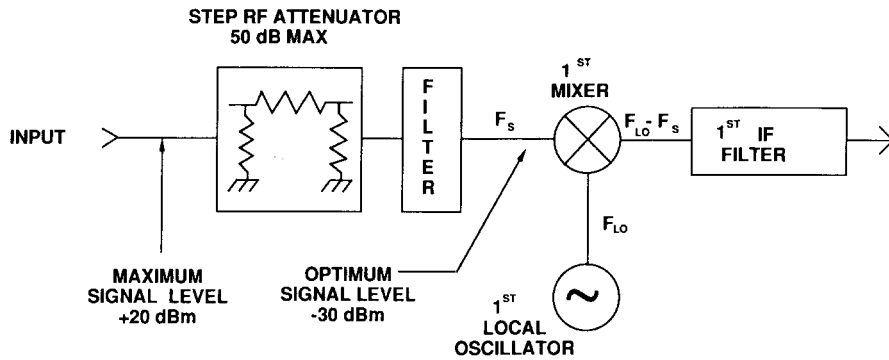
### Sweeping or superheterodyne analyzer

The sweeping analyzer is basically a tuned receiver whose center frequency can be swept electronically. It has adjustable bandwidth, and detects the rms amplitude of the input spectrum over its passband. Heterodyne means to mix (translate frequency), and super refers to super-audio frequencies.



The simplified diagram above shows the basic operation of the analyzer. The input signal is low-pass filtered (*why*), mixed with a signal from a local oscillator, and the mixing products bandpass filtered. Any signals within the bandpass of this intermediate frequency filter will be rectified, amplified and digitized, and used to provide a vertical displacement on the cathode ray tube. A ramp generator tunes the local oscillator in proportion to the ramp voltage, and also provides horizontal displacement of the CRT.

In addition to the low pass filter at the input, we will find an attenuator to maintain the required signal level at the mixer:

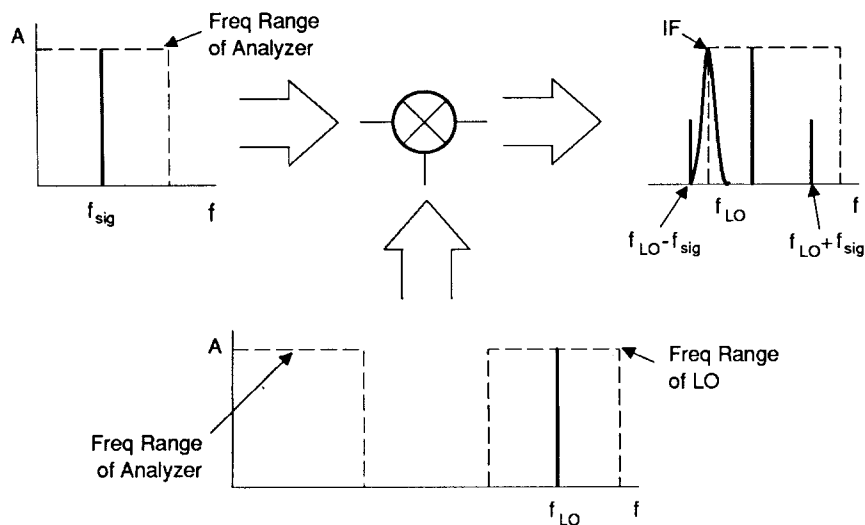


It is very important that the total signal level - at any frequency - is below the level that would cause damage to the analyzer components. DC current may also damage a spectrum analyzer.

The local oscillator frequency and the bandpass filter center frequency are chosen to allow detection of the mixer product

$$f_{IF} = f_{LO} - f_{signal}$$

The IF frequency (filter) is fixed, and ramping the LO frequency brings successive signal frequencies through the bandpass filter to the detector. The example below shows the signal just below the passband of the filter; increasing the LO frequency will bring the mixing product into the IF passband and a signal will be seen on the display. The horizontal axis of the CRT display can be calibrated in terms of the input frequency. Typical frequencies are  $3.6 \text{ GHz} < f_{LO} < 6.5 \text{ GHz}$ ,  $f_{IF} = 3.6 \text{ GHz}$ , for an analyzer that tunes up to 2.9 GHz.

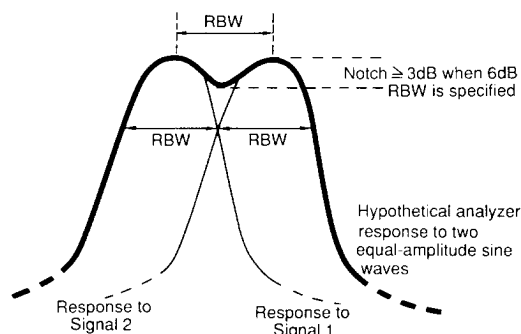




The purpose of the low-pass filter at the analyzer input is to reject input signals at which the mixer product  $f_{IF} = f_{\text{signal}} - f_{LO}$  would result in a detected signal after the IF filter. Also, the low pass filter must reject input signals at the IF frequency itself, which are present in the mixer output.

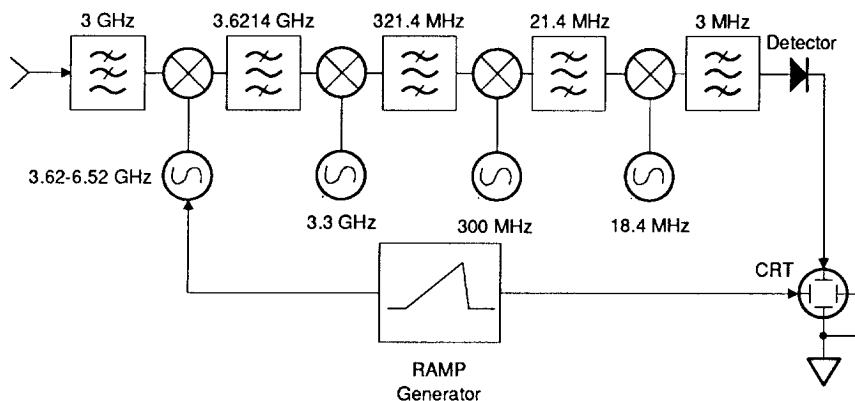
The resolution of an analyzer is a function of the bandwidth (**resolution bandwidth, RBW**) of the IF bandpass filter. The shape of a signal on the spectrum analyzer is a combination of the shape of the signal and the IF filter. In order to separate two equal sinusoids closely spaced in frequency, the filter must have a 3dB bandwidth equal or less than the signal separation.

The resolution is defined as the frequency separation of two signals which merge with a 3 dB notch:



If we are dealing with signals that are not equal in amplitude, the smaller signal may be lost in the skirts of the filter response. To characterize this, another specification, the selectivity or shape factor, is used in defining the bandpass filters. The selectivity is the ratio of bandwidth at 60 dB down from maximum, to the bandwidth at 3 dB (or 6 dB) down from maximum. Typical selectivity of filters for high performance analyzers might be 11:1 (60:3 dB ratio).

Narrow IF bandwidths, perhaps into the range of 10's of Hz, are difficult to achieve at high frequencies. In order to obtain high resolution, several mixing stages are employed:



The required resolution bandwidth is a function of both the resolution and selectivity of the IF filter, and the separation and amplitudes of the signals we wish to resolve.

Some spectrum analyzers also contain a digital filter to achieve the highest resolution (lowest resolution bandwidth). In this case the signal is mixed down to low frequency, passed through a narrowband analog filter, amplified, sampled and digitized. The signal is acquired in the time-domain and put through a Fast Fourier Transform algorithm which filters the data with a highly selective filter. The analyzer then steps to the next frequency in the span (by changing the LO frequency), and another time-domain sample is taken and analyzed and then displayed.

Another factor affecting the resolution is the stability of the local oscillator. Modulation of the local oscillator frequency will result in products from the mixer which are not present in the input signal. Residual FM of the local oscillator signal may limit the resolution of low-cost analyzers (with simple YIG-tuned oscillators as the LO source). Phase noise is present on all spectrum analyzer LO systems, and manifests itself as a broad skirt around a signal when displayed above the noise-floor of the analyzer. Note that the noise-floor varies with RBW since the noise power is proportional to bandwidth.

The resolution bandwidth of the analyzer imposes significant restrictions on the sweep time. The sweep rate must be slow enough that the filters can respond and reach peak amplitude in the time that a signal is within the filter passband. The time in the passband is

$$T_{\text{passband}} = \text{RBW}/(\text{span}/\text{sweep time})$$

and the rise time of the filter is

$$T_{\text{filter}} \approx 0.3/\text{RBW}$$

then if we equate these times the sweep time is related to the resolution bandwidth by

$$\text{sweep time} \approx 0.3 (\text{span})/(\text{RBW})^2$$

and this is a lower limit on the sweep time for CW signals. Selection of RBW is particularly important in measurements of pulsed signals, where the time duration of the input signal must be accounted for also.

The IF filter output is converted to a video signal by an envelope detector. The detector will put out a dc voltage for a CW sinusoidal input that gets through the IF filter, the voltage dependent on the amplitude of the signal. The video signal contains the information on the input signal, and also noise introduced by the analyzer itself. This signal may be low-pass filtered to reduce noise. When the video filter has a passband less than the IF filter, the video system cannot follow the rapidly changing variation of the envelope detector, resulting in averaging or smoothing of the displayed signal. The **video bandwidth (VBW)** should be used with caution, if set below the RBW it may affect the amplitude of the signals if the sweep rate is not adjusted to allow the filter signal to maximize. The VBW is usually set equal to the RBW as a default.

The spectrum analyzer may also be used in CW mode, where the LO is fixed. The video output then may be used to monitor amplitude changes in a signal at a fixed frequency.

Digital spectrum analyzers (most modern analyzers are digital) allow video averaging, where each displayed point is averaged in with the previously averaged data:

$$A_{\text{avg}} = [(n-1)/n]A_{\text{prior avg}} + (1/n)A_n$$

where  $A_{\text{avg}}$  = new average value  
 $A_{\text{prior avg}}$  = average from prior sweep  
 $A_n$  = measured value on current sweep  
 $n$  = number of current sweep

The noise-figure of a spectrum analyzer relates the signal-to-noise ratio at the input to that at the output. We simplify this by noting that the output signal level (indicated on the display) is made to be equal to the input signal level, then the noise figure becomes

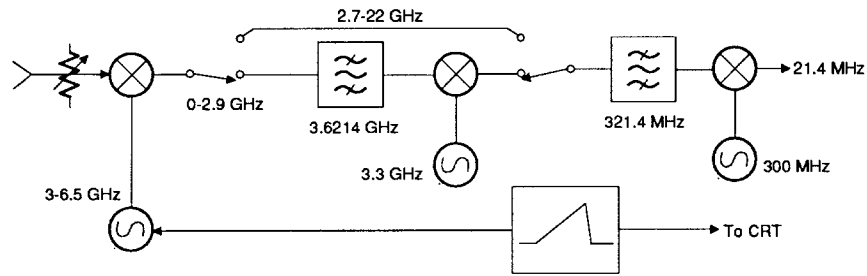
$$F = N_o/N_i$$

We know that the input noise level for room temperature, for a 1 Hz bandwidth, and with the input terminated in  $50\Omega$  is

$$N_i = kTB = -174 \text{ dBm}$$

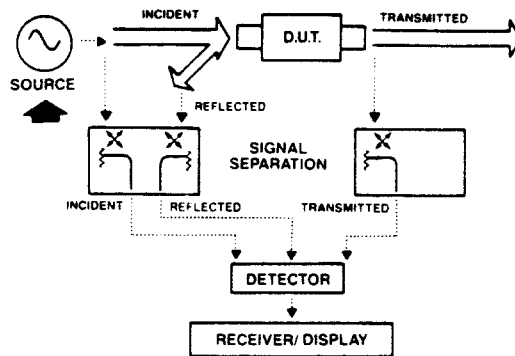
The noise figure is then the measured noise converted to a 1 Hz bandwidth (the measured noise will be for the RBW), minus the input noise (measurements in dBm). Typically, the noise figure may be 24 dB. A preamplifier may be used to improve the system noise figure.

The discussion so far has been for an analyzer of relatively low frequency range, perhaps a few GHz. If we wish to measure higher frequency signals, we must remove the low-pass filter at the input and we may switch to a different IF, this time lower in frequency than the tuning range of interest. If we limit the span, and apply bandpass filtering where necessary, frequencies up to tens of GHz may be analyzed:

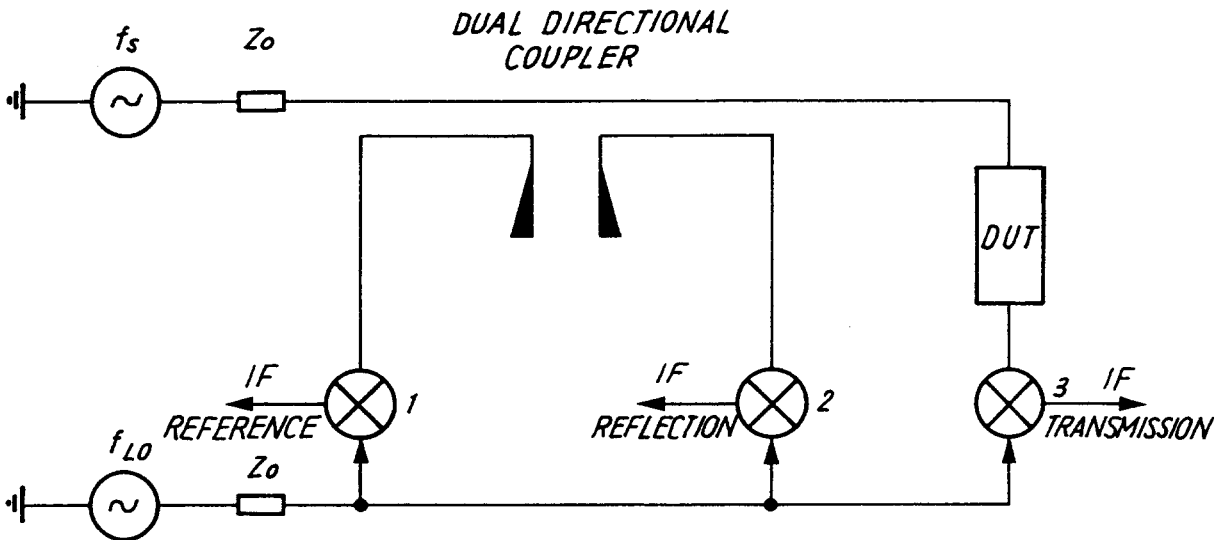


## Network analyzers

Network analysis tells us how a system responds to a given input. Network analyzers measure the amplitude and phase (for vector network analyzers) of the response of a system to sinusoidal input signals. In some ways the network analyzer may be thought of as a spectrum analyzer with a tracking generator, but this is not strictly true. The basic functions of a vector network analyzer are to measure the magnitude and phase of signals transmitted through and reflected from a device, with respect to the source signal. A scalar network analyzer is less complicated and does not allow phase information to be discerned.

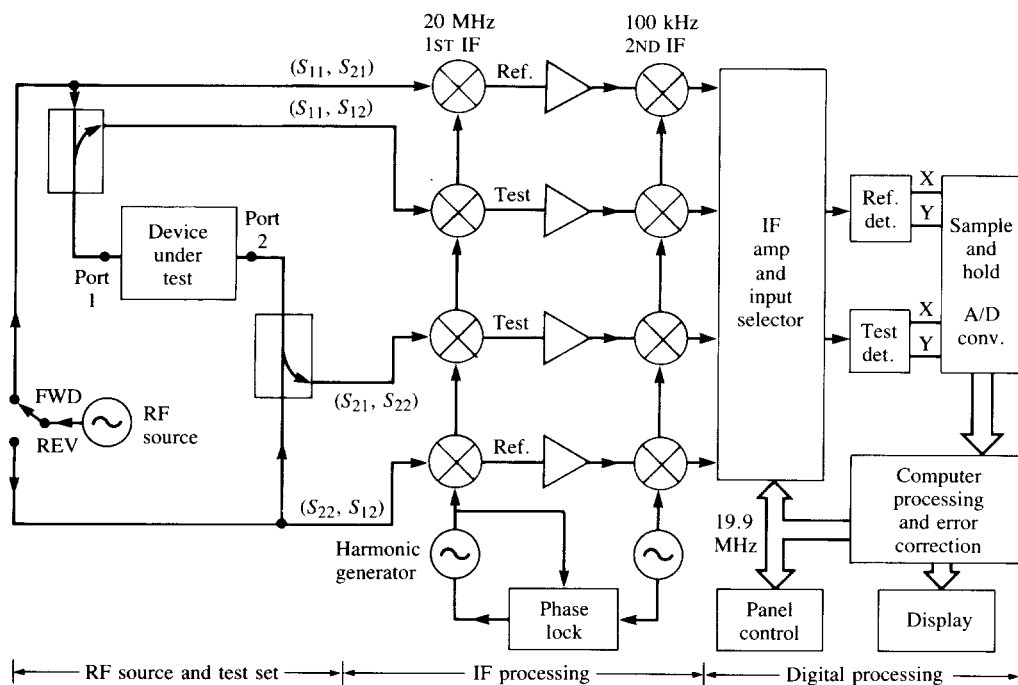


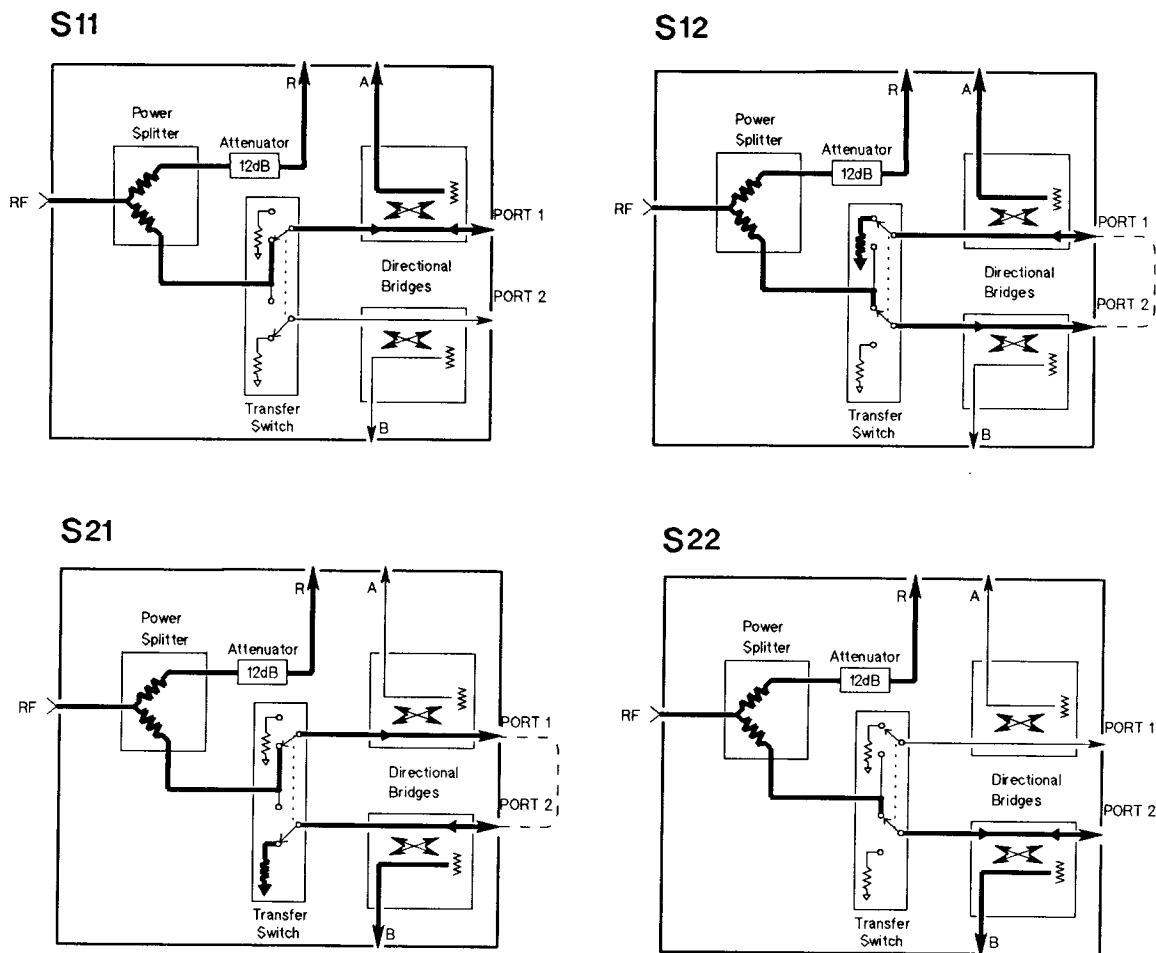
Two signals are used, both variable in frequency (swept or stepped), but locked to each other by a phase-locked-loop (PLL), such that their difference frequency is kept constant at some IF.



After mixing, the IF contains the full phase and amplitude information of the RF signal to be measured. The signal source may be a sweep oscillator or a synthesized sweeper, providing a signal which may be swept over a range of frequencies of interest. A synthesized sweep oscillator allows the production of very accurate synthesized CW signals which may be stepped to provide the desired frequency span. The IF of mixer 1 gives a signal to a PLL which maintains the local oscillator at the required frequency difference from the RF signal ( $f_s$  in the above diagram). The IF signals are amplified and mixed down to 100 kHz where they are detected. A phase sensitive detector is used to measure the phase against a 100 kHz reference oscillator. The phase and amplitude signals are digitized and sent to the CRT display.

The basic network analyzer has an RF output port and three input ports; the reference (R), port 1 signal (A), and port 2 signal (B). The analyzer controls the frequency of the RF signal and detection electronics, and displays the data. Modern analyzers have onboard computers which allow manipulation of the data and can display in various formats, including SWR, return loss, phase, group delay, impedance, Smith chart etc. Using a dual-reflectorometer, or S-parameter test set, input and output reflection coefficients, as well as the forward and reverse transmission coefficients, can be measured without disconnecting the device under test.





Factors affecting accuracy are similar to those discussed for the spectrum analyzer, in particular concerns over IF bandwidth and sweep time. Another control to improve accuracy of measurements is the power output of the analyzer RF signal.

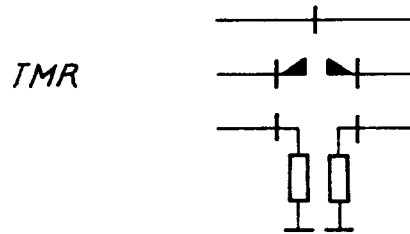
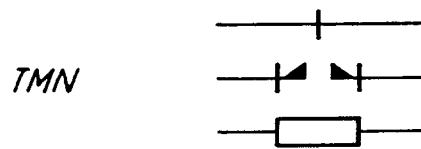
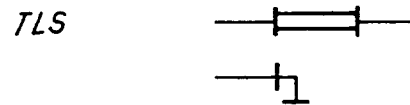
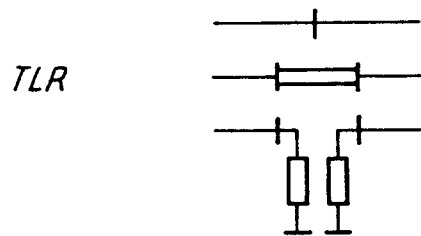
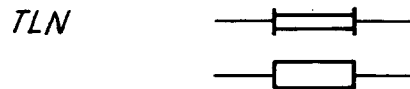
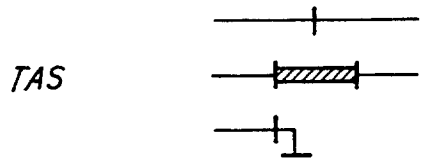
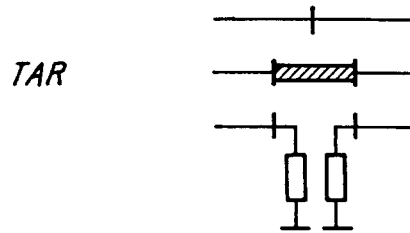
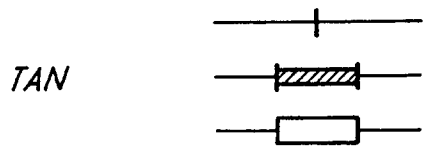
Network analysis measurements contain systematic errors that can be measured and corrected for. A measurement is the vector sum of the actual device response plus all error terms. These errors are due to the finite directivity of the couplers in the test-set, impedance mismatch at the RF source, impedance mismatch at the load (port 2), finite isolation of signal paths within the analyzer (crosstalk), and frequency response of all devices in the forward and reverse signal paths (tracking). By connecting known terminations at each port (open circuit, short circuit, and matched load), and by connecting the two ports together directly, these 12 (6 in each direction) systematic error terms can be calculated and in a calibration routine, and correction applied to the measured signals. The full 2-port, 12 point calibration routine requires all S-parameters to be measured to determine the correction for any one S-parameter. Simpler correction routines are used for 1-port measurements.

Calibration kits consisting of open, short, load, through are available for standard coaxial lines, but other techniques are available using different reference measurements, and which may find application in measurements with non-standard transmission lines.

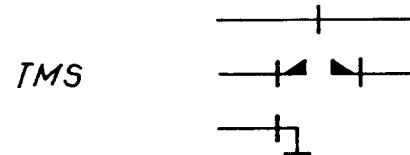
Another means of removing some unwanted effects, such as multiple reflections, is to use the FFT capabilities of modern analyzers, transforming into time domain, applying a time gate to remove reflections, and then transforming back into frequency domain.

It is also possible to generate "synthetic pulses" by shaping the frequency domain signal and transforming to time domain.



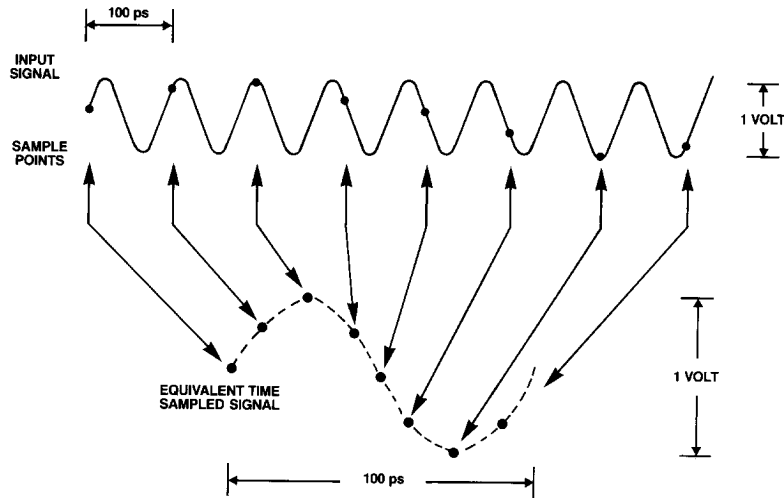


*A = Attenuation*  
*L = Line*  
*M = Matched load*  
*N = Unknown network*  
*R = Unknown reflection*  
*S = Short*  
*T = Thru*

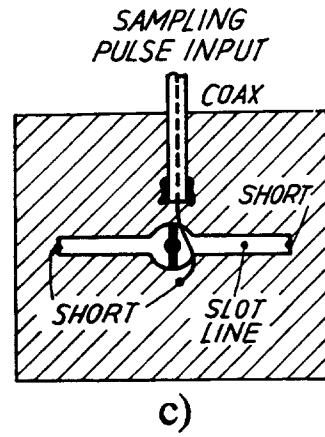
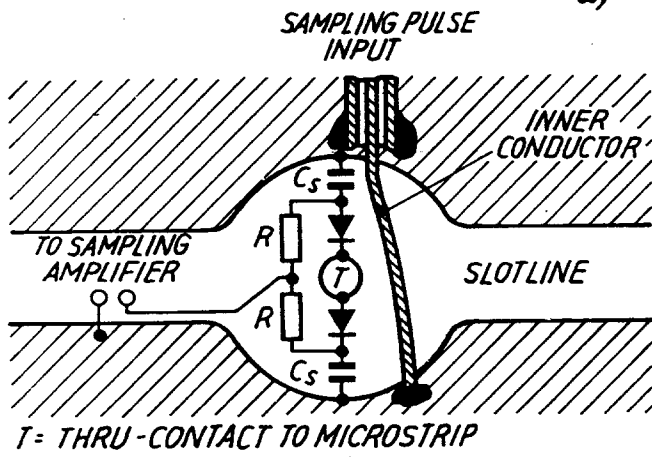
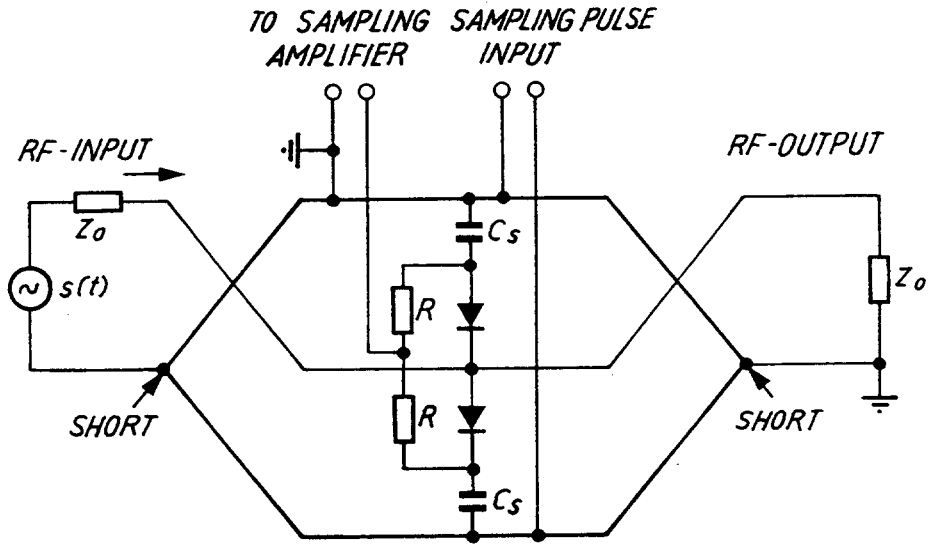


## *Sampling oscilloscopes*

Real-time oscilloscopes have bandwidths limited to  $\approx 1$  GHz. In order to see faster signals on repetitive waveforms sampling 'scopes are used. The equivalent time sampling technique samples the input waveform at least once in its repetitive period, then the time of the next sample is delayed slightly, and so on, and generates a waveform similar to the input waveform by ordering the measured samples appropriately.



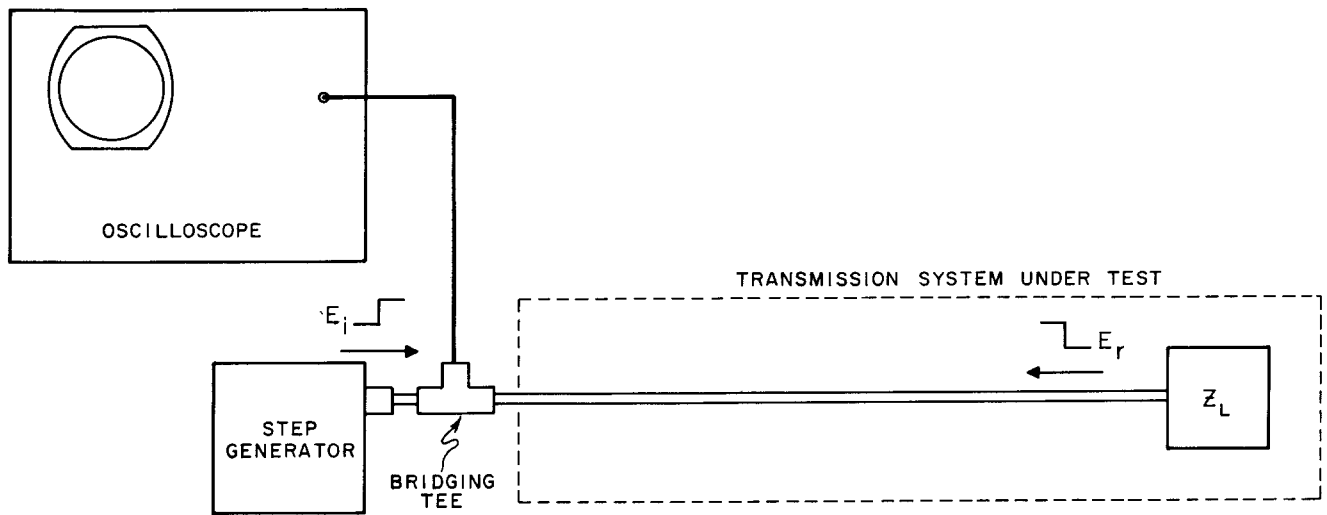
The sampling heads must have very short measurement time to avoid averaging the signal. Step-recovery diodes, which change their conductivity very rapidly between the conducting and non-conducting state, are used to generate the sampling pulse. The actual sampling switch is a Schottky diode which becomes conductive during the sampling pulse and allows the input signal to charge a capacitor. The capacitor forms part of a sample-and-hold circuit, the output of which is read and forms the vertical displacement on the CRT display. Sampling head bandwidths of 50 GHz are achievable with monolithic microwave integrated circuits.



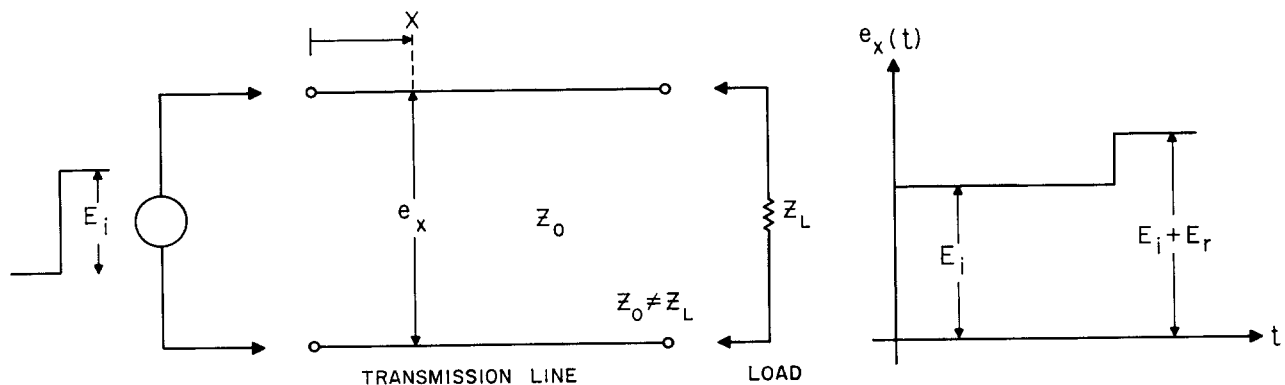
## Time domain reflectometry

Time domain reflectometry (TDR) allows measurement of characteristic impedance, reflection coefficient, and nature (resistive, inductive, capacitive) and value of complex impedances on coaxial lines. It also allows the location in time (distance) of mismatches on the transmission line.

A voltage step is propagated down the transmission line under test, and the incident and reflected voltages are monitored by an oscilloscope. A sampling oscilloscope is used, since the step rise time is typically 25 ps and cannot be resolved by real time 'scopes.



Once the incident and reflected voltages are measured on the oscilloscope, the reflection coefficient and impedance of the mismatch may be calculated.



$$\rho = E_r/E_i = (Z_L - Z_0)/(Z_L + Z_0)$$

The location of an impedance mismatch may be found by timing the arrival of the pulse reflected from the mismatch ( $E_r$ ). The distance from the reference plane to the mismatch is

$$d = v T/2 = (c/\sqrt{\epsilon_r}) T/2$$

where  $v$  is the velocity of the wave on the transmission line,  $T$  is the measured time interval, and  $\epsilon_r$  the relative dielectric constant of the material of the coaxial line. The time measured is from the arrival of the incident pulse at the reference plane, to its return from the discontinuity, and so is twice the time of travel to the discontinuity itself.

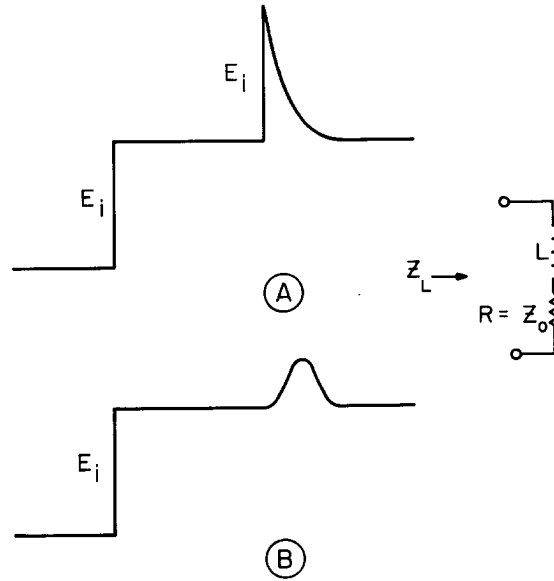
The spatial resolution may be related to the step risetime by assuming that two discontinuities are indistinguishable if separated by less than the risetime. Then

$$d_{\min} = (c/\sqrt{\epsilon_r}) T_{\text{rise}}/4$$

TDR displays for resistive loads:

TDR displays for complex loads

Note that the ideal waveforms of the previous page are smeared out as a result of the finite bandwidth of the system, which is less than the time constant of the reactive circuit for small enough reactances.



# Microwave Devices and components

## *Transmission lines*

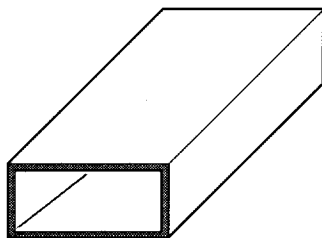
Transmission lines are used to carry microwave signals in an efficient manner, allowing the incorporation or connection to other microwave devices. In order to choose an appropriate transmission line for a given application, several factors have to be considered:

- signal frequency
- signal bandwidth
- power handling capability
- attenuation of signal
- size of transmission line
- ease of fabrication

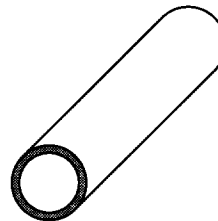
Generally a transmission line is chosen with a compromise between these requirements.

Three basic, common, types of transmission line are shown here:

Waveguide



(c) Rectangular waveguide



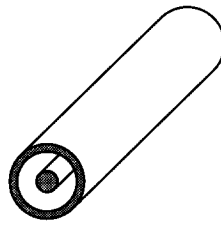
(d) Circular waveguide

Waveguides are low-loss and have high power handling capability, but limited bandwidth (low frequency cut-off and multi-mode propagation at high frequencies). Large size at low frequencies. Generally the height of the waveguide is approximately half the width, and the type of waveguide used is determined by the requirement that only the  $TE_{10}$  mode propagates within the frequency band of the signal.



The  $TE_{20}$  mode has the next lowest cut-off, and to avoid propagation of higher-order-modes the waveguide width must be chosen such that the wavelength at the upper operating frequency is less than the guide width. For this reason the bandwidth is generally a little less than an octave. Circular waveguides may be used in applications where less attenuation is required than can be achieved with rectangular guide, but overmoding is more problematic.

## Coaxial lines



(b) Coaxial line

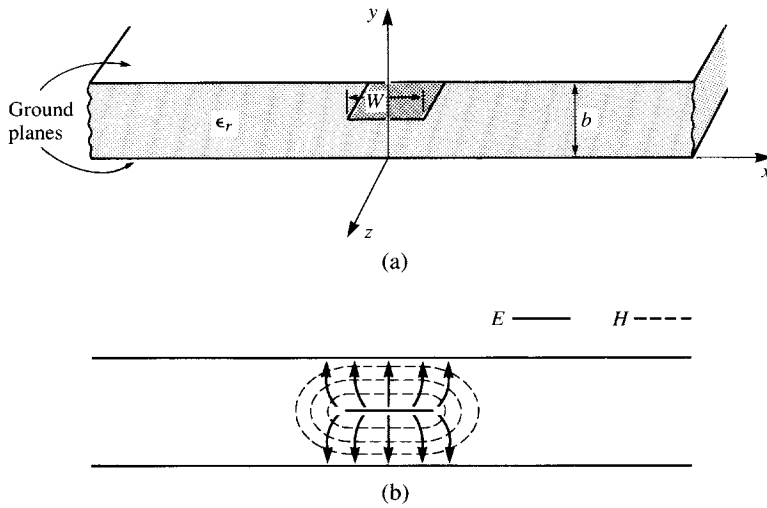
Coaxial lines accommodate TEM waves and have broad bandwidth and small size. Attenuation is relatively high and power handling capability is less than waveguide. Note that Teflon may be incorporated in some coaxial cable types, and such cables may not be suitable for high radiation environments around accelerators. Most cables are  $50 \Omega$  characteristic impedance, although other values are used, notably  $75 \Omega$  for TV and video use. The dominant waveguide mode on a coaxial line is the  $TE_{11}$  mode, and the approximate cut-off frequency for this mode is given by

$$f_c \approx c/(\pi(a+b))$$

Coaxial connectors can be found in various designs, usually in male/female threaded pairs.

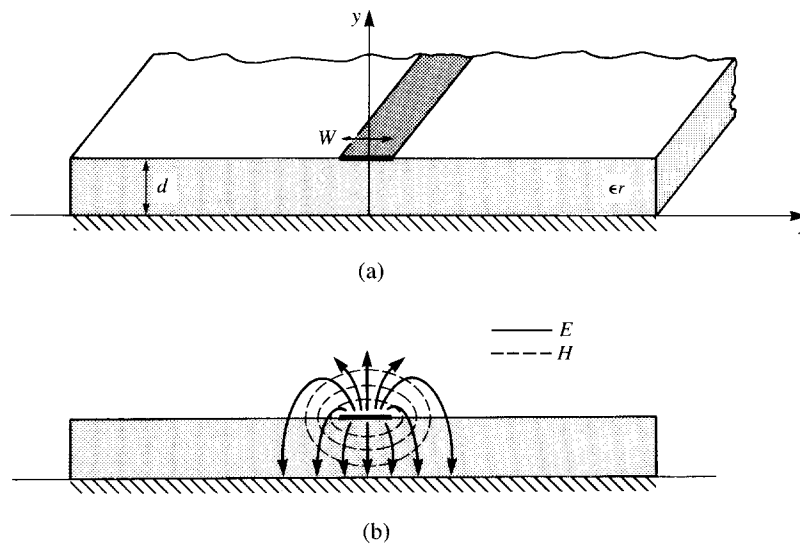
|         |  |
|---------|--|
| N-type  | In common usage, recommended upper operating frequency about 11 GHz, precision versions up to 18 GHz.  |
| SMA     | Smaller and lighter than the N-type, cheap, re-connection not reliable after several applications, can be used up to 18 GHz, some versions up to 25 GHz. |
| APC-3.5 | Similar to SMA but has no solid dielectric filling and can be used up to 34 GHz, with high repeatability. Expensive. Can mate with SMA.                  |
| APC-7   | Precision sexless connector, used up to 18 GHz with high repeatability.  |
| BNC     | Low frequency connector, quick-release, usually used up to $\approx 1$ GHz.  |

## Stripline



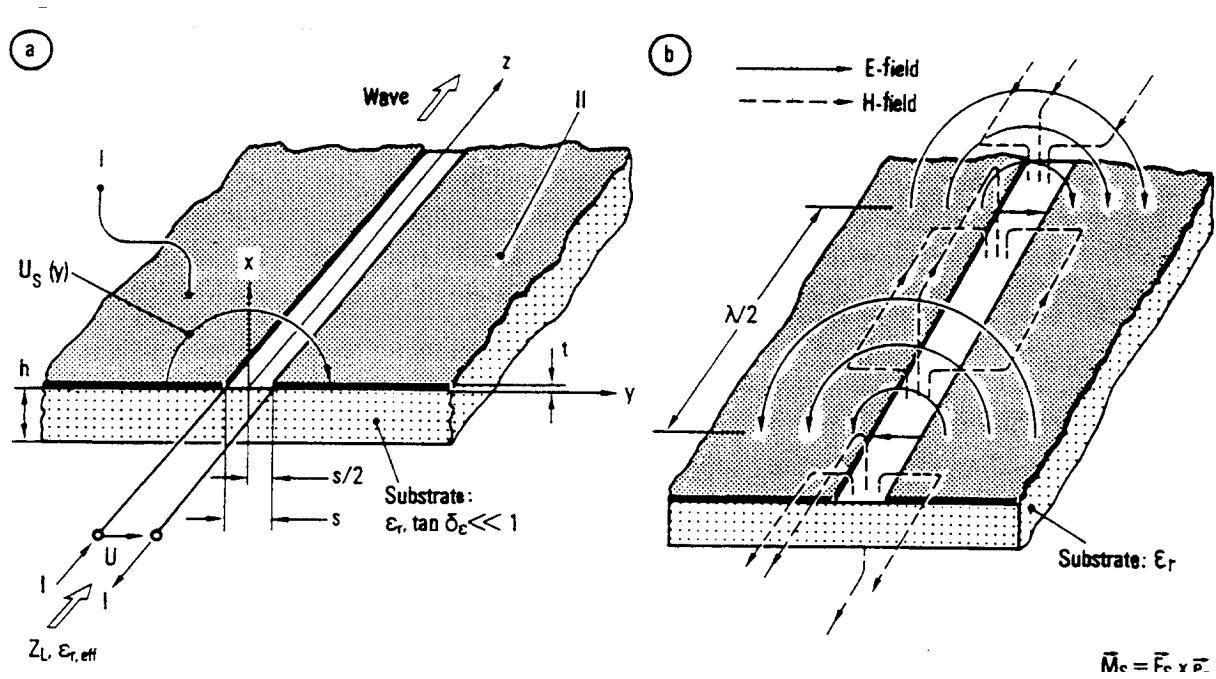
Stripline may be thought of as a "flattened out coax", and lends itself well to photolithographic fabrication techniques. Since stripline contains two conductors and a homogeneous dielectric, it can support TEM waves. Higher order TM and TE modes may be generated for frequencies where the spacing between the ground planes is greater than a half-wavelength.

## Microstrip



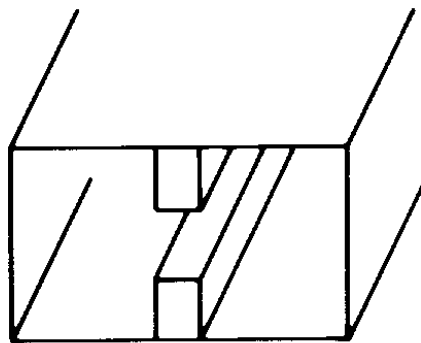
Microstrip is another very common planar transmission line, which is easily manufactured and integrates well with other microwave devices. Microstrip does not support pure TEM waves, attenuation is high and power handling capabilities are low.

## Slotline



Similar to microstrip but with a thin slot in the ground plane on one side of the dielectric.

## Ridged waveguide

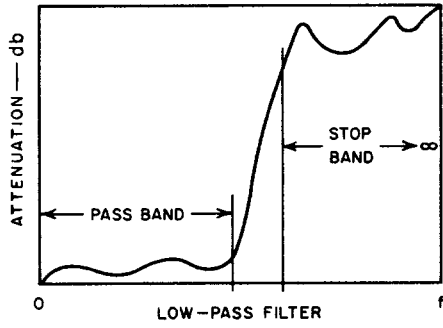


Ridges on the top and/or bottom of a waveguide lower the frequency of the dominant mode, increasing bandwidth. Often used in impedance matching transitions since the impedance is easily controlled by the ridge dimensions.

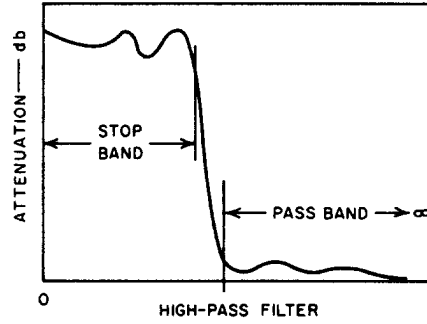
# Filters

Filters are frequency-selective devices which pass only frequencies within a desired band, and reject signals at other frequencies. Typically four types of filter passband characteristics are used:

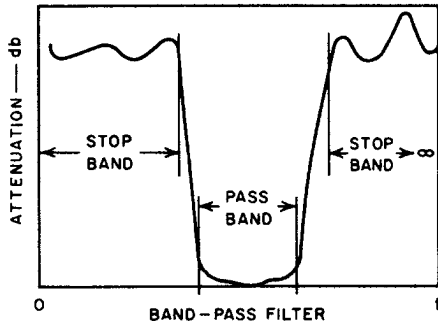
Lowpass



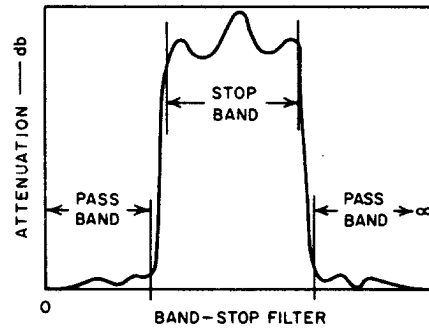
Highpass



Bandpass



Bandstop



Important specifications for filters are:

Cut-off frequency (lowpass and highpass filters)

Center frequency (bandpass filters)

Bandwidth (bandpass filters)

Lower stopband frequency

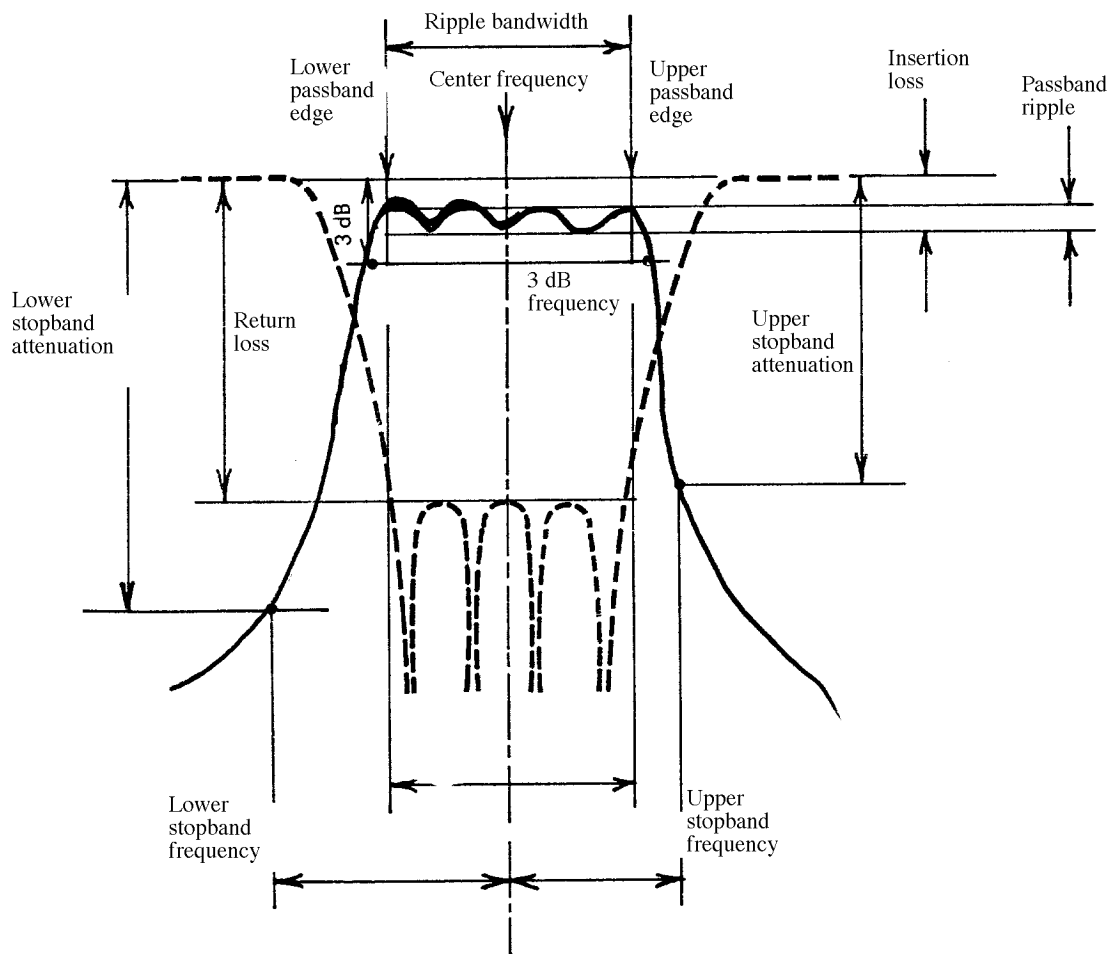
Upper stopband frequency

Out-of-band rejection

Insertion loss

Return loss

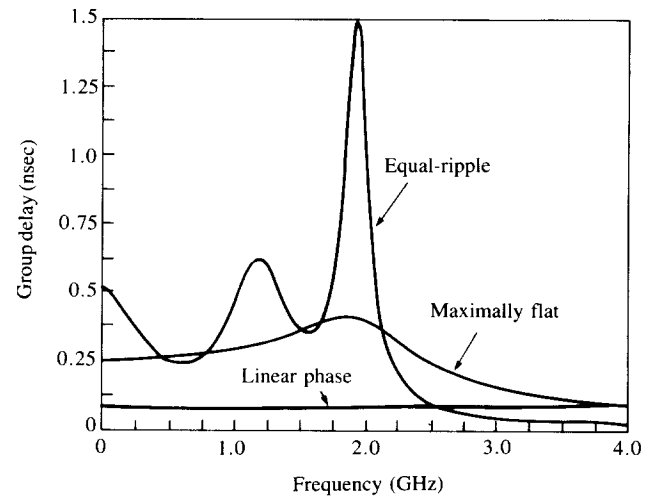
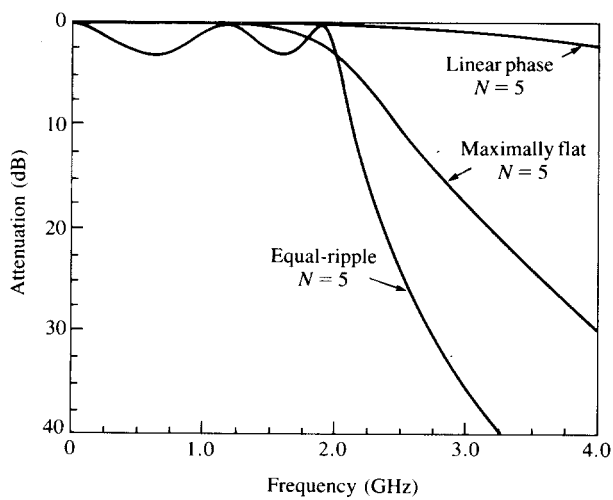
Passband ripple



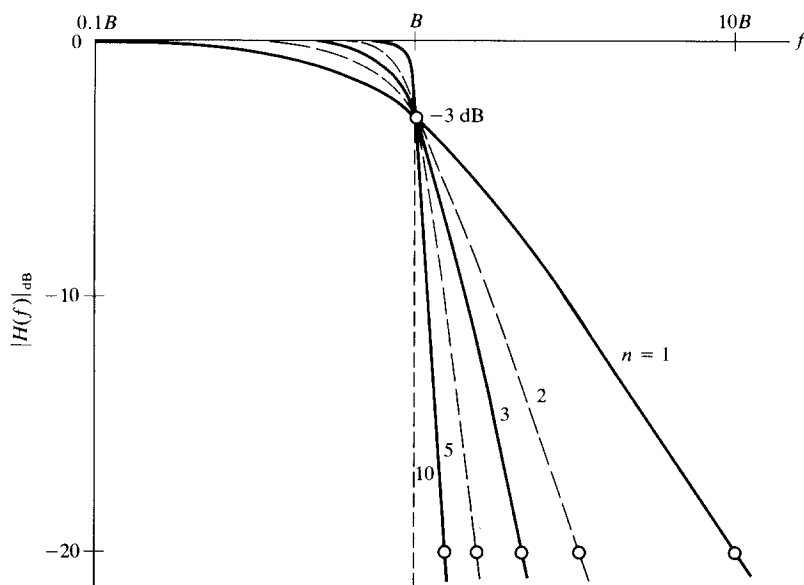
The required filter response determines the mathematical description used in the design of the filter, and several types are in common usage including:

- Maximally flat (or binomial or Butterworth)
- Chebyshev (or equal-ripple)
- Linear phase

Once the mathematical description is selected, the order of the transfer function necessary to achieve the required specifications can be computed.



Transfer function for Butterworth lowpass filters of order  $n$ :

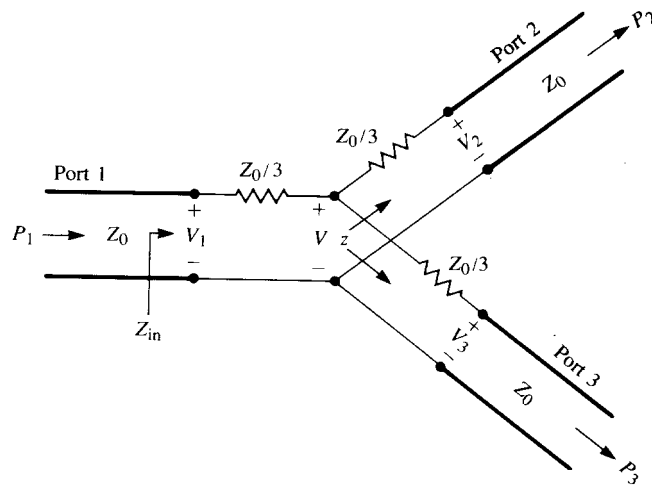


## *Power dividers, power couplers*

Power dividers are used to split a signal from one transmission line into other lines, or to combine power from two or more lines. Typically, a power divider is a three-port network and the division is into two equal lines each -3 dB less in power than the incident line, but the split may be into more lines or different power ratios.

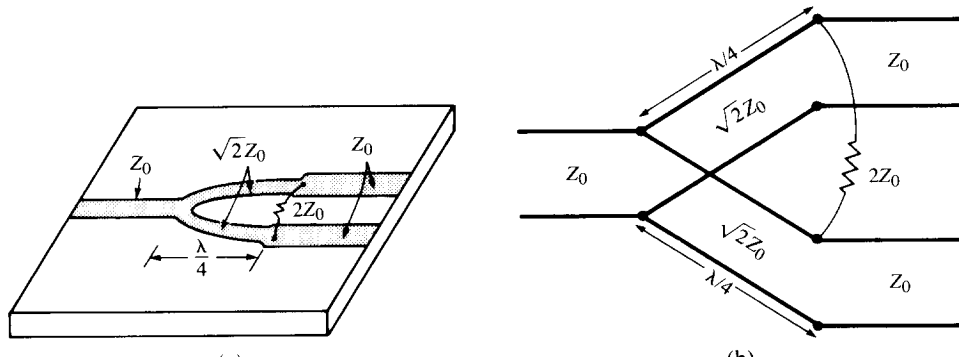
A simple T-junction allows lossless transmission of power into two arms, with the power ratio determined by the characteristic impedance of each arm. While the input impedance may be matched, the impedance into the coupled arms is not. Also, the ports of this splitter are not isolated.

Resistive dividers allow matching of all three ports, but introduce a 3 dB loss in total power, and no isolation between ports.

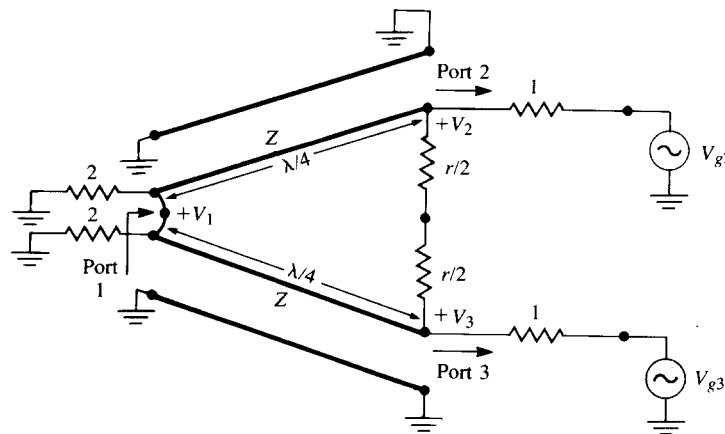




The Wilkinson power divider allows matching of all ports and isolation between the output ports. The input and output lines are connected by lines  $\sqrt{2} Z_0$ , and a resistor of  $2 Z_0$  between the output lines. This resistor does not introduce loss in the power-splitting since the two output arms are in phase and there is not voltage across the resistor, but it does attenuate power coupled into the arms out-of-phase and provides isolation between the output arms.



The symmetry of the Wilkinson divider allows a simple analysis using the even-odd mode technique. We normalize all impedances to the characteristic impedance  $Z_0$ , add voltage generators at the output ports, and draw the circuit below:

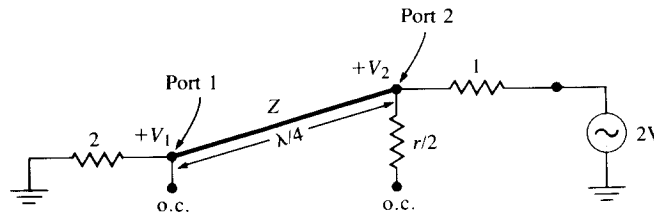


We can define two modes of excitation:

the even mode, where  $V_{g2} = V_{g3} = 2 \text{ V}$   
the odd mode, where  $V_{g2} = -V_{g3} = 2 \text{ V}$

By superposition of the two modes we have  $V_{g2} = 4 \text{ V}$ , and  $V_{g3} = 0$ .

For the **even mode**  $V_{g2} = V_{g3} = 2\text{V}$ , and  $V_2 = V_3$ , there is no current flow through the resistors  $r/2$ , or through the short circuit at port 1. Bisecting the network with open circuits at the center line, looking into port 2 we see a  $\lambda/4$  line, and the input impedance at port 2 is that of a quarter-wave transformer  $Z_{in}^{even} = \frac{Z^2}{R_{load}}$ ;



$$Z_{in}^{even} = \frac{Z^2}{2}$$

Thus port 2 will be matched if  $Z = \sqrt{2}$ , and all power goes to port 1.

To find  $S_{12}$  we use the transmission line equations. The voltage on the line is ( $x = 0$  at port 2 and  $x = \lambda/4$  at port 1):

$$V_x = V^+ (e^{-j\beta x} + \Gamma e^{j\beta x})$$

$$V_0 = V^+ (1 + \Gamma) = V_2 = V$$

$$V_1 = V \frac{\lambda}{4} = jV^+ (\Gamma - 1) = jV \frac{\Gamma - 1}{\Gamma + 1}$$

using  $\Gamma = \frac{Z_{in} - Z_0}{Z_{in} + Z_0}$  we have

$$\Gamma = \frac{2 - \sqrt{2}}{2 + \sqrt{2}}$$

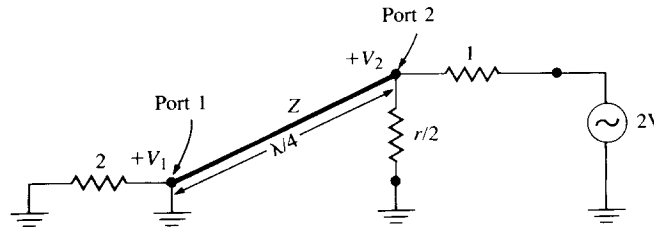
and

$$V_1 = -jV \frac{1}{\sqrt{2}}$$

$$S_{12} = \frac{V_1}{V_2} = \frac{-j}{\sqrt{2}}$$

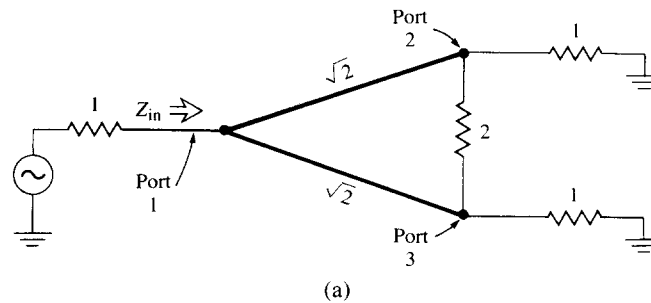
By symmetry  $S_{13} = -j/\sqrt{2}$ , and  $S_{33} = 0$

Now for the **odd mode**  $V_{g2} = -V_{g3} = 2V$ , and  $V_2 = -V_3$ , the circuit can be grounded along the center line:

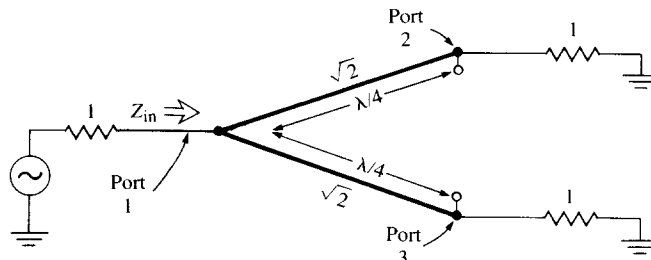


Looking into port 2 we see an impedance of  $r/2$ , the port is matched ( $S_{22} = 0$ ) if  $r = 2$ . In this mode all power is delivered to the resistors and none gets to port 1.

For the input match  $S_{11}$  we terminate ports 2 and 3 in matched loads and the resulting circuit is similar to the even mode:



(a)



(b)

No current flows through the resistor, so it can be removed in the analysis, and we have two quarter-wave transformers in parallel. The input impedance is then matched

$$Z_{\text{in}} = \frac{1}{2} \frac{(\sqrt{2})^2}{1} = 1$$

We now have all of the S parameters:

$$S_{11} = S_{22} = S_{33} = 0$$

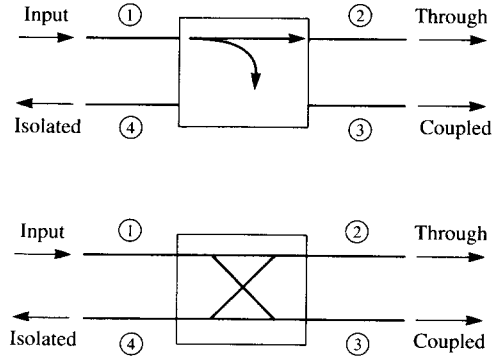
$$S_{12} = S_{21} = S_{13} = S_{31} = -j/\sqrt{2}$$

$$S_{23} = S_{32} = 0$$

When the outputs are matched, the divider is lossless and power from ports 2 or 3 is dissipated in the resistor.

## Directional couplers

Directional couplers are 4-port devices which sample power traveling in one direction down a transmission line.



If the 4-port device is reciprocal and matched at all ports the [S] matrix has the form

$$[\mathbf{S}] = \begin{bmatrix} 0 & S_{12} & S_{13} & S_{14} \\ S_{12} & 0 & S_{23} & S_{24} \\ S_{13} & S_{23} & 0 & S_{34} \\ S_{14} & S_{24} & S_{34} & 0 \end{bmatrix}$$

and for a lossless network the matrix is unitary (energy conservation). Then we have for the dot products of rows 1 and 2, and rows 3 and 4:

$$S_{13}^* S_{23} + S_{14}^* S_{24} = 0$$

$$S_{14}^* S_{13} + S_{24}^* S_{23} = 0$$

from which we find

$$S_{14}^* \left( |S_{13}|^2 - |S_{24}|^2 \right) = 0 \quad (\text{a})$$

Similarly for rows 1 and 3, and rows 4 and 2:

$$S_{12}^* S_{23} + S_{14}^* S_{34} = 0$$

$$S_{14}^* S_{12} + S_{34}^* S_{23} = 0$$

and

$$S_{23}^* \left( |S_{12}|^2 - |S_{34}|^2 \right) = 0 \quad (\text{b})$$

(a) and (b) may be satisfied if  $S_{14} = S_{23} = 0$ , which results in a directional coupler. Then the self-products of  $[S]$  give:

$$\begin{aligned} |S_{12}|^2 + |S_{13}|^2 &= 1 \\ |S_{12}|^2 + |S_{24}|^2 &= 1 \\ |S_{13}|^2 + |S_{34}|^2 &= 1 \\ |S_{24}|^2 + |S_{34}|^2 &= 1 \end{aligned}$$

implying that  $|S_{13}| = |S_{24}|$ , and  $|S_{12}| = |S_{34}|$ .

We may choose the reference phases such that  $S_{12} = S_{34} = \alpha$ ,  $S_{13} = \beta e^{j\theta}$ ,  $S_{24} = \beta e^{j\phi}$ . Note that:

$$\alpha^2 + \beta^2 = 1$$

Taking the dot product of rows 2 and 3 we have:

$$S_{12}^* S_{13} + S_{24}^* S_{34} = 0$$

from which

$$\theta + \phi = \pi \pm 2n\pi$$

and we find two common choices:

For the symmetrical coupler  $\theta = \phi = \pi/2$ , and

$$[S] = \begin{bmatrix} 0 & \alpha & j\beta & 0 \\ \alpha & 0 & 0 & j\beta \\ j\beta & 0 & 0 & \alpha \\ 0 & j\beta & \alpha & 0 \end{bmatrix}$$

For the antisymmetrical coupler  $\theta = 0$ ,  $\phi = \pi$ , and

$$[S] = \begin{bmatrix} 0 & \alpha & \beta & 0 \\ \alpha & 0 & 0 & -\beta \\ \beta & 0 & 0 & \alpha \\ 0 & -\beta & \alpha & 0 \end{bmatrix}$$

Power supplied to port 1 is coupled to port 3 with a coupling factor  $|S_{13}|^2 = \beta^2$ . The coupling factor is the fraction of the input power which is coupled to the output port:

Coupling (dB) =  $C = 10 \log (P_1/P_3) = -20 \log \beta$   
the remainder is delivered to port 2  $|S_{12}|^2 = \alpha^2 = 1 - \beta^2$ .

In an ideal coupler no power arrives at port 4 (the isolated port), and the isolation measures the fraction of the incident power to the power at the isolated port:

$$\text{Isolation (dB)} = I = 10 \log (P_1/P_4) = -20 \log |S_{14}|$$

The directivity is a measure of the coupled power to the power at the isolated port:

$$\text{Directivity (dB)} = D = 10 \log (P_3/P_4) = 20 \log (\beta/|S_{14}|)$$

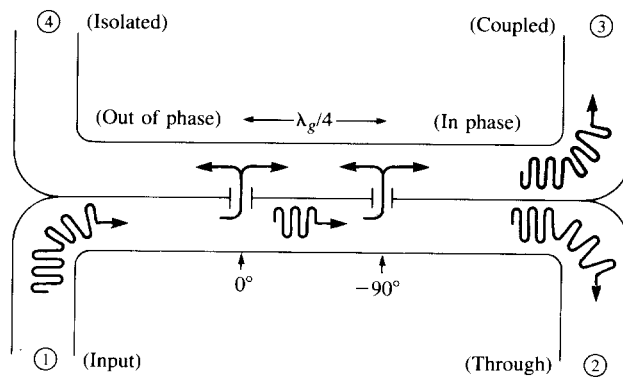
The isolation, directivity, and coupling are related by

$$I = D + C \quad (\text{dB})$$

Ideally, both isolation and directivity are infinite.

Couplers are readily made in many different forms. In waveguide they are often found as single-hole, multi-hole, and branch-line couplers. In stripline and microstrip they are often found as branch-line and coupled-line configurations.

The operation of multihole waveguide couplers can be understood from the following diagram.



Apertures between the waveguide broad walls are spaced by  $\lambda/4$ , most of the power input at port 1 travels to port 2 but some power is coupled through the apertures. As the wave travels along the through-guide it excites forward and backward waves at each aperture. If the reference phase at the first hole is  $0^\circ$ , the phase of the incident wave at the second aperture is  $-90^\circ$ . The forward waves are in phase, but the backward waves are  $180^\circ$  out-of-phase and cancel, thus port 4 is isolated from port 1 and port 3 is coupled by a factor dependent on the dimensions and spacing of the apertures.

Coupling through the apertures may be described by small-hole (or Bethe) coupling in terms of electric and magnetic polarizabilities. Clearly the isolation and directivity are sensitive to frequency, but the coupling is less sensitive.

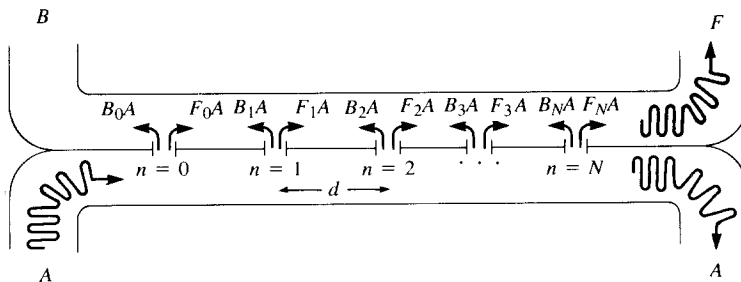


If we assume that the coupling is small and the incident wave is the same amplitude at each aperture, then the amplitude of the forward and backward waves can be written

$$= Ae^{-j\beta Nd} \sum_{n=0}^N f_n$$

$$B = A \sum_{n=0}^N b_n e^{-2j\beta nd}$$

where  $f_n$  is the forward coupling coefficient of the  $n$ th aperture, and  $b_n$  is the backward coupling coefficient of the  $n$ th aperture. These coupling coefficients are proportional to the polarizabilities of the apertures, and are functions of frequency.

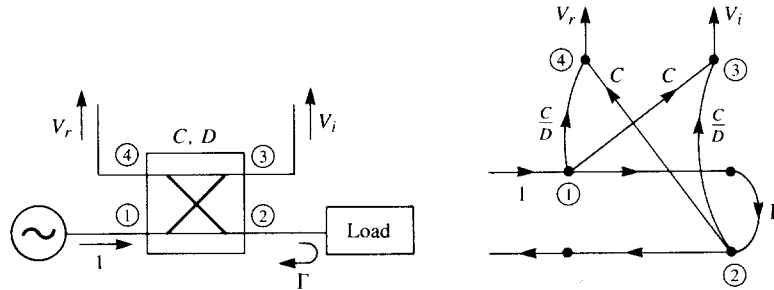


The coupling and directivity are:

$$C = -20 \log |F/A| = 20 \log \left| \sum_{n=0}^N f_n \right|$$

$$D = 20 \log |F/B| = 20 \log \left| \frac{\sum_{n=0}^N f_n}{\sum_{n=0}^N b_n e^{-2j\beta nd}} \right|$$

A common component in network analyzers is the reflectometer, which uses a directional coupler to separate samples of forward and reflected signals.



For a unit incident wave from the source, and a load reflection coefficient of  $\Gamma$  the "incident" port will receive a signal of amplitude

$$V_i = \beta + \frac{\beta}{d} \Gamma e^{j\theta}$$

and the "reflected" port will receive

$$V_r = \frac{\beta}{d} + \beta \Gamma e^{j\phi}$$

where  $\beta$  is the (linear) coupling factor and  $d = \beta/|S_{14}|$  the (linear) directivity,  $\theta$  and  $\phi$  unknown phase delays through the coupler. The maximum and minimum values of F and R are then

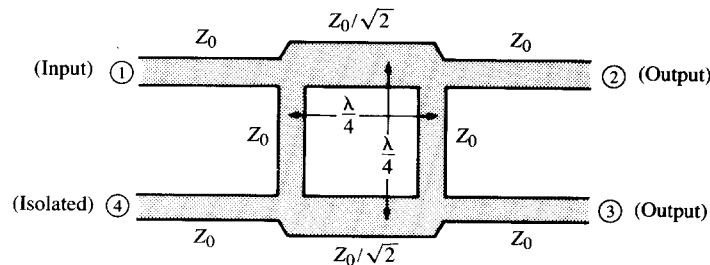
$$\frac{|V_r|}{|V_i|_{\max}} = \frac{|\Gamma| \pm \frac{1}{d}}{1 \mp \frac{|\Gamma|}{d}}$$

leading to an uncertainty of approximately  $\pm(1 + |\Gamma|)/d$ . Thus it can be seen that good directivity is required for accurate measurements, preferably  $d > 100$  ( $D > 40$  dB)

## Hybrids

Hybrids are 3 dB directional couplers with a phase difference between the output arms of either  $90^\circ$  (quadrature hybrid) or  $180^\circ$ . Hybrids are also useful as signal combiners.

A typical  $90^\circ$  hybrid is the branch-line design shown here, although other types of couplers can be used as quadrature hybrids.



The  $[S]$  matrix has the form

$$[S] = \frac{-1}{\sqrt{2}} \begin{bmatrix} 0 & j & 1 & 0 \\ j & 0 & 0 & 1 \\ 1 & 0 & 0 & j \\ 0 & 1 & j & 0 \end{bmatrix}$$

and power input at port 1 is evenly divided between ports 2 and 3, with a  $90^\circ$  phase shift between these ports. Note the symmetrical properties of the devices, and the isolation between the output ports.

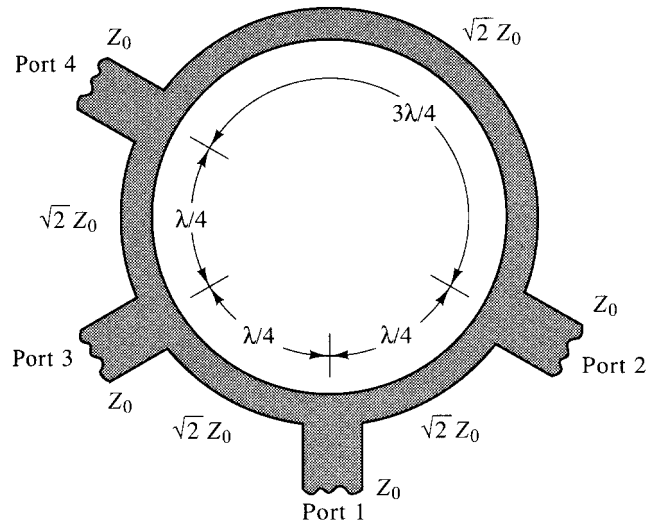
The  $180^\circ$  hybrid has an  $[S]$  matrix of the form

$$[S] = \frac{-j}{\sqrt{2}} \begin{bmatrix} 0 & 1 & 1 & 0 \\ 1 & 0 & 0 & -1 \\ 1 & 0 & 0 & 1 \\ 0 & -1 & 1 & 0 \end{bmatrix}$$

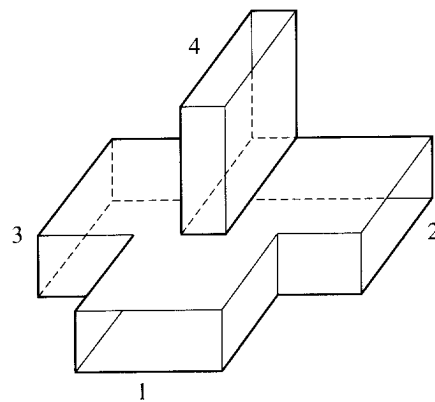
and can also be operated so that the outputs are in phase. A signal input at port 1 will be evenly split into two in-phase components at ports 2 and 3, port 4 is isolated. Applying the input signal to port 4 yields two equal components  $180^\circ$  out of phase at ports 3 and 2, and port 1 is isolated.

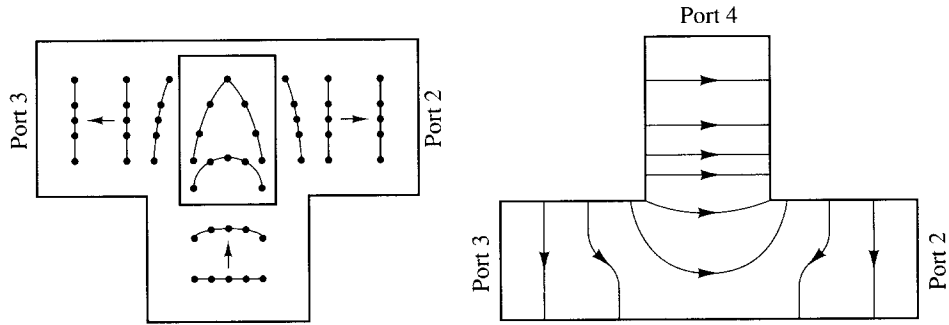
Applying two input signals to ports 2 and 3 yields the sum of the signals at port 1, and the difference at port 4. For this reason ports 1 and 4 are referred to as the sum and difference ports respectively. A common type of  $180^\circ$  hybrid is the ring or rat-race hybrid shown. Waveguide magic-T junctions are also  $180^\circ$  hybrids.

### Ring hybrid



### Waveguide magic-T



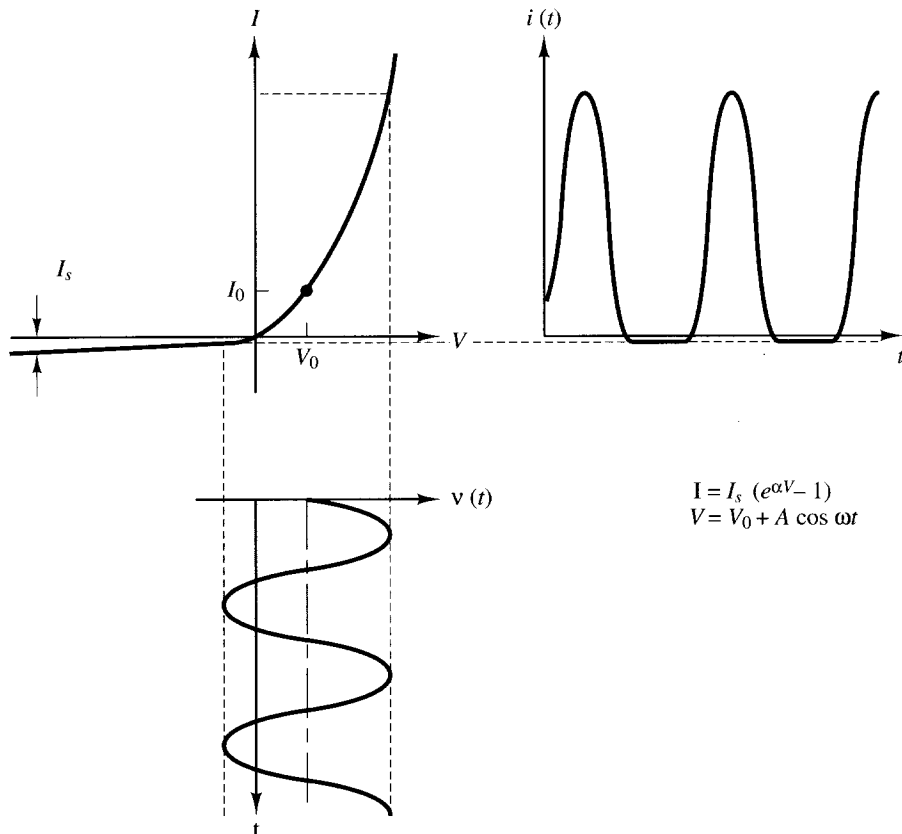


## Diode detectors

The DC voltage-current characteristic of a diode may be written:

$$I(v) = I_s(e^{\alpha V} - 1)$$

where  $I_s$  is the reverse saturation current,  $\alpha = \frac{q_{\text{electron}}}{nkT}$ , and  $n$  is the ideality factor (close to unity), such that  $\alpha \approx 1/25 \text{ mV}^{-1}$ .



If  $V = V_0 + v$ , where  $v$  is a small AC voltage and  $v \ll V_0$ , then a Taylor series expansion about  $V_0$  may be written:

$$I(V) = I_0 + v \left( \frac{dI}{dV} \right)_{V_0} + \frac{1}{2} v^2 \left( \frac{d^2 I}{dV^2} \right)_{V_0} + \dots$$

where  $I_0 = I(V_0)$  is the DC bias current. The first derivative is:

$$\left( \frac{dI}{dV} \right)_{V_0} = \alpha I_s e^{\alpha V_0} = \alpha (I_0 + I_s) = G_d = \frac{1}{R_j}$$

$R_j$  is the diode junction resistance and  $G_d$  the dynamic conductance of the diode. The second derivative is:

$$\left( \frac{d^2 I}{dV^2} \right)_{V_0} = \left( \frac{dG_d}{dV} \right)_{V_0} = \alpha^2 I_s e^{\alpha V_0} = \alpha^2 (I_0 + I_s) = \alpha G_d = G'_d$$

The expansion in  $I(V)$  may be written

$$I(V) = I_0 + i = I_0 + v G_d + \frac{v^2}{2} G'_d + \dots$$

If the diode voltage consists of a DC bias and a small RF voltage

$$V = V_0 + v_0 \cos \omega_0 t$$

then taking the first three terms of the expansion in  $I$

$$I(V) = I_0 + v_0 G_d \cos \omega_0 t + \frac{v_0^2}{2} G'_d \cos^2 \omega_0 t$$

using  $2 \cos^2 x = \cos 2x + 1$  we get

$$I(V) = I_0 + \frac{v_0^2}{4} G'_d + v_0 G_d \cos \omega_0 t + \frac{v_0^2}{4} G'_d \cos 2\omega_0 t$$

$I_0$  is the DC bias current, and  $\frac{v_0^2}{4} G'_d$  is the DC rectified current. Note that the output also contains AC signals at the original frequency and higher harmonics. These may be filtered out with a low-pass filter.

When used as a detector, the nonlinearity of the diode is used to demodulate and RF carrier. The diode voltage can be written as:

$$v = v_0 (1 + m \cos \omega_m t) \cos \omega_0 t$$

where  $m$  is the modulation index,  $\omega_m$  is the modulation frequency and  $\omega_m \ll \omega_0$ . The diode current is then:

$$i(t) = v_0 G_d \left[ (1 + m \cos \omega_m t) \cos \omega_0 t + \frac{v_0^2}{2} G_d' (1 + m \cos \omega_m t)^2 \cos^2 \omega_0 t \right]$$

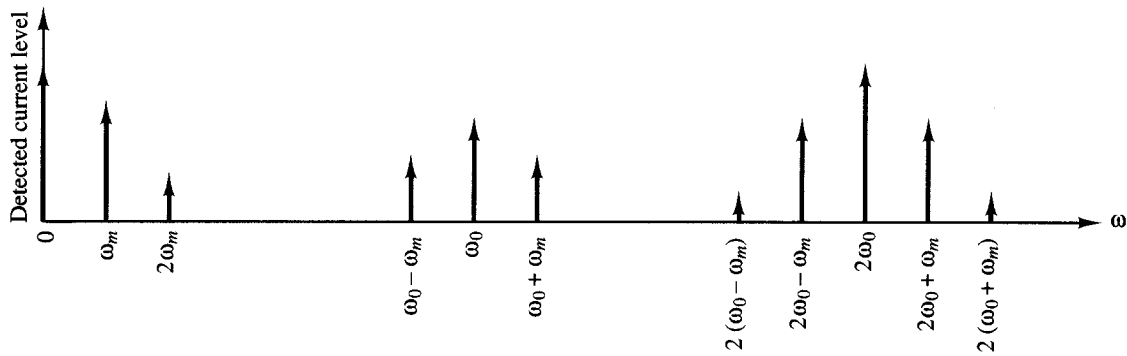
$$i(t) = v_0 G_d \left[ \cos \omega_0 t + \frac{m}{2} \sin (\omega_0 + \omega_m) t + \frac{m}{2} \sin (\omega_0 - \omega_m) t \right]$$

$$+ v_0^2 G_d' \left[ 1 + \frac{m^2}{2} + 2m \cos \omega_m t + \frac{m^2}{2} \cos 2\omega_m t + \cos 2\omega_0 t \right.$$

$$+ m \sin (2\omega_0 + \omega_m) t + m \sin (2\omega_0 - \omega_m) t + \frac{m^2}{2} \cos 2\omega_0 t$$

$$\left. + \frac{m^2}{4} \sin 2(\omega_0 + \omega_m) t + \frac{m^2}{4} \sin 2(\omega_0 - \omega_m) t \right]$$

The output current terms contain components which are linear in diode voltage, occurring at frequencies  $\omega_0$  and  $\omega_0 \pm \omega_m$ , and components at other frequencies including the modulation frequency  $\omega_m$  which are proportional to the square of the input signal. This **square-law** region is the usual operating condition for detector diodes.

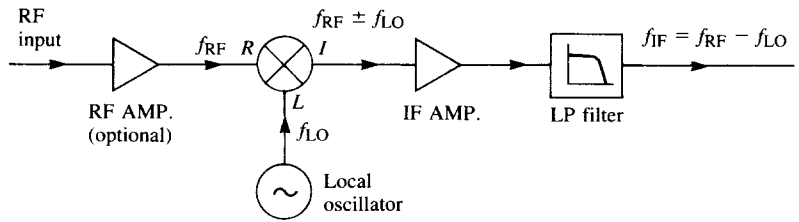


## Mixers

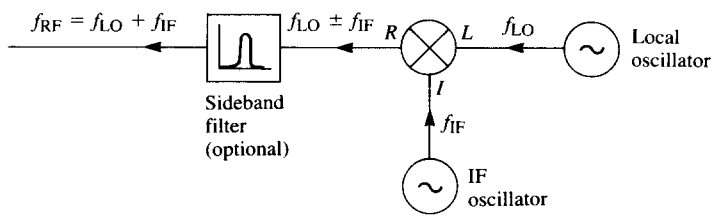
A mixer uses the non-linearity of a diode (or diodes) to generate output at the sum and difference frequencies of two input signals. In **heterodyne** receiver applications the mixer translates the incoming RF signal to a lower intermediate frequency, where gain can be implemented with a low-noise amplifier before detection occurs. This scheme improves receiver sensitivity and noise characteristics compared to the direct detection with a diode. A mixer may also be used to offset a signal, for example in a transmitter.

The desired mixer output signals are the sum and difference frequency terms of the diodes (generally one term is required, the other is filtered out)

$$V_{out} \approx k V_{signal} V_{LO} [\cos(\omega_{LO} - \omega_{signal})t - \cos(\omega_{LO} + \omega_{signal})t]$$



(a)



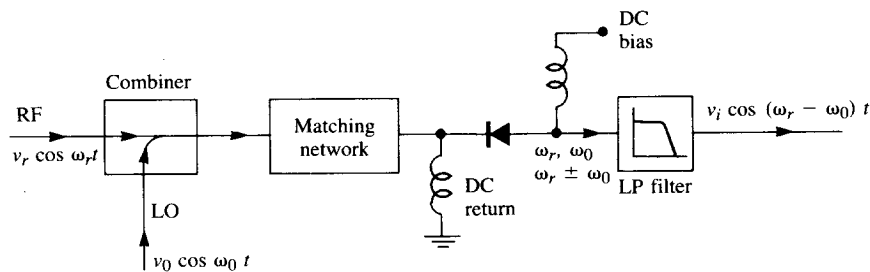


Mixer design involves the matching of the three ports, which is complicated by having to work over several frequencies and their harmonics. An important figure of merit for a mixer is the **conversion loss,  $L_c$** :

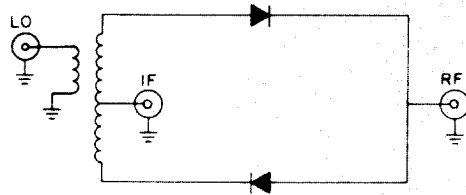
$$L_c = 10 \log \frac{\text{available RF input power}}{\text{IF output power}} \text{ (dB)}$$

$L_c$  is generally between 4 and 7 dB. Other important characteristics include isolation between the ports, input power levels, and harmonic distortion.

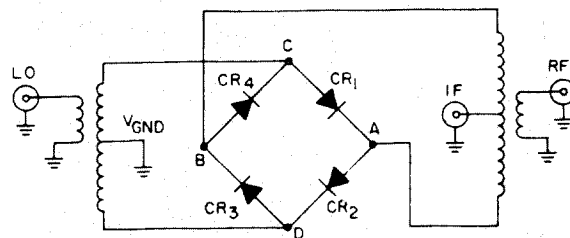
The simplest mixer is the single-ended mixer, which uses one diode and provides reasonable performance:



A single-balanced mixer improves input SWR and isolation between RF and LO:



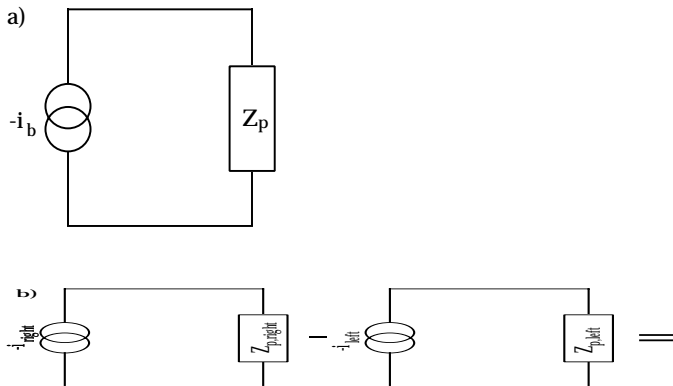
A commonly used design is the double-balanced mixer, which suppresses even harmonics of the LO and RF signals, leading to a very low conversion loss. It has excellent isolation but the input SWR is poor.



# Beam Signals

## *General Approach*

Consider a beam pickup modeled as a simple circuit



The response of the circuit to a current  $I$  is the convolution of the current with impulse response of the circuit.

$$V(t) = \int_{-\infty}^{\infty} dt' i(t') W_p(t - t')$$

In the frequency domain, the convolution becomes a product

$$V(\omega) = \tilde{i}(\omega) Z_p(\omega)$$

Strategy: derive the beam signal in time and frequency domain and either convolve or multiply with PU response.

## Single Particle Current

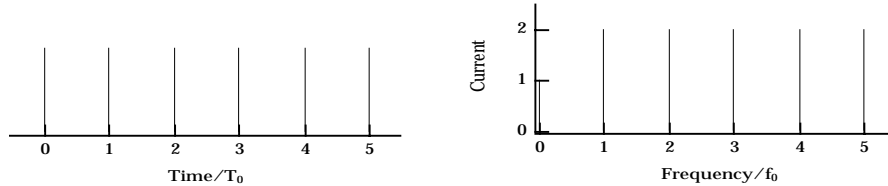
Consider a point particle going around a storage with revolution period  $T_0$  and rotation frequency  $f_0=1/T_0$ . The current at a fixed point in the ring is given by

$$\begin{aligned} i(t) &= e \sum_{n=-\infty}^{n=+\infty} \delta(t-nT_0) = e \omega_0 \sum_n e^{jn\omega_0 t} \\ &= e f_0 + 2e f_0 \sum \cos(n\omega_0 t) \end{aligned}$$

The FT of this given by

$$I(\omega) = e \omega_0 \sum_k \delta(\omega - k\omega_0)$$

The spectrum is a comb with signal only at the rotation harmonics



(Negative frequency components can be folded onto positive frequency. AC components are 2X DC component.)

Allow the particle to make synchrotron oscillations with angular frequency  $\omega_s$  of amplitude (in time) of  $\tau_s$

$$i(t) = e \sum_n \delta(t - nT_0 + \tau_s \cos(\omega_s t))$$

The FT of this signal is given by

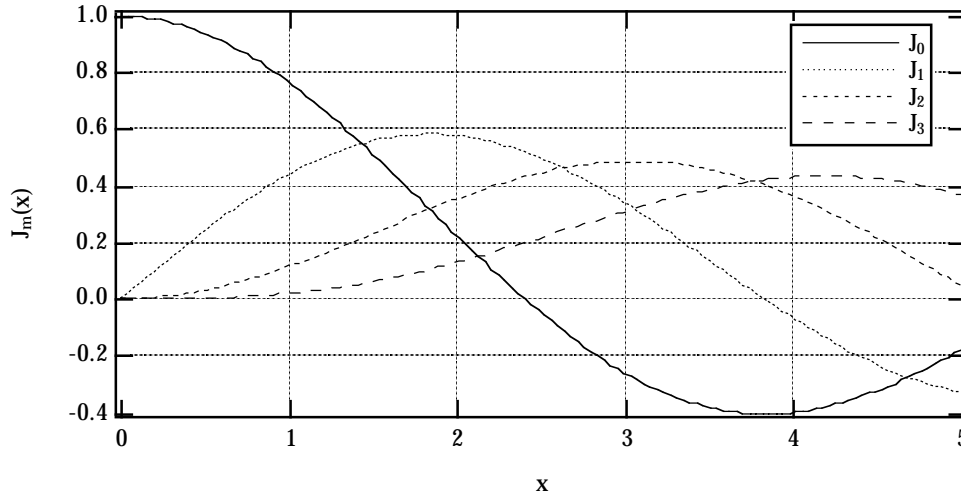
$$\begin{aligned} I(\omega) &= e \omega_0 \sum_n e^{-jn\omega_0(t + \tau_s \cos \omega_s t)} \\ &= e \omega_0 \sum_m j^{-m} J_m(\omega \tau_s) \sum_k \delta(\omega + m\omega_s - k\omega_0) \end{aligned}$$

where the relation

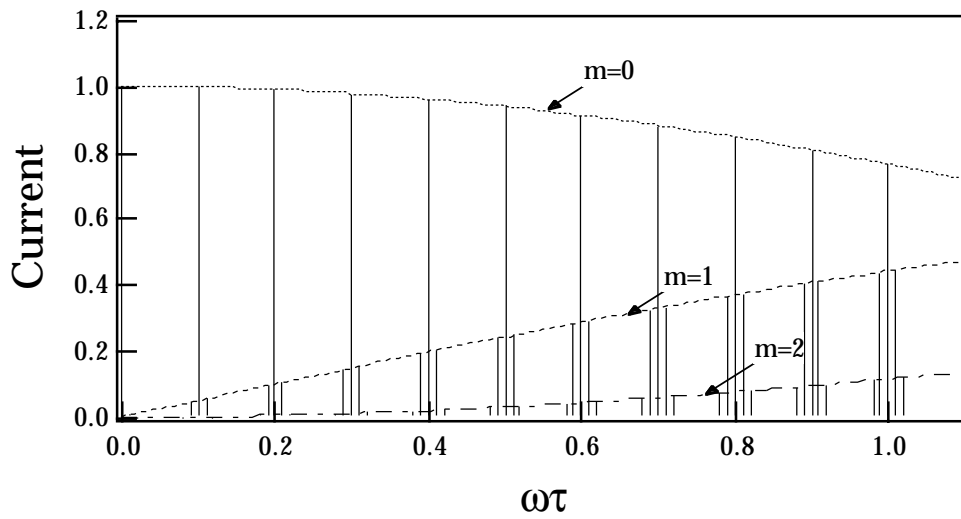
$$e^{jx \cos \theta} = \sum_m j^m J_m(x) e^{jm\theta}$$

has been used.

The comb spectrum has added FM sidebands which are contained within Bessel function envelopes.



Rotation harmonics follow  $J_0$ , first order sidebands follow  $J_1$ , etc.



Note that the rotation harmonics disappear at the zeros of  $J_0(\omega\tau)$ .

## Single Particle Dipole Signal

The dipole signal at a fixed point is the  $d(t)=x(t)*i(t)$

For an offset  $X_0$  and betatron oscillation amplitude  $x_\beta$ , the dipole signal is (no synch oscillations)

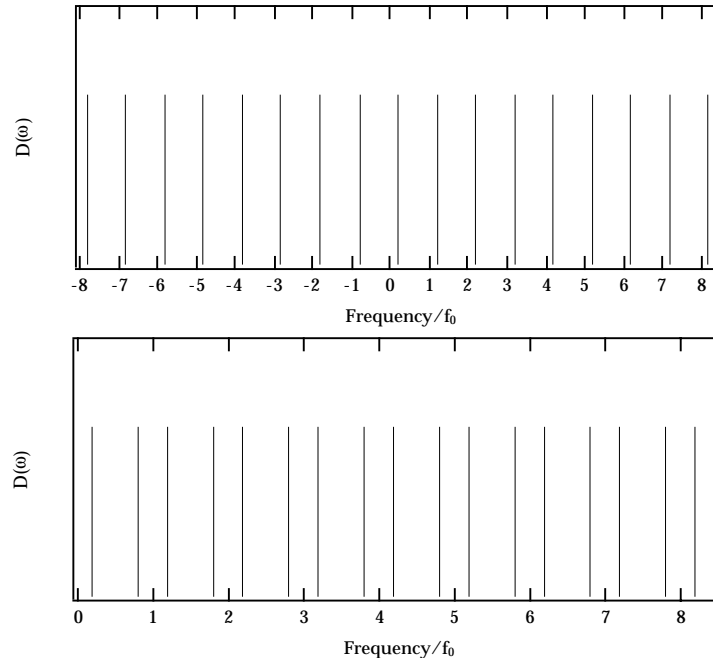
$$d(t)=e(X_0+x_\beta \cos(\omega_\beta t)) \sum_n \delta(t-nT_0)$$

where  $\omega_\beta=Q_\beta\omega_0$  is the betatron angular frequency.

The frequency spectrum is given by

$$D(\omega)=e \omega_0 X_0 \sum_k \delta(\omega-k\omega_0) + e \omega_0 x_\beta \sum_k \delta(\omega-(\omega_\beta+k\omega_0))$$

The result is a comb spectrum at rotation harmonics with betatron sidebands. (Negative frequencies fold over to become lower sidebands in this form.)



The integer part  $Q_\beta$  of cannot be determined from this measurement.

Allow the particle to also make synchrotron oscillations

$$d(t) = e(X_0 + x_\beta \cos(\omega_\beta t) + \eta \delta \sin(\omega_s t)) \sum_{n=-\infty}^{n=+\infty} \delta(t - nT_0 + \tau_s \cos(\omega_s t))$$

where the additional AM comes from dispersion ( $\eta$ ) at the measurement point and PM from the longitudinal oscillations.

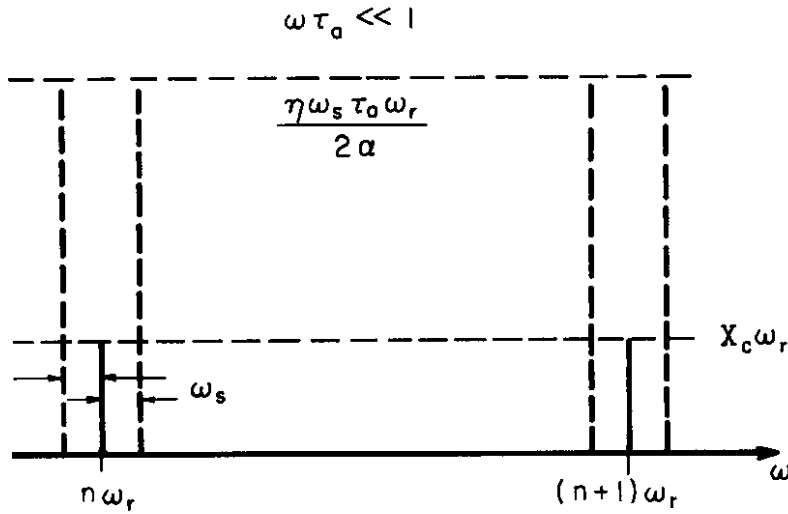
The contribution to the frequency spectrum of this signal is similar to the current signal and is

$$D_{\text{coe}}(\omega) = e \omega_0 \eta \delta \sum_{\mathbf{m}} j^{-\mathbf{m}} J_{\mathbf{m}}(\omega \tau_s) \sum_{\mathbf{k}} \delta(\omega + \mathbf{m} \omega_s - \mathbf{k} \omega_0)$$

The contribution from the energy oscillations is given by

$$D_\delta(\omega) = e \omega_0 X_0 \sum_{\mathbf{m}} j^{-\mathbf{m}} J_{\mathbf{m}}((\omega - \omega_s) \tau_s) \sum_{\mathbf{k}} \delta(\omega + \mathbf{m} \omega_s - (\mathbf{k} + 1) \omega_0) - \sum_{\mathbf{m}} j^{-\mathbf{m}} J_{\mathbf{m}}((\omega + \omega_s) \tau_s) \sum_{\mathbf{k}} \delta(\omega + \mathbf{m} \omega_s - (\mathbf{k} - 1) \omega_0)$$

The spectrum becomes a combination of AM and PM sidebands. These signals are visible at much lower frequency compared to PM signals.



Chromaticity complicates the signal even further. The betatron tune is given by

$$Q_\beta = Q_{\beta 0}(1 + \xi\delta)$$

where the chromaticity is defined as

$$\xi = \frac{dQ/Q}{dE/E}$$

The rate of change of the betatron phase is given by

$$\frac{d\psi_\beta}{dt} = Q_{\beta 0}(1 + \xi\delta)\omega_0(1 - \dot{\tau}) \approx \omega_{\beta 0}(1 + \dot{\tau}) + \omega_\xi \dot{\tau}$$

( $\delta(t) = \frac{1}{\alpha} \dot{\tau}(t)$  and  $\omega_\xi \equiv \omega_{\beta 0} \xi / \alpha$  is called the chromatic frequency.)

The instantaneous betatron phase is given by

$$\psi_\beta = \omega_{\beta 0} t + (\omega_\xi - \omega_{\beta 0}) \tau_s \cos(\omega_s t)$$

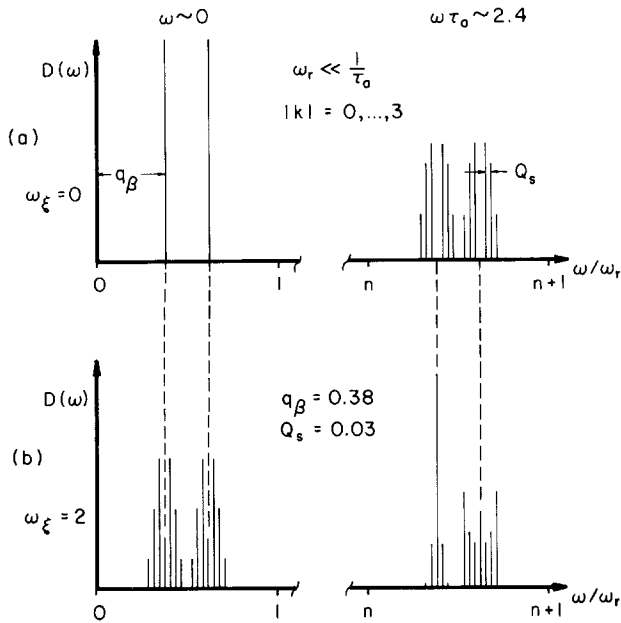
The dipole signal is given by (ignoring c.o.e. and dispersion)

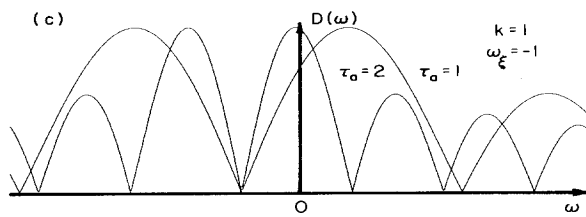
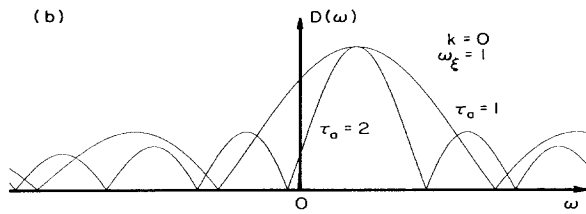
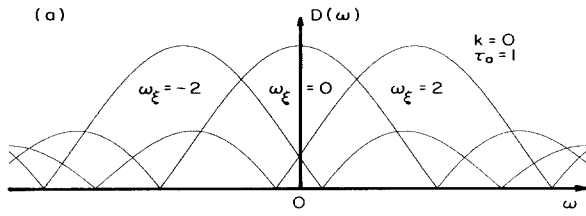
$$d(t) = e x_\beta \cos(\psi_\beta) \sum_n \delta(t - nT_0 + \tau_s \cos(\omega_s t))$$

The FT of this signal is

$$D_\xi(\omega) = e \omega_0 x_\beta \sum_m j^{-m} J_m((\omega - \omega_\beta + \omega_\xi) \tau_s) \sum_k \delta(\omega - (k\omega_0 + \omega_\beta - m\omega_s))$$

This gives the betatron sidebands synchrotron sidebands following a Bessel function envelope.







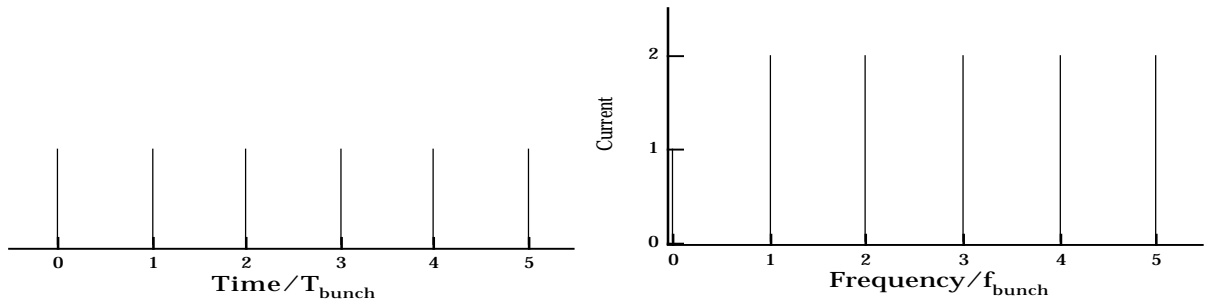
## Multibunch Signals

For the case of multiple bunches in a storage ring, the current at a given point is just the single particle current summed over many bunches

$$i(t) = e \sum_{m=1}^N \sum_n \delta(t - nT_0 - T_m) = e \sum_{m=1}^N \sum_n e^{jn\omega_0 t} e^{jn\omega_0 T_m}$$

where  $T_m$  is the arrival time of bunch  $m$ .

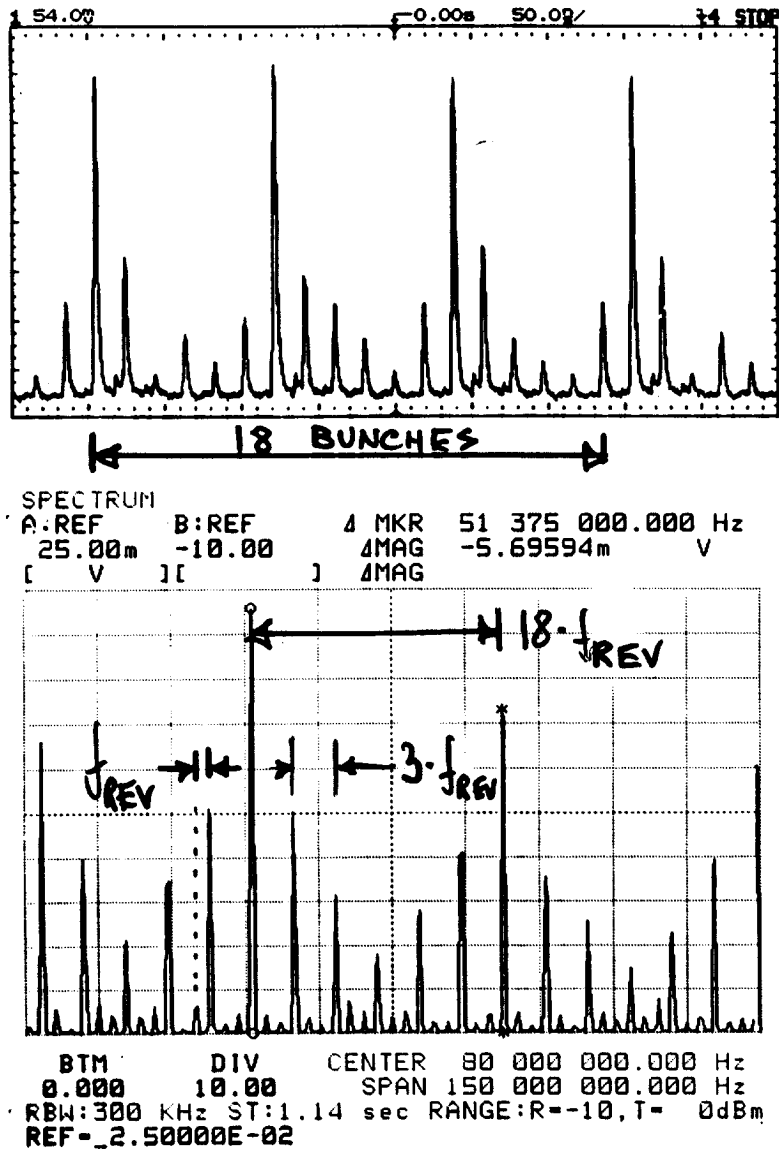
For the case of a symmetric fill pattern (equal bunch charges with equal spacing), the signal is a periodic delta function with a repetition frequency of the bunch rate. All of the signal goes into the bunch harmonics.



The signal is identical to the single bunch except the repetition period is  $T_0/N_{\text{bunch}}$  and thus the spacing of the comb spectrum is  $N_{\text{bunch}}f_0$ . All intermediate rotation harmonics disappear. For every bucket filled, this implies that the first current harmonic appears at the RF frequency and other harmonics at multiples of the RF frequency.

For asymmetric fill patterns, (i.e. unequal bunch charges and/or unequal spacing), the signal leaks into the rotation harmonics between bunch harmonics.

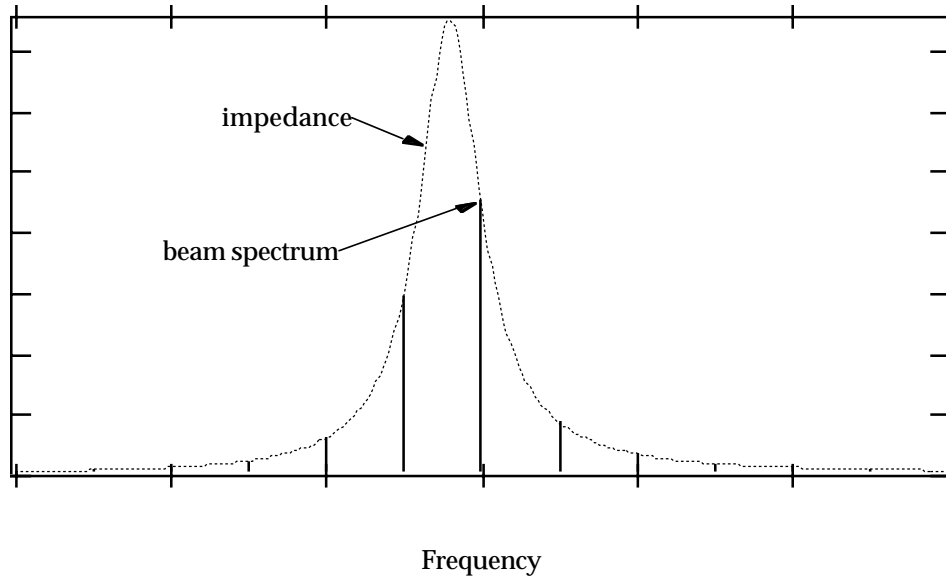
Example:



Asymmetric fill pattern at ADONE. The upper plot shows the time domain signal of the fill pattern of 18 bunches. The lower plot is the frequency spectrum which shows intermediate rotation harmonics reflecting the time domain bunch pattern. (Courtesy of M. Serio.)

## Beam Induced Signals

Given a particular fill pattern or bunch spectrum, how do we calculate the signal induced in a RF cavity or a pickup? If the cavity or pickup represent a beam impedance  $Z_{||}(\omega)$ , (with a corresponding impulse response  $W(t)$ ), the total signal out is a convolution of the input with the response. In the frequency domain, this is just a multiplication of the beam spectrum with the impedance.



The beam induced voltage is given by

$$V(\omega) = I(\omega) Z_{||}(\omega)$$

or in the time domain

$$V(t) = \frac{1}{2\pi} \sum_{n=0}^{\infty} I(n\omega_0) Z_{||}(n\omega_0) e^{jn\omega_0 t}$$

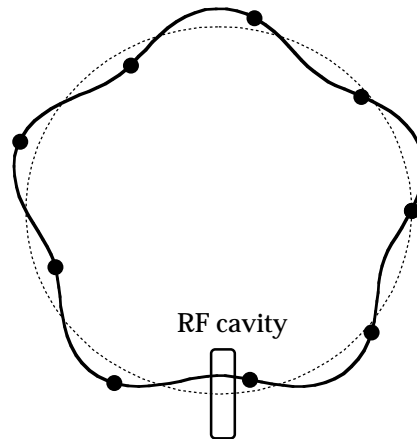
The power dissipated in the impedance is

$$P = \left(\frac{1}{2\pi}\right)^2 \sum_0^{\infty} |I(n\omega_0)|^2 Z_{||}(n\omega_0)$$

This approach can be applied to any impedance: cavity fundamental or HOM, pickup, etc.

## *Coupled Bunch Oscillations*

Wakefields which last from bunch to bunch can couple the oscillations of the the bunches. Under certain conditions, the coupled oscillation can resonate with the cavity mode and grow exponentially and destroy the beam quality (or even the beam!) Coupled bunch (CB) oscillations also have distinct signals in the frequency domain which can be useful for diagnosis.

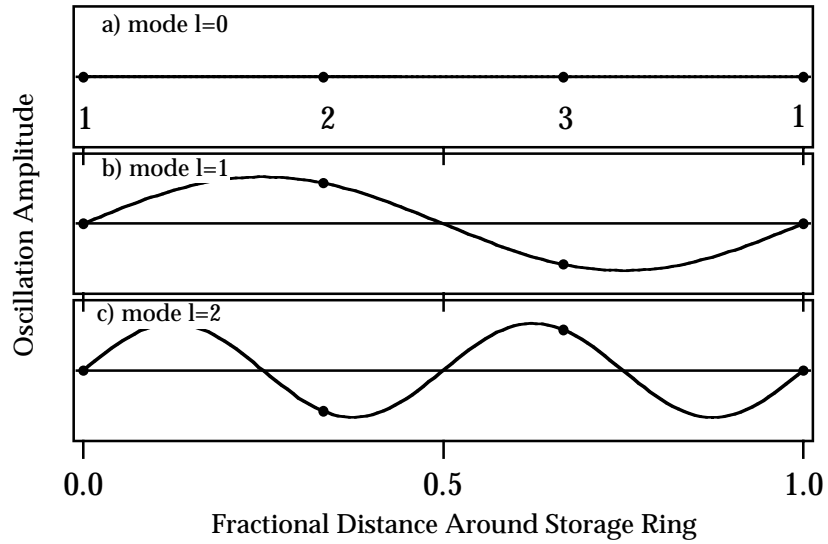


**A coherent coupled bunch oscillation created by coupled through and RF cavity.**

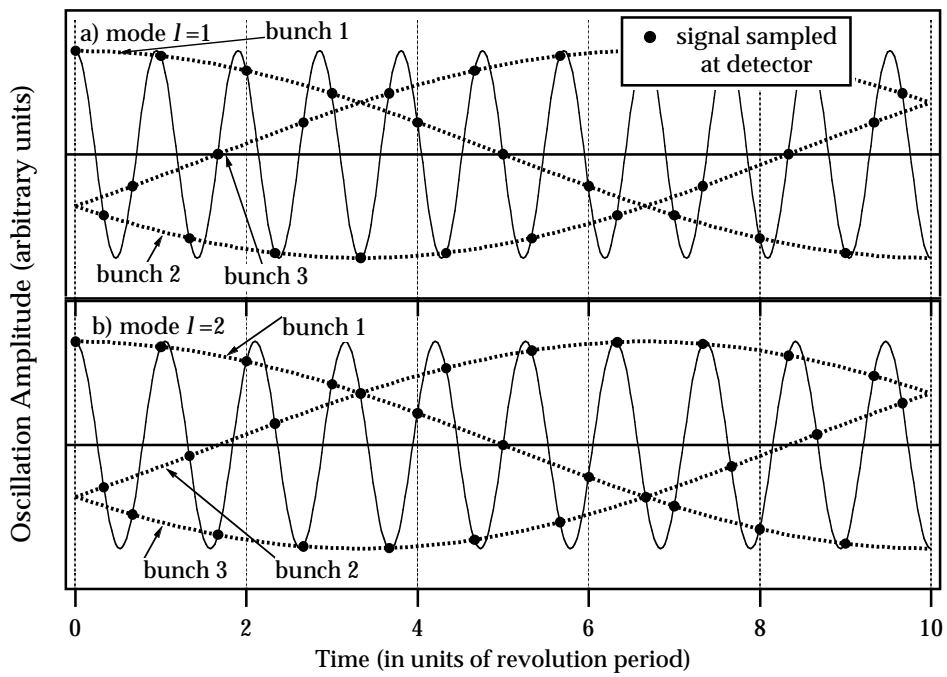
For the case of a symmetric bunch pattern, the normal modes of oscillation can be described by the relative phase of oscillation of the individual bunches. For N bunches, the relative phase of consecutive bunches in mode l is given by

$$\Delta\phi = \frac{2\pi l}{N}$$

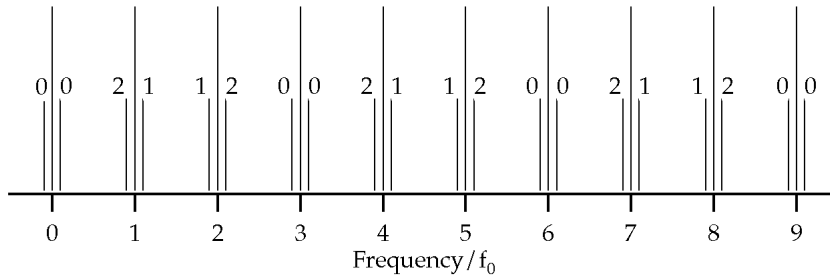
For example, the case of 3 bunches is shown below. The figure illustrates a snapshot picture of the relative phase of the three bunches for each normal mode.



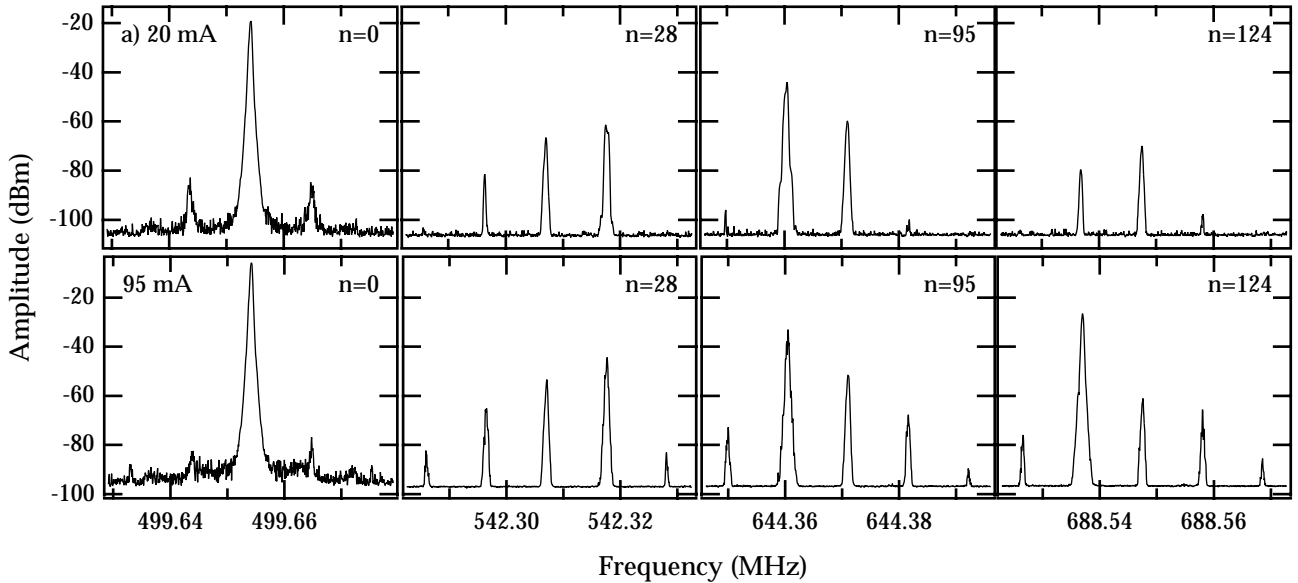
The signal observed at a single point in the ring for each bunch is shown below. Although each bunch oscillates at the synchrotron frequency, the frequency of the mode is much higher.



The signal for the coupled bunch oscillations in the frequency domain appears as sidebands of rotation harmonics as shown below.



Below is some raw spectra of a BPM sum signal from the ALS showing coupled bunch oscillations. The measurement was made with 328 bunches (all RF buckets) filled as equally as possible. The number of rotation harmonics from the RF frequency is given in each graph. The upper graph was measured at 20 mA and the lower at 95 mA.

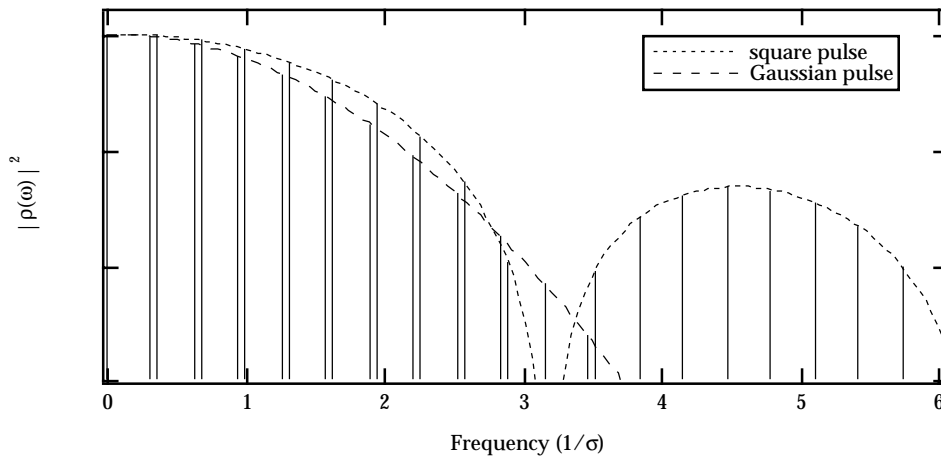


The relatively small signals at the intermediate rotation harmonics come from a small variation in the individual bunch charges. The amplitude of each CB mode is found from the ratio of the sideband to the bunch harmonic and not the intermediate rotation harmonics.

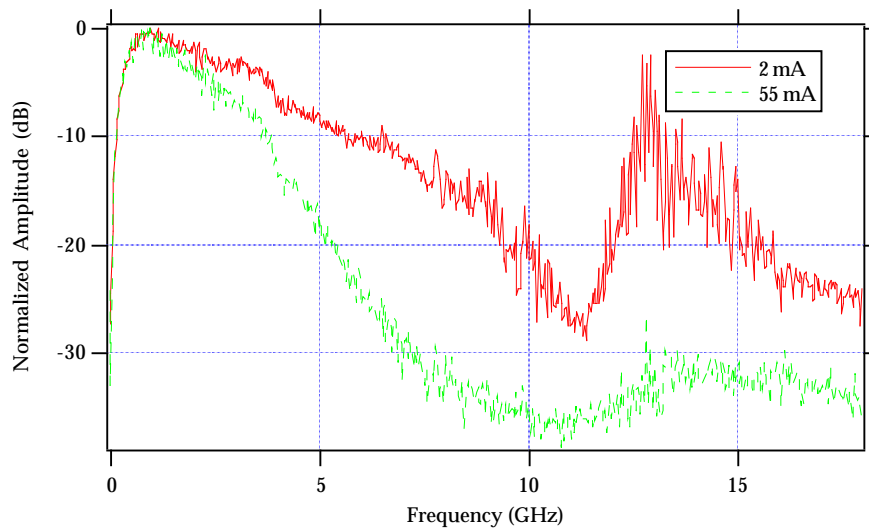
## Single Bunch Spectra

So far the bunch has been treated as a point particle. Real bunches have a longitudinal distribution of charge,  $\rho(t)$ . The frequency spectrum of a stored bunch is given by the convolution of the bunch distribution with the signal from a point particle. This gives the frequency spectrum as the product of the FTs of the distribution and and the point particle signal.

$$I(\omega) = e \omega_0 \tilde{\rho}(\omega) \sum_k \delta(\omega - k\omega_0)$$



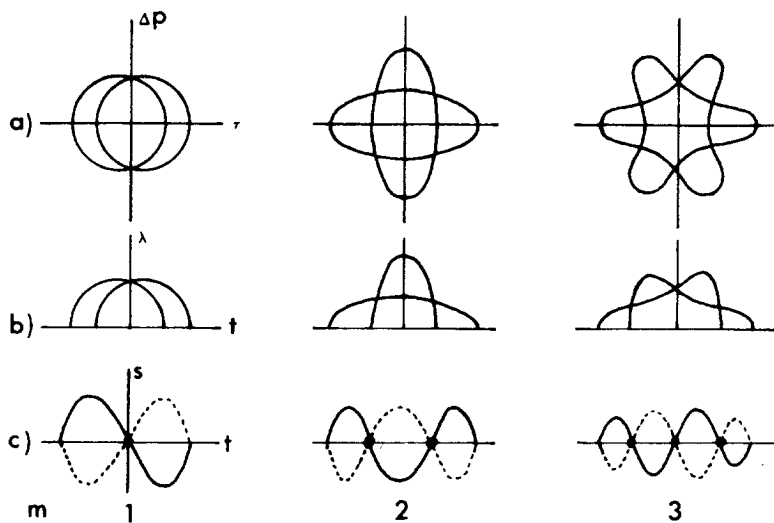
Below are some examples of broadband measurements on the ALS. The actual spectra is not Gaussian because of the frequency response of the button BPM used. The bunch has lengthened significantly at 55 mA shown by a narrowing of the frequency spectrum.



## Single Bunch Oscillations

### Longitudinal

So far the bunch has been treated as either a point particle or a rigid distribution of charge. However, short range wakefields generated by bunches with a lot of charge can have a significant effect on the stability of motion within the bunch. The standard approach is to describe the intrabunch motion in terms of normal modes. Shown below is a representation of the first three normal modes. The upper plot shows the relative phase space distribution and the lower shows the corresponding line density.



Representation of first three longitudinal bunch modes. a) Phase space picture. b) Linear charge density. c) Deviation of linear charge density from stationary charge density.

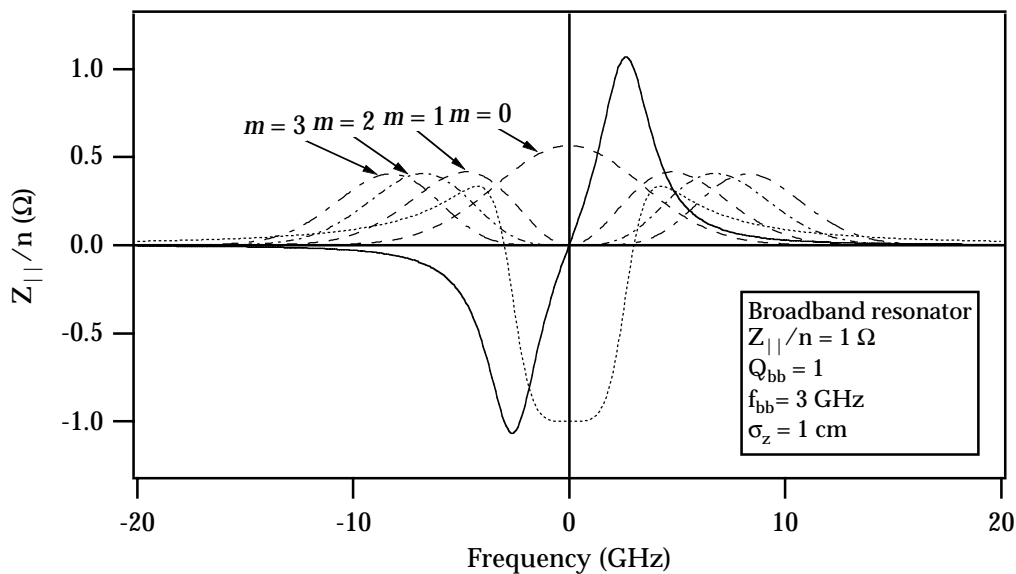
From the symmetry of the phase space distribution, it can be seen that each mode appears to oscillate in time with a frequency of  $m\omega_s$  and appear as upper and lower sidebands of rotation harmonics.



## Frequency Spectra of Bunch Motion

From the difference signal seen in part c) of the previous figure, the frequency spectrum of the signal from each mode peaks at  $\sim 1/\text{wavelength}$  of the signal, given by  $f_{\text{peak}} = (m+1)/2\tau_l$ , where  $\tau_l$  is the bunch length. The signal extends over a bandwidth of  $2\pi/\tau_l$ .

For a Gaussian bunch, small perturbations to the distribution have been shown to be described by a series of Hermitian eigenmodes shown below.



Envelope of the frequency spectrum of first three longitudinal bunch modes (including the stationary distribution) for a Gaussian bunch of rms length 1 cm. The mode spectra are superimposed over an arbitrary broadband impedance to illustrate the different overlap.

## *Head Tail Oscillations*

The transverse motion of the bunch is bit more complicated than the longitudinal motion because the longitudinal position within the bunch can influence the transverse motion.

Consider a bunch of two particles.



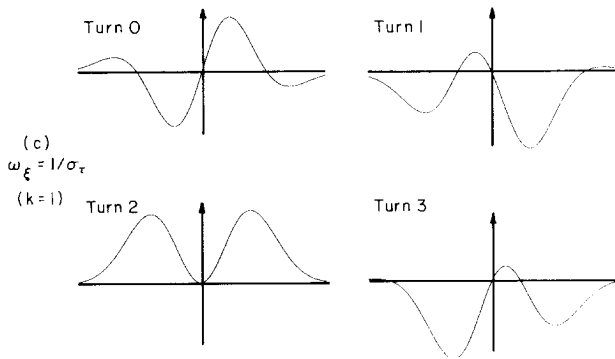
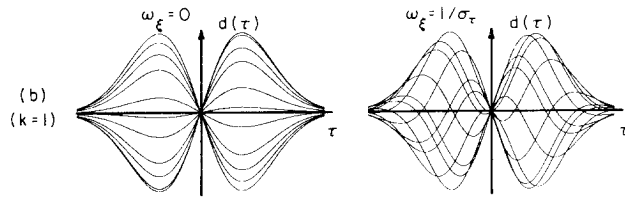
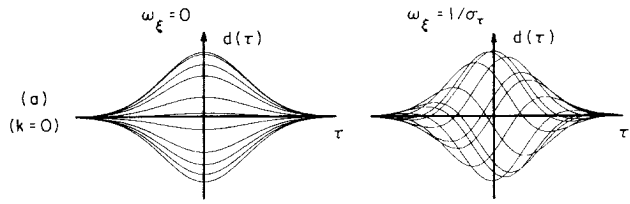
Over the first half the synchrotron period, the head drives the tail. During the second half, the particles switch places and the former tail drives the former head. In this sense the synchrotron oscillations provide a natural damping mechanism.

For real bunches, the motion is broken down in normal modes as shown below.

As in the longitudinal case, the higher modes of motion occur at increasingly higher frequencies.

The situation is more complex with presence of chromaticity (dependence of the betatron tune on energy.)

\



## *Schottky Signals*

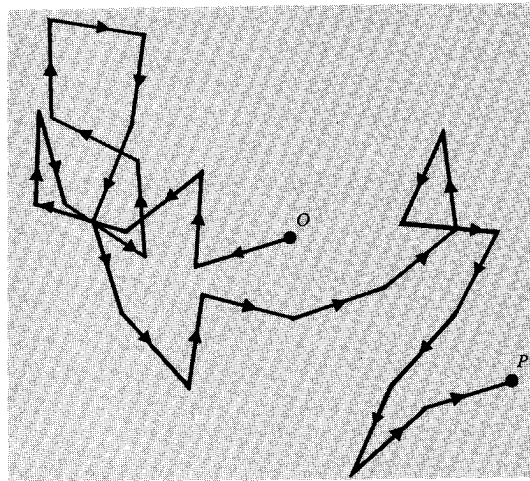
### Coasting Beam

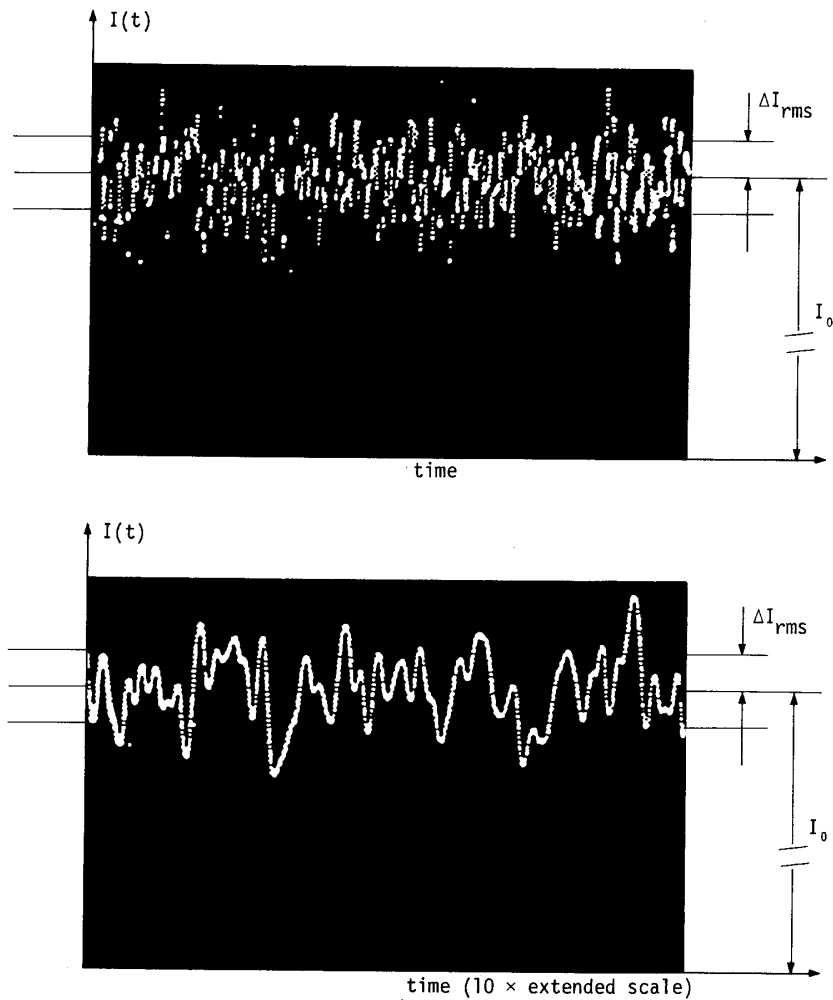
A coasting beam is one in which no RF acceleration is applied. It usually has no RF structure imposed on the beam and is somewhat uniformly spread around the ring.

For a perfectly uniform beam of  $N$  particles, the current signal would be a comb spaced by  $Nf_0$  because the phase of the signals from individual particles don't add coherently at intermediate rotation harmonics. For large  $N$ , the frequency of the first harmonic would be too large to observe with any reasonable detector and the only signal measurable is the DC current (assuming you have a DC current monitor!)

However, real coasting beams are not perfectly uniform. The relative phases of the signals are randomly distributed. Consider the signals of individual particles as steps in a random walk. The rms amplitude of the signal will be (on average) proportional to

$$\sqrt{N}$$





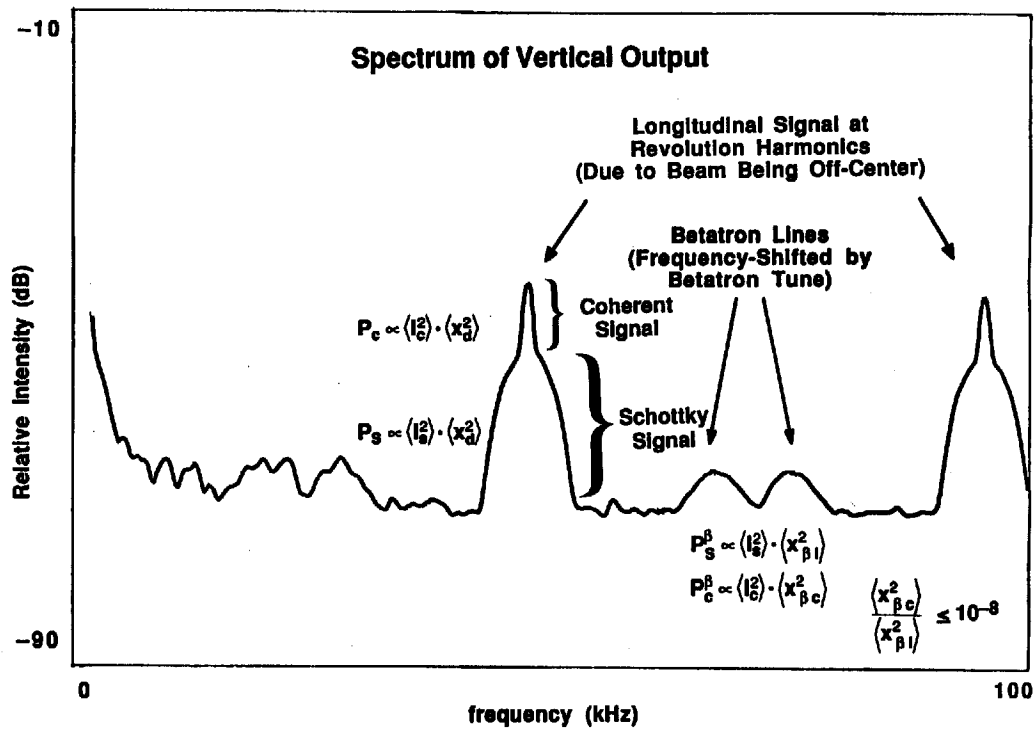
The pickup current from a coasting beam shows a DC component and an AC component from the random fluctuations in the current. (From D. Mohl, CERN 84-15)

The frequency spectrum of the signal is also strongly dependent on the energy spread of the beam because of the energy dependence of the rotation frequency on the energy.

Stochastic cooling systems are simply feedback systems which try to reduce the random fluctuations of the beam by slightly reorganizing the distribution of particles.

# Bunched Beam

The Schottky signals of a bunched beam are very similar to those of a coasting beam. However, it is much more difficult in practice to observe the signals because of the large coherent signal already present on the beam from the bunching. The presence of the coherent signal requires electronics with a large dynamic range while retaining low S/N.

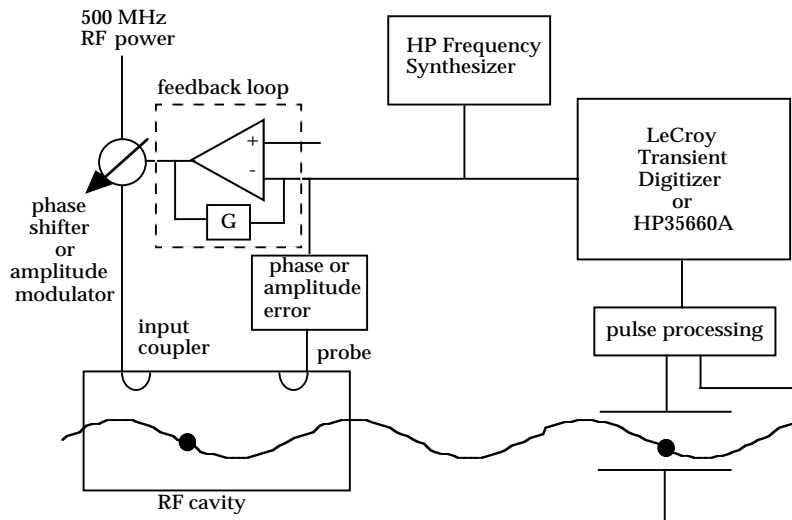


Bunched beam Schottky spectrum taken at Fermilab using a transverse cavity detector. (Courtesy D. Goldberg)

## *Beam Transfer Functions*

All of the beam signals we've mentioned so far are observed with a passive detector. Another important class of beam signals are observed via a beam transfer function.

The idea is to drive beam oscillations and measure the amplitude and phase response. This setup is typically used for betatron tune measurements on a spectrum analyzer with a tracking generator. The information in a BTF can also be measured by pinging the beam (i.e. impulse response=transfer function.)

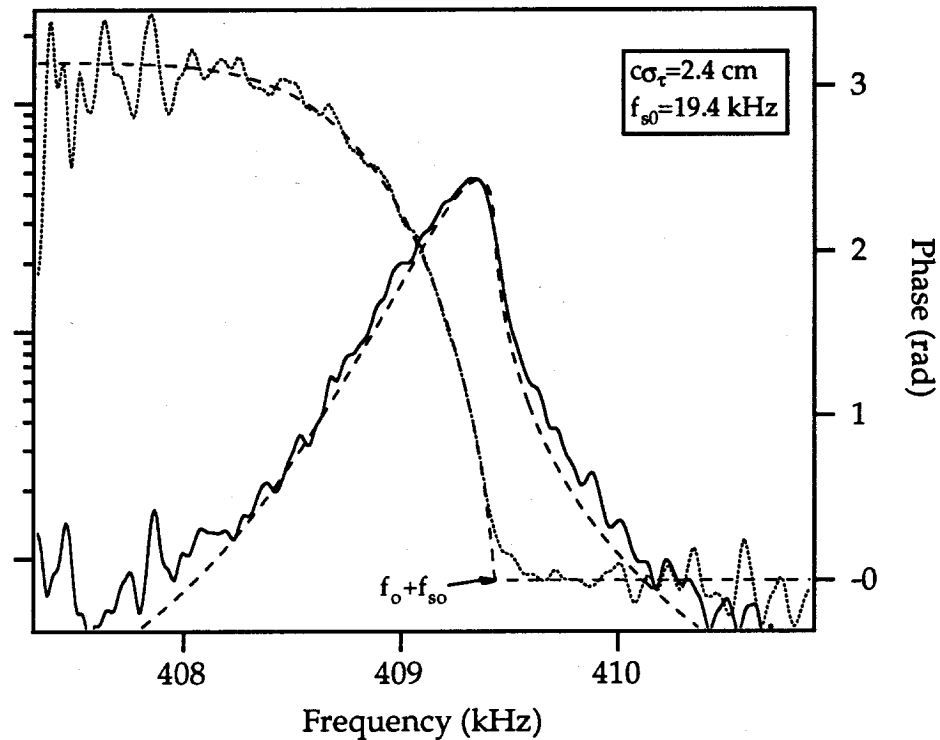


Setup for a BTF measurement using phase modulation of the RF cavity to drive longitudinal oscillations.

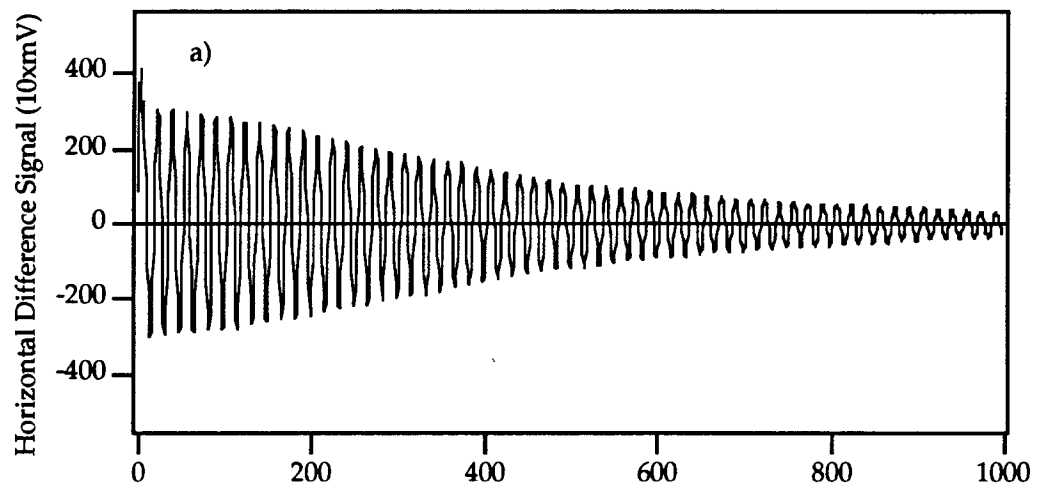
BTF measurements are useful for

- sensitive tune measurements
- beam impedance/instability measurements
- bunch length measurements
- FB system characterization

## Examples



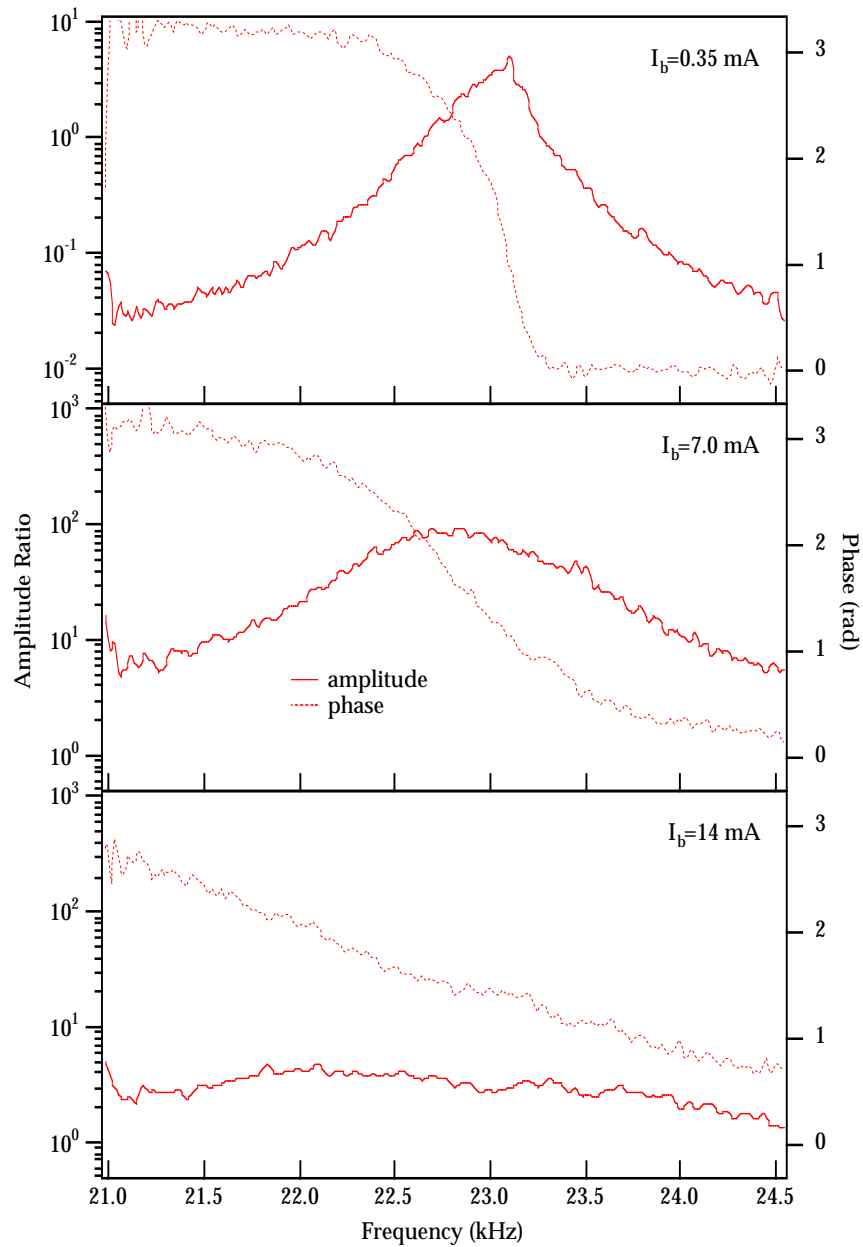
Longitudinal BTF measured at CESR at low bunch current. The dashed curve is the calculated response for a bunch length of 2.4 cm.



Longitudinal impulse response of a single bunch measured at CESR. The FT transform of this signal is equivalent to the BTF shown above.



## More Examples



BTF measurement of the longitudinal coupled bunch mode showing the effect of Robinson damping.

# RF Cavities

## *Introduction:*

RF cavities are useful in accelerators for interacting with beams of particles in order to supply energy for acceleration, extract information (energy) in the form of a pick-up or modulate the energy of particles as a kicker. These interactions are generally characterized by coupling impedances in the longitudinal and transverse planes.

## *Simple equivalent circuit, transmission-line analogy:*

The generalized transmission-line formulation shown in figure 1 describes any guided transmission medium in terms of a capacitance and inductance per unit length with a series resistance and shunt admittance to account for losses,

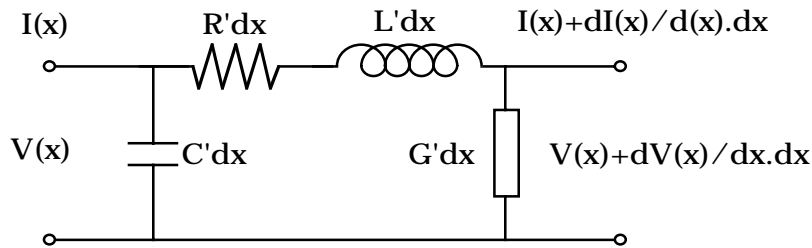


Figure 1: General transmission-line element

Waves in this medium have the general solution:

$$V(x,t) = V_1 e^{-\alpha x} e^{i(\omega t - kx)} + V_2 e^{\alpha x} e^{i(\omega t + kx)}$$

which is a superposition of forward and backward traveling waves of frequency  $\omega$  with attenuation  $\alpha$ . Phase velocity,  $v_p = \omega/k$ , group velocity,  $v_g = \partial\omega/\partial k$  and wavelength  $\lambda = 2\pi/k$ .

Similarly for current:

$$I(x,t) = \frac{V_1}{Z_0} e^{-\alpha x} e^{i(\omega t - kx)} - \frac{V_2}{Z_0} e^{\alpha x} e^{i(\omega t + kx)}$$

where  $Z_0$  is the characteristic impedance of the line:

$$Z_0 = \frac{V_1}{I_1} = -\frac{V_2}{I_2} = \sqrt{\frac{R' + i\omega L'}{G' + i\omega C'}}$$

For the lossless case  $G' = R' = 0$

$$Z_0 = \sqrt{\frac{L'}{C'}}, \alpha = 0, k = \omega\sqrt{L'C'}, \lambda = \frac{2\pi}{\omega\sqrt{L'C'}}, v_p = v_g = \frac{1}{\sqrt{L'C'}}$$

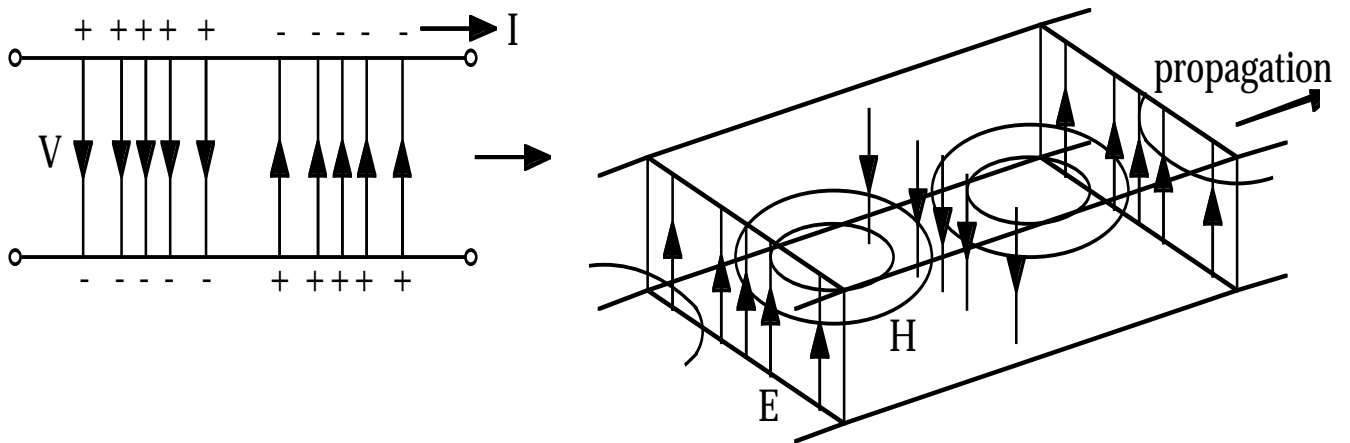
and

$$V(x,t) = V_1 e^{i(\omega t - kx)} + V_2 e^{i(\omega t + kx)}$$

$$I(x,t) = \frac{V_1}{Z_0} e^{i(\omega t - kx)} - \frac{V_2}{Z_0} e^{i(\omega t + kx)}$$

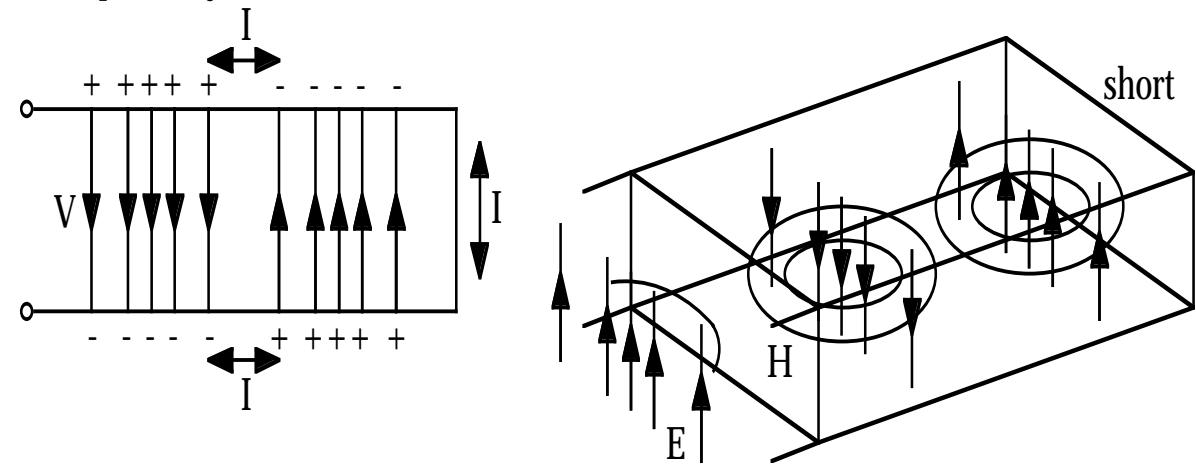
### Traveling wave on a transmission line

Field pattern moves in the direction of propagation, current in phase with voltage.



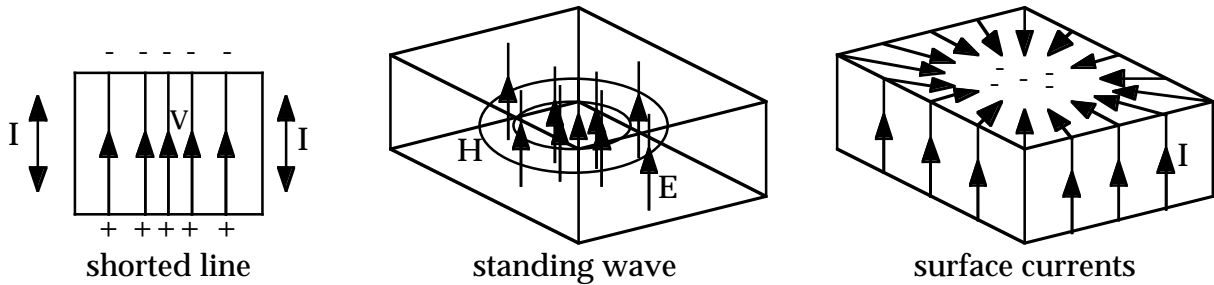
### Reflection from a short circuit:

Superposition of forward and reflected waves gives pure standing wave. Field pattern is stationary with time varying amplitude. Current and voltage are out of phase by  $90^\circ$  ( $\pi/2$  rad.)

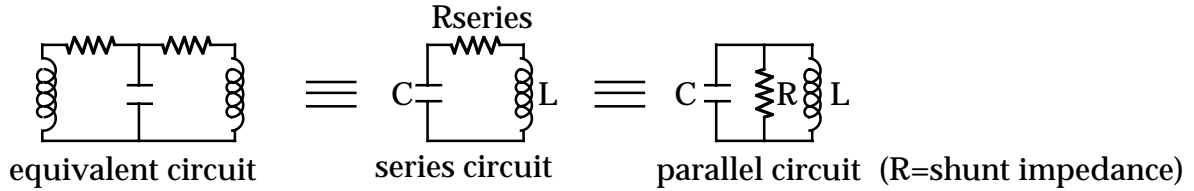


### Standing wave between two shorts:

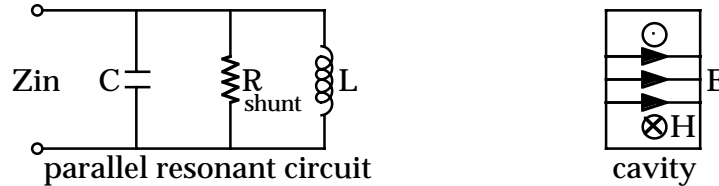
Resonant line between two short circuits is a pure standing wave with an integer number of half-wavelengths.



Shorted line can be represented by a lumped-element equivalent circuit:



**Properties of parallel resonant circuit and real cavity:**



The input impedance of the equivalent circuit can be expressed as:

$$\begin{aligned}
 z_{in} &= \left( \frac{1}{R} + \frac{1}{j\omega L} + j\omega C \right)^{-1} \\
 &= \frac{R}{1 + jQ\left(\frac{\omega}{\omega_0} - \frac{\omega_0}{\omega}\right)} \approx \frac{R}{1 + jQ^2\left(\frac{\delta\omega}{\omega_0}\right)}
 \end{aligned}$$

where  $\omega_0 = \frac{1}{\sqrt{LC}}$  and  $Q = \omega_0 RC$  or  $Q = \frac{R}{\omega_0 L}$  (see homework problem #1).

For a cavity the **shunt impedance**, **R**, is defined in terms of the voltage produced in the cavity for a given power dissipation,  $R = V^2 / 2P$ , where the voltage is considered as the integral of the electric field along the flight path of a particle,  $V = \int \mathbf{E} \cdot d\mathbf{l}$ . N.b.: In some physics texts the shunt impedance is defined as  $R = V^2 / P$  and may or may not include the transit-time factor.

The **quality factor Q** of the cavity or equivalent circuit is a measure of the sharpness of the resonance and also of the enhancement of the voltage and current compared to a simple traveling wave. The Q is defined as the ratio between the stored energy and the power dissipation per radian or  $Q = \omega U / P$

The ratio **R/Q** is a figure of merit for the shape of the cavity and is independent of the material and it can be shown also that

$$- = \sqrt{\frac{L}{C}} = \frac{1}{\omega_0 C} = \omega_0 L$$

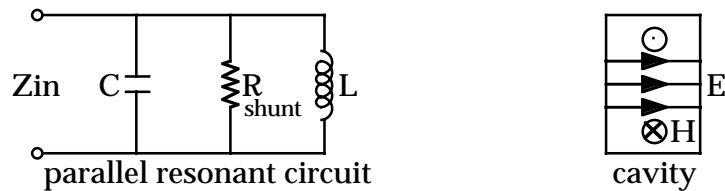
which gives a clue as to how to optimize the cavity shape once the field distributions are known (see section on “real cavities”).

If the time taken for a particle to cross the cavity is a significant fraction of the RF period then the effective voltage seen or induced by the particle is reduced because of the  $\cos(\omega t)$  time dependence of the fields. The factor by which it is reduced is called the **transit-time factor**, **T**, and is defined as the ratio of the energy actually received to that which would be received if the field were constant at the maximum value. The **longitudinal beam impedance**  $Z_{||}$  (sometimes  $R_{||}$ ) is the product of the shunt impedance and the square of the transit-time factor,

$$Z_{||} = RT^2$$

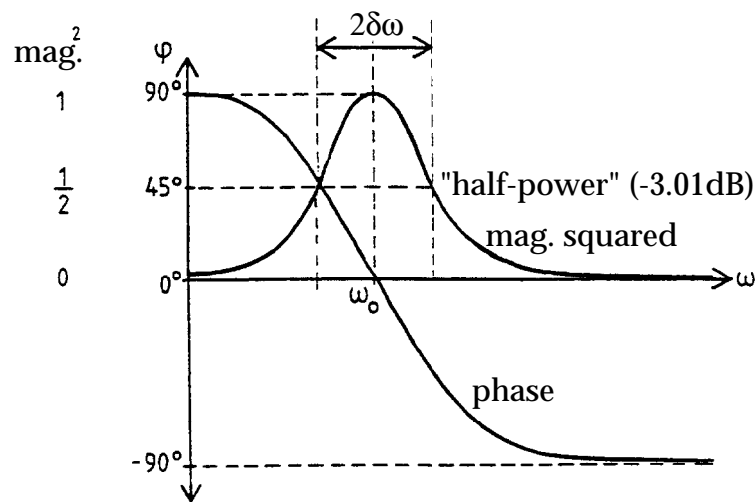
(note: this is different from the impedance of the cavity as a pick-up which is  $RT^2/4$ ).

## Magnitude and phase of parallel circuit and cavity:



The resonant nature of the circuit is clearly seen by looking at the magnitude and phase of the impedance as a function of frequency.

Note that at resonance the impedance is purely resistive and equal to the shunt impedance. Below resonance the impedance is inductive and above resonance it is capacitive. In the cavity there will be other modes with higher resonant frequencies and the impedance will become inductive, resistive and capacitive again for each in turn as the frequency increases.



## Transmission ( $S_{21}$ ) measurement:

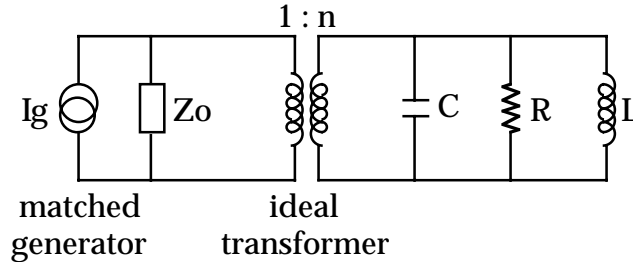
The impedance response can be measured by the transmission between two probes coupled to the cavity. If the probes are weakly coupled then the Q is not changed significantly, otherwise the coupling factor of the probes must be measured and taken into account.

The Q can be measured from the resonance curve by taking the bandwidth at the half-power ( $1/\sqrt{2}$  voltage, or -3.01dB) points.

$$Q = \frac{\omega_0}{2\delta\omega}$$

### Coupling to matched source/load:

To supply energy to the cavity from an external source or extract signal power induced by the beam requires a means of coupling the cavity fields to an external circuit. This can be represented in the equivalent circuit by an idealized transformer of turns ratio 1:n linking the cavity voltage to a transmission line which is matched to an ideal current source representing the generator.



This circuit can be used to transform the cavity impedance into the transmission line to observe the load presented to the generator (fig a) or to transform the generator current and source impedance into the cavity so that the total cavity voltage from generator- and beam-induced currents can be calculated (fig. b).

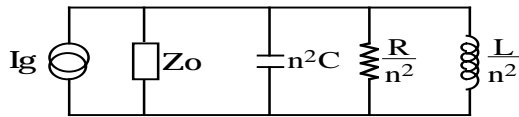


fig. a cavity referred to input

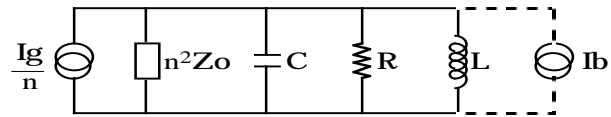


fig. b source referred to cavity

The **coupling factor**  $\beta$  is defined as the ratio of the power loss in the external circuit to that in the cavity. A loaded  $Q$ ,  $Q_L$ , can be defined as the ratio of the stored energy to the total loss per radian, and an external  $Q$ ,  $Q_{ext}$ , can be defined as the ratio of the stored energy to the loss in the external circuit per radian. It can thus be shown that:

$$\beta = \frac{\text{power loss in ext. cct}}{\text{power loss in cavity}} = \frac{Q_o}{Q_{ext}} = \frac{R}{n^2 Z_o}, \quad \frac{1}{Q_L} = \frac{1}{Q_o} + \frac{1}{Q_{ext}}, \quad \text{and } Q_o = (1+\beta)Q_L$$

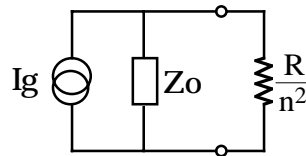
When the cavity is matched to the source at resonance (without beam):

$$\beta = 1, \quad Q_L = \frac{Q_o}{2}, \quad \text{and } n^2 = \frac{R}{Z}$$

### Reflection coefficient looking toward cavity at resonance:

Away from resonance most of the power incident on the cavity is reflected but close to resonance the response may come closer to or go through a matched condition, depending on the coupling. At resonance the resistive impedance  $R$  is

transformed in to the external circuit so the reflection coefficient is simple to calculate:



cavity impedance at resonance referred to input

$$\text{Reflection coefficient } \Gamma = \frac{\frac{R}{n^2} - Z_o}{\frac{R}{n^2} + Z_o} = \frac{\beta - 1}{\beta + 1}$$

$$\text{while } \text{VSWR} = \frac{1+|\Gamma|}{1-|\Gamma|}$$

$$\begin{aligned} \text{so } 0 < \beta < 1 \text{ (under-coupled)} & \quad \text{VSWR} = 1/\beta \\ \beta = 1 \text{ (matched)} & \quad \text{VSWR} = 1 \\ \beta > 1 \text{ (over-coupled)} & \quad \text{VSWR} = \beta \end{aligned}$$

### Measurement of cavity properties from $S_{11}$ :

Provided the losses in the coupler can be neglected\*, the coupling factor  $\beta$ , and the loaded and unloaded  $Q$ 's can be calculated from an accurate measurement of  $S_{11}$  looking towards the cavity. As described above, the coupling factor can be determined from the reflection coefficient at resonance. If the coupling can be adjusted it is often a simple matter to determine whether the system is under- or over- coupled. If the VSWR dips towards unity through the range of adjustment but a match is never achieved then the system is undercoupled (and  $\beta_{\max} = 1/\text{VSWR}_{\min}$ ). If the VSWR goes to 1 then rises to a local maximum the system is overcoupled (and  $\beta_{\max} = \text{local max. VSWR}$ ). With the phase information available on the network analyzer the complex impedance can be plotted on a Smith chart and it is easily determined whether the system is under- or over-coupled. Once the coupling factor is known the value of  $S_{11}$  or the VSWR at the loaded or unloaded half-power points can be calculated, or these points can be found on the Smith chart (once the electrical delay has been adjusted to refer the impedance to the detuned-short position)

For the unloaded half-power points ( $Q_o$ ):

$$|S_{11}| = \sqrt{\frac{5S_o^2 - 2S_o + 1}{S_o^2 - 2S_o + 5}} \qquad \text{VSWR} = \frac{2 + \beta^2 + \sqrt{4 + \beta^4}}{2\beta}$$

---

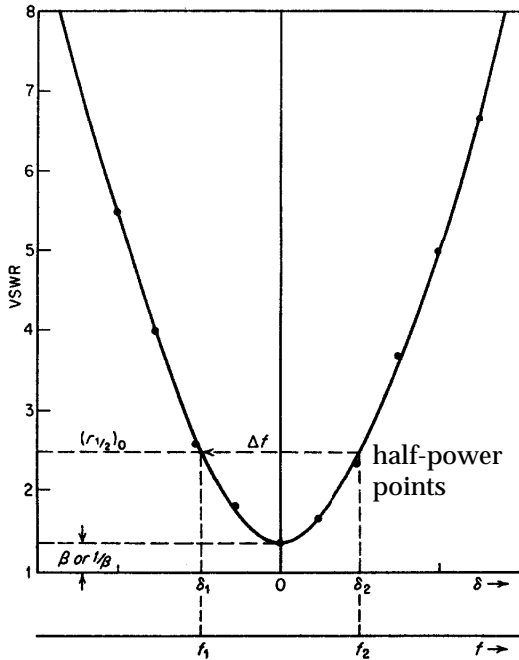
\* the coupler loss and self-inductance are not represented in this simple equivalent circuit



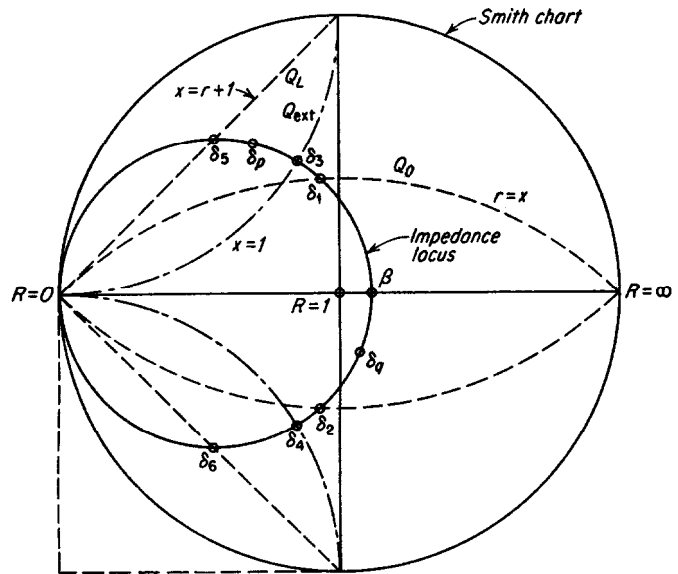
For the loaded half-power points ( $Q_L$ ):

$$|S_{11}| = \sqrt{\frac{S_o+1}{2}}$$

$$SWR = \frac{1+\beta+\beta^2+(1+\beta)\sqrt{1+\beta^2}}{\beta}$$



VSWR close to resonance

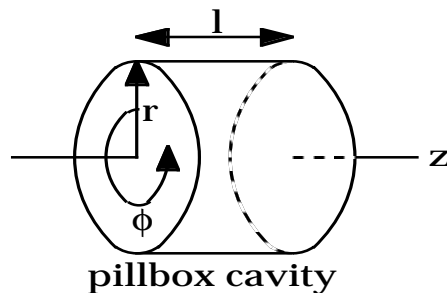


Identification of the half-power points from the Smith chart.

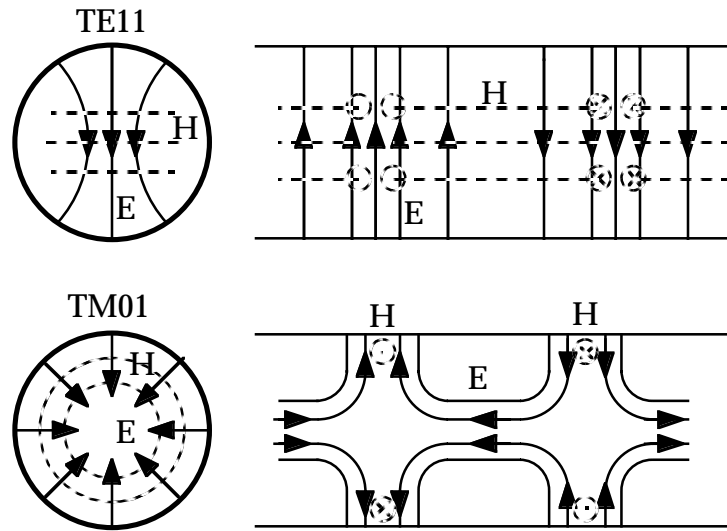
$Q_0$  locus is given by  $X=R$ ;  $Q_L$  by  $X=R+1$ ,  $Q_{ext}$  by  $X=1$

### "Pillbox" cavity modes

The "pillbox" is a simple closed shape for which analytical solutions can be derived for the field and current distributions of the resonant modes. Such a shape could in fact be used as an accelerating structure, however more efficient shapes are usually used in practice. Study of the modes of the pillbox is instructive however and provides much of the nomenclature that is used to describe modes in other axis-symmetric structures.

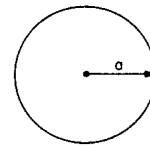
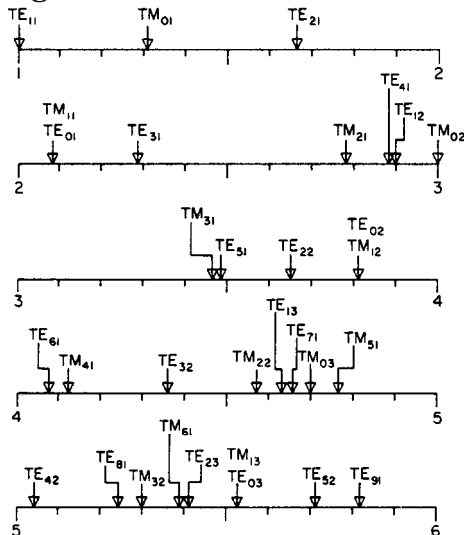


As presented above in the transmission-line analogy, cavity modes can be thought of as resonances between two short circuit planes in a waveguide. In the case of the pillbox this is a length of circular waveguide with a short-circuit boundary condition at each end, so the solutions are standing-waves of the TE and TM circular waveguide modes with an integer number of half-wavelengths between the end-plates. The boundary conditions also allow for TM modes with zero variation in the z axis, which are of particular interest for accelerator cavities. The waveguide modes (TE/M<sub>mn</sub>) are denoted by two subscripts, the first is the number of full periods in  $\phi$  and the second is the number of radial zeros in the field. For cavity modes a third subscript is added which is the number of half-period variations in the z direction.



First two modes in circular waveguide

The following chart shows the cut-off frequencies for modes in circular waveguide, normalized to that of the lowest mode (TE<sub>11</sub>).

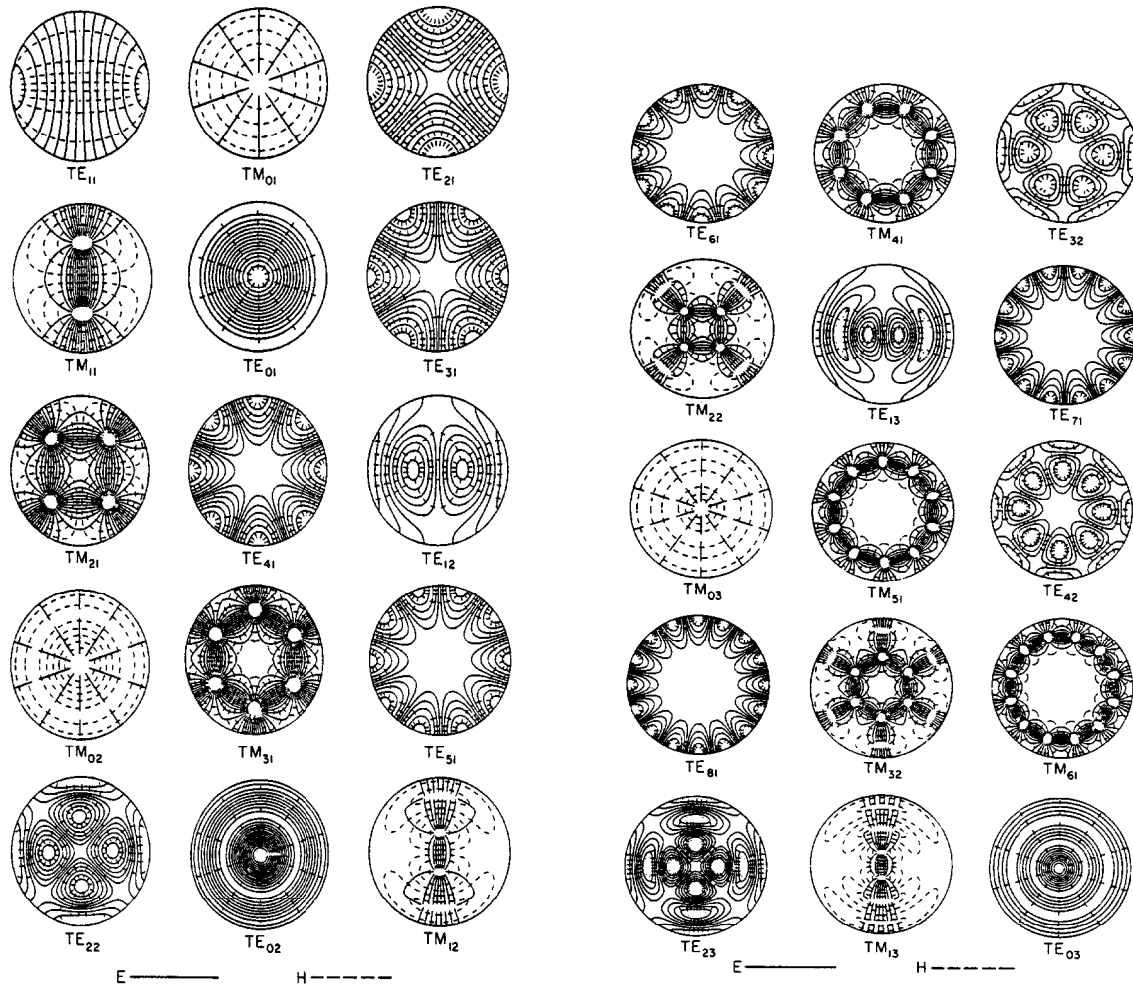


$$k_{\text{TE11}} = \frac{1.841}{a}$$

$$\lambda_{\text{TE11}} = 3.41a$$

$$f_{\text{TE11}} = \frac{0.293}{a\sqrt{\mu\epsilon}}$$

The figures below show plots of the E and H fields for the first thirty modes [Lee et.al., IEEE Trans. MTT, vol. MTT-33, No. 3, March 1985, p 274].



Only those modes with a component of electric field in the direction of motion of the particle can interact with the beam (Panofsky-Wenzel). For the pillbox this means only the TM modes are of interest. The transverse variations of the longitudinal field are solutions of Maxwell's equations within a circular boundary condition and are Bessel functions of the first kind.

$$z(r, \phi) = E_0 J_m(k_{mn} r) \cos m \phi$$

where:  $J_m$  are the first order Bessel functions  
 $k_{mn} = x_{mn}/r$  is the transverse wave number  
 $x_{mn}$  are the roots of the Bessel functions  $J_m$

For modes with  $E_z(z) = \text{constant}$  ( $k_z = 0$ ),  $\omega = ck_{mn}$

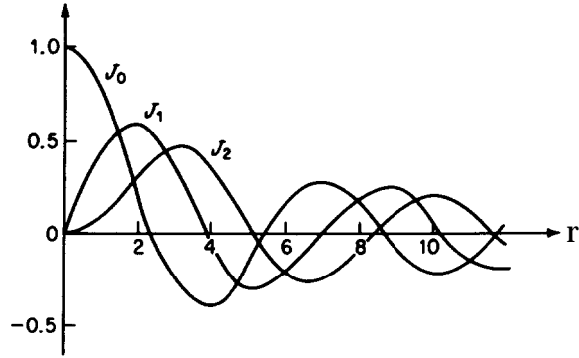
For modes with  $E_z(z) \propto \cos(k_z z)$ , where  $k_z$  is the axial wave number:

$$\omega^2 = k_{mn}^2 + k_z^2 \quad \text{or} \quad \omega_0 = c \sqrt{k_{mn}^2 + k_z^2}$$

For  $TM_{mnz}$  modes the fields are thus:

$$z(r,z,t,\phi) = E_0 J_m\left(\frac{X_{mn}r}{a}\right) e^{j\omega t} \cos(m\phi) \cos(k_z z)$$

$$H_\phi(r,z,t,\phi) = H_0 J'_m\left(\frac{X_{mn}r}{a}\right) e^{j\omega t} \cos(m\phi) \cos(k_z z)$$



Low-order Bessel functions of the first kind

**ZEROS AND ASSOCIATED VALUES OF BESSEL FUNCTIONS AND THEIR DERIVATIVES**

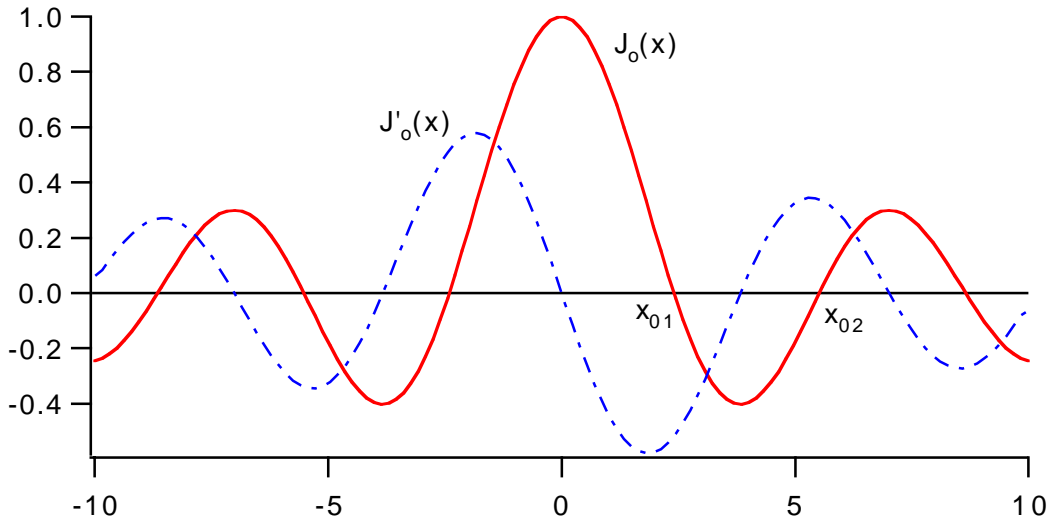
| $s$ | $j_{0,s}$      | $J'_0(j_{0,s})$ | $j_{1,s}$ | $J'_1(j_{1,s})$ | $j_{2,s}$ | $J'_2(j_{2,s})$ |
|-----|----------------|-----------------|-----------|-----------------|-----------|-----------------|
| 1   | 2.40482 55577  | -0.51914 74973  | 3.83171   | -0.40276        | 5.13562   | -0.33967        |
| 2   | 5.52007 81103  | +0.34026 48065  | 7.01559   | +0.30012        | 8.41724   | +0.27138        |
| 3   | 8.65372 79129  | -0.27145 22999  | 10.17347  | -0.24970        | 11.61984  | -0.23244        |
| 4   | 11.79153 44391 | +0.23245 98314  | 13.32369  | +0.21836        | 14.79595  | +0.20654        |
| 5   | 14.93091 77086 | -0.20654 64331  | 16.47063  | -0.19647        | 17.95982  | -0.18773        |

| $s$ | $j_{3,s}$ | $J'_3(j_{3,s})$ | $j_{4,s}$ | $J'_4(j_{4,s})$ | $j_{5,s}$ | $J'_5(j_{5,s})$ |
|-----|-----------|-----------------|-----------|-----------------|-----------|-----------------|
| 1   | 6.38016   | -0.29827        | 7.58834   | -0.26836        | 8.77148   | -0.24543        |
| 2   | 9.76102   | +0.24942        | 11.06471  | +0.23188        | 12.33860  | +0.21743        |
| 3   | 13.01520  | -0.21828        | 14.37254  | -0.20636        | 15.70017  | -0.19615        |
| 4   | 16.22347  | +0.19644        | 17.61597  | +0.18766        | 18.98013  | +0.17993        |
| 5   | 19.40942  | -0.18005        | 20.82693  | -0.17323        | 22.21780  | -0.16712        |

**Monopole modes (m=0):**

Modes which have no azimuthal variation are labelled “monopole” modes and TM modes of this type have longitudinal electric field on axis and thus can interact strongly with the beam. The radial distribution of  $E_z$  follows  $J_0$ , where the zeros satisfy the boundary condition that  $E_z = 0$  at the conducting wall at radius  $a$ . Similarly  $H_\phi$  and  $E_r$  (if present) follow  $J'_0$  and are zero in the center and have a finite value at the wall.



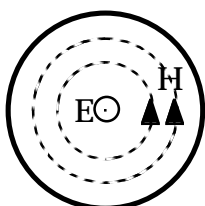
For  $TM_{0ni}$  modes:

$$E_z = E_0 J_0(k_{0n}r) \cos(k_z z) \text{ where } k_{0n} = x_{0n}/a \text{ and } k_z = i\pi/\text{length} \text{ (} i \geq 0 \text{)}$$

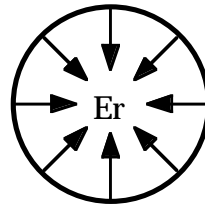
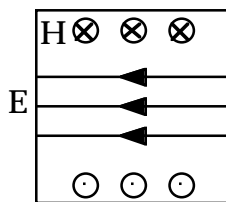
$$H_\phi = H_{\phi 0} J'_0(k_{0n}r) \cos(k_z z) \quad x_{01} = 2.405$$

$$E_r = E_{r0} J'_0(k_{0n}r) \sin(k_z z) \quad x_{02} = 5.520$$

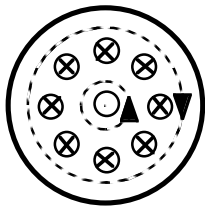
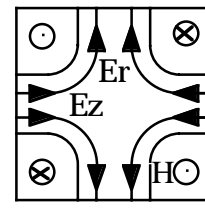
$$x_{03} = 8.654$$



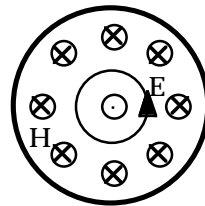
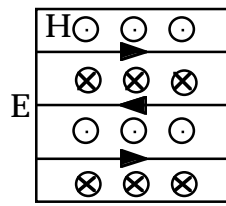
$TM_{010}$



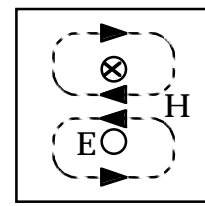
$TM_{011}$



$TM_{020}$



$TE_{011}$



### Dipole modes ( $m=1$ ):

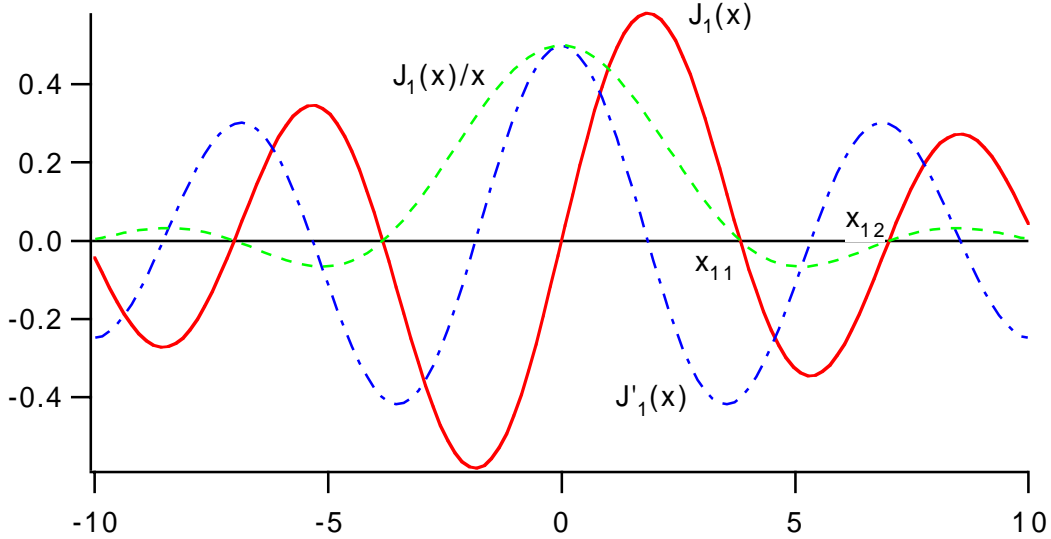
Dipole modes have one full period of variation around the azimuth. For TM modes this means there is no longitudinal field on axis and that the field strength grows linearly with radius close to the center, with opposite sign either side of the axis. This transverse gradient to the longitudinal field gives rise to a transverse voltage kick which is proportional to the beam current and the beam offset. This can be expressed through a **transverse impedance  $Z_{\perp}$** :

$$Z_{\perp}[\Omega m^{-1}] = j \frac{-V_x}{I_b x_0}$$

where  $I_b(0)x_0$  is the dipole moment of the beam. It can be shown that  $Z_{\perp}$  is related to  $Z_{||}$  by

$$Z_{\perp}[\Omega m^{-1}] = \frac{Z_{||}(r)}{kr^2}$$

where  $Z_{||}(r)$  is the longitudinal impedance evaluated at radius  $r$



For  $TM_{1ni}$  modes:

$$E_z = E_0 J_1(k_{1n}r) \cos(\phi) \cos(k_z z) \text{ where } k_{1n} = x_{1n}/a \text{ and } k_z = i\pi/\text{length} \text{ (} i \geq 0 \text{)}$$

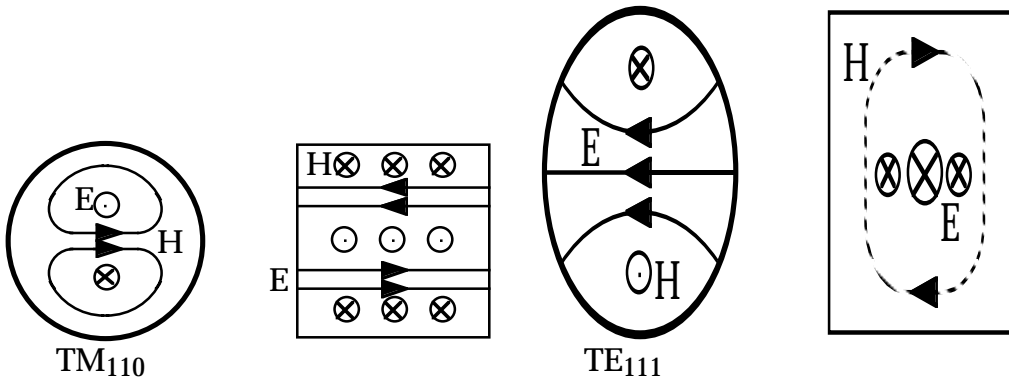
$$H_{\phi} = H_{\phi 0} J_1'(k_{1n}r) \cos(\phi) \cos(k_z z)$$

$$x_{11} = 3.383171$$

$$|H_r| = H_{r0} \frac{J_1'(k_{1n}r)}{r} \sin(\phi) \cos(k_z z)$$

$$x_{12} = 7.01559$$

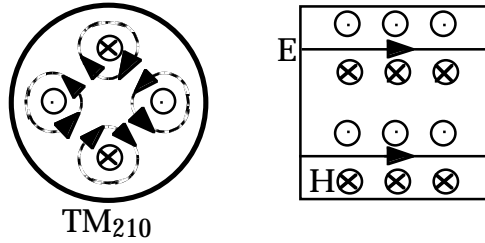
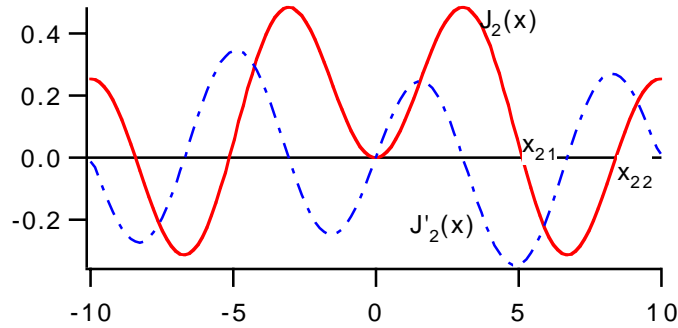
$$x_{13} = 10.17347$$



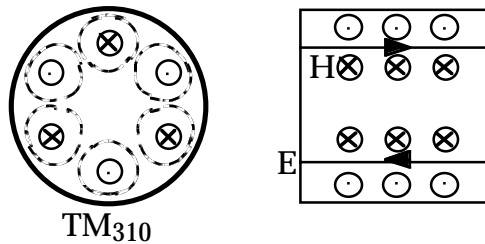
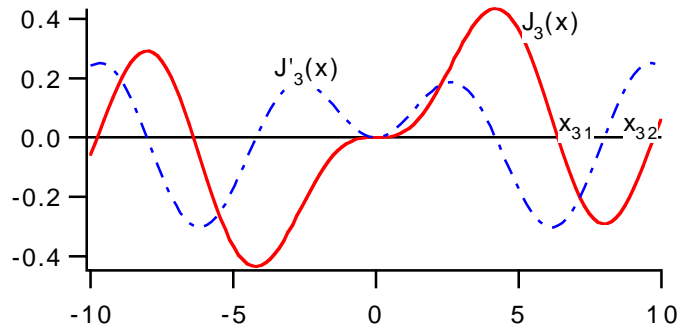
### Higher-order modes ( $m > 1$ ):

For modes with higher azimuthal order ( $m=2$ , quadrupole,  $m=3$ , sextupole etc.), the fields close to the beam axis become progressively weaker as the stored energy is concentrated towards the outer edge of the cavity. Modes with even  $m$  have no sign reversal across the axis so do not drive coupled-bunch instabilities. Modes with odd  $m$  may couple weakly to transverse motion of the beam but are generally not problematic.

For quadrupole modes  $E_z$  goes as  $J_2(k_{2n}r)\cos(2\phi)\cos(k_z z)$  etc.

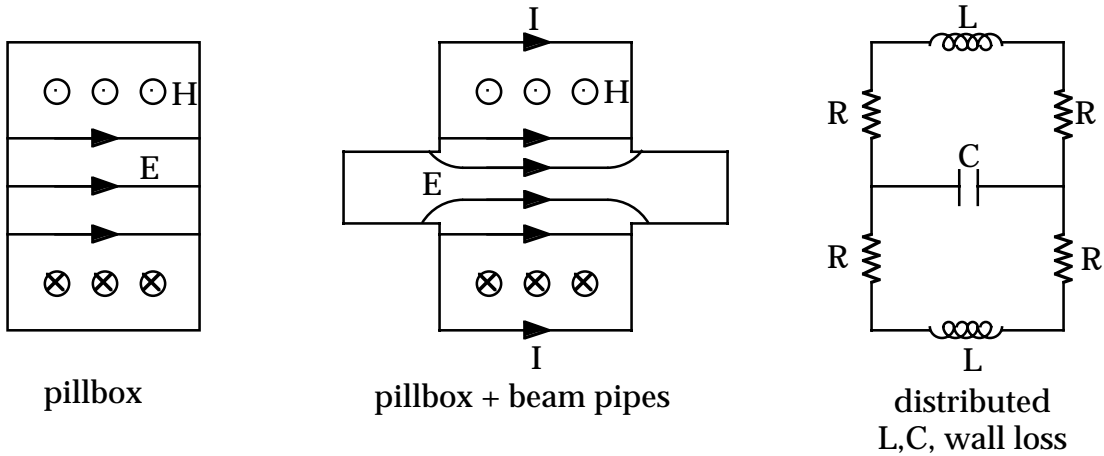


For sextupole modes  $E_z$  goes as  $J_3(k_{3n}r)\cos(3\phi)\cos(k_z z)$  etc.



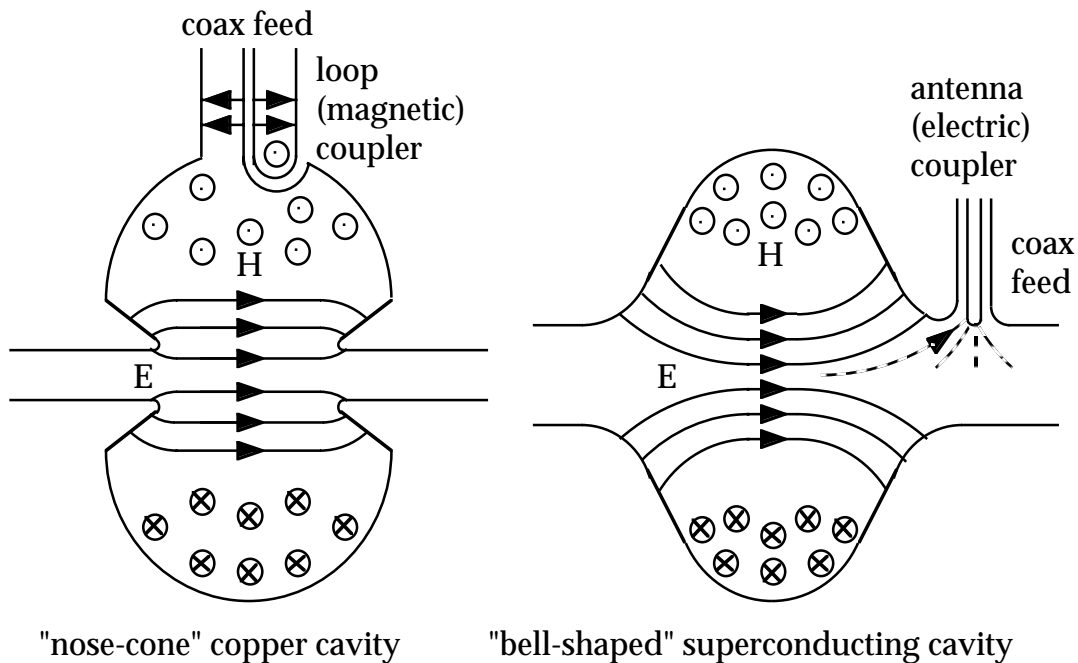
**Real cavities:**

In practice the simple pillbox cavity shape can be improved upon to maximize the shunt impedance for acceleration. The shape must also be modified to allow passage of the beam and addition of one or more couplers



For copper cavities it is desirable to maximize the shunt impedance to make most efficient use of available power. From the equivalent circuit it is known that  $R/Q = \sqrt{L/C}$  so it is generally good to maximize  $L$  and minimize  $C$ , while keeping the optimum interaction length (max.  $T$ ), and maximum  $Q$ . The "nose-cone" or re-entrant cavity does this by increasing the volume occupied by the magnetic field and the surface area carrying the current and decreasing the surface area in the capacitive region (nose tips). The limiting factors to achievable gradient are wall-power dissipation and E-field strength at the nose-tips.

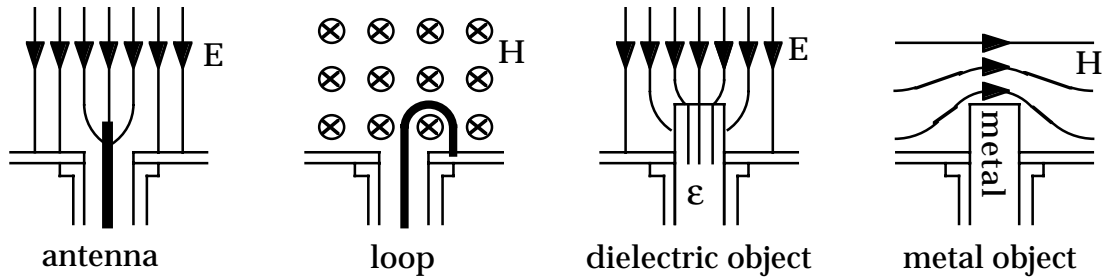
For superconducting cavities the smooth shape is determined by the need to avoid field emission from the surface.  $R/Q$  is low but  $Q$  is very high.





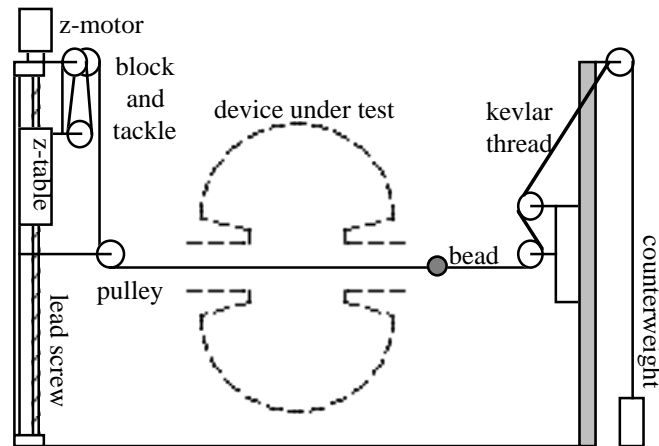
## Field measurement

Information about the field distribution and mode orientation can be obtained by observing the coupling to E and H field components at various places in the cavity. This can be done using E-field antennas or H-field loops or by introducing perturbing objects of dielectric, ferrite or metal.



Introduction of a dielectric object in a region of electric field produces a negative shift in the resonant frequency while introducing a metal object into a region of magnetic field causes a positive frequency shift. If both fields are present when a metal object is inserted the resulting frequency shift will depend on the relative strengths of the E and H fields.

Small objects pulled through the cavity on a string can be used to map the field distributions of the modes and determine the beam impedances.

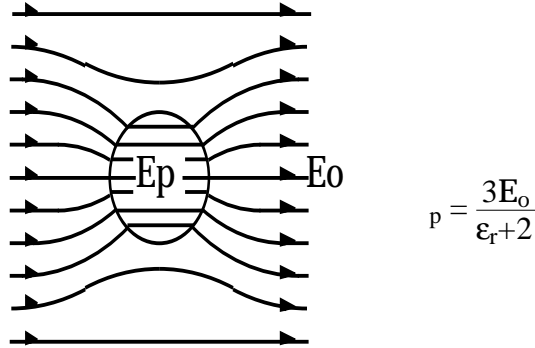


schematic of a motorized bead-puller apparatus

## Perturbation measurement:

It has been shown (by Slater and others), that the change in resonant frequency upon introducing an object into the cavity field is proportional to the relative change in stored energy:

$$\frac{\Delta\omega}{\omega} = \frac{\Delta U_M - \Delta U_E}{U} = \frac{\int_{\Delta V} (\mu H^2 - \epsilon E^2) dV}{\int_V (\mu H^2 + \epsilon E^2) dV}$$



perturbation of a uniform E-field by a dielectric bead

For the case of a small non-conducting sphere, radius  $r$ , where the unperturbed field may be considered uniform over a region larger than the bead, it can be shown that:

$$\frac{\Delta\omega}{\omega} = \frac{\Delta U}{U} = - \frac{\pi r^3}{U} \left[ \epsilon_0 \frac{\epsilon_r - 1}{\epsilon_r + 2} E_0^2 + \mu_0 \frac{\mu_r - 1}{\mu_r + 2} H_0^2 \right]$$

and since  $U = PQ/\omega$

$$\frac{\Delta\omega}{\omega} = \frac{\Delta U}{U} = - \frac{\omega \pi r^3}{PQ} \left[ \epsilon_0 \frac{\epsilon_r - 1}{\epsilon_r + 2} E_0^2 + \mu_0 \frac{\mu_r - 1}{\mu_r + 2} H_0^2 \right]$$

so to calculate the absolute fields the  $Q$  and the input power must be known, however to get  $R/Q$  from the longitudinal field distribution these are not required.

### Cases of special interest:

For a dielectric bead ( $\mu_r = 1$ ) the expression reduces to:

$$\frac{\Delta\omega}{\omega} = - \frac{\pi r^3}{U} \left[ \epsilon_0 \frac{\epsilon_r - 1}{\epsilon_r + 2} E_0^2 \right]$$

For a metal bead ( $\epsilon_r \rightarrow \infty, \mu_r \rightarrow 0$ ):

$$\frac{\Delta\omega}{\omega} = - \frac{\pi r^3}{U} \left[ \epsilon_0 E_0^2 - \frac{\mu_0}{2} H_0^2 \right]$$

A metallic bead can be used to measure the electric field if the magnetic field is known to be zero (e.g.: on axis of a monopole mode), and gives a larger frequency shift than common dielectric materials such as Teflon ( $\epsilon_r = 2.08$ ) or Alumina ( $\epsilon_r = 9.3$ ). Shaped beads such as needles or disks can be used to enhance the perturbation and give directional selectivity. The enhancement or “form factor” can be calculated for ellipsoids or calibrated in a known field.

### Calculation of R, R/Q:

By mapping the longitudinal distribution of  $E_z$  and integrating, the cavity shunt impedance can be determined

$$RT^2 = \frac{(VT)^2}{2P} = \frac{\left[ \int E_z(z) e^{j\omega \frac{z}{v}} dz \right]^2}{2P}$$

where  $v$  is the velocity of the particles (usually  $\approx c$ ), while

$$E^2 = - \frac{\Delta\omega PQ(\epsilon_r+2)}{\omega^2 \pi r^3 \epsilon_0 (\epsilon_r-1)}$$

so

$$T^2 = - \frac{Q(\epsilon_r+2)}{\omega \pi r^3 \epsilon_0 (\epsilon_r-1)} \cdot \frac{\left[ \int \sqrt{\frac{\Delta\omega}{\omega}}(z) (\cos \frac{\omega z}{c} + j \sin \frac{\omega z}{c}) dz \right]^2}{2}$$

If the cavity is symmetric in  $z$  and  $t=0$  at  $z=0$  in the center,

$$\frac{RT^2}{Q} = - \frac{(\epsilon_r+2)}{4\pi^2 f r^3 \epsilon_0 (\epsilon_r-1)} \cdot \left[ \int \sqrt{\frac{\Delta f}{f}}(z) (\cos \frac{2\pi f z}{c}) dz \right]^2$$

Values of  $\Delta f/f$  can be measured at discrete intervals and the function

$$\sqrt{\frac{\Delta f}{f}}(z) (\cos \frac{2\pi f z}{c}) dz$$

can be tabulated, integrated numerically and multiplied by the constants to obtain  $RT^2/Q$ . If  $Q$  is measured at the same time then the beam impedance  $Z_{||} = RT^2$  can be calculated. This process is often automated, using a computer to move a motorized bead positioning apparatus, take frequency data from a network analyzer and calculate the integrals. For modes with weak fields where the frequency perturbation may be hard to measure it may be advantageous to measure the phase shift with the source fixed at the unperturbed resonant frequency. This is a more sensitive measurement and the phase data can be used directly to calculate  $RT^2$ , eliminating the need to measure the  $Q$ .

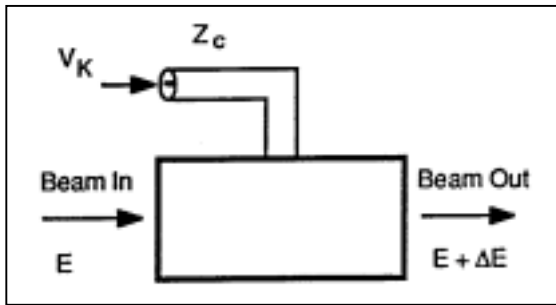
# Pickups and kickers

A charged particle beam generates electromagnetic fields which in turn interact with the beam's surroundings. With suitably designed sensing electrodes, these fields can provide information on various properties of the beam. Such electrodes are generally known as *pickups*.

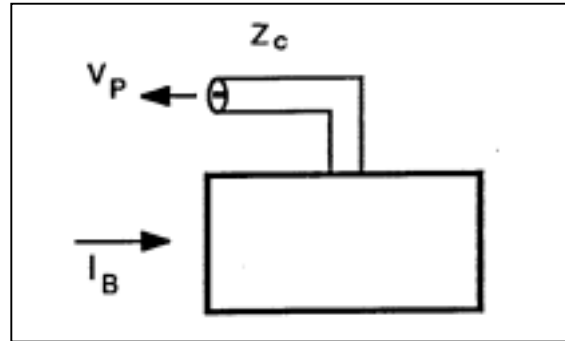
Similarly, charged particle beams respond to the presence of externally imposed electromagnetic fields. Devices used to generate such fields are generally known as *kickers*.

We may represent the pickup or kicker schematically:

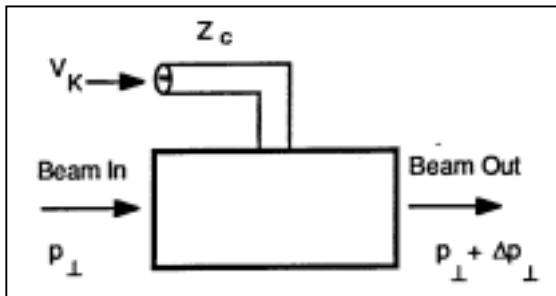
Longitudinal kicker



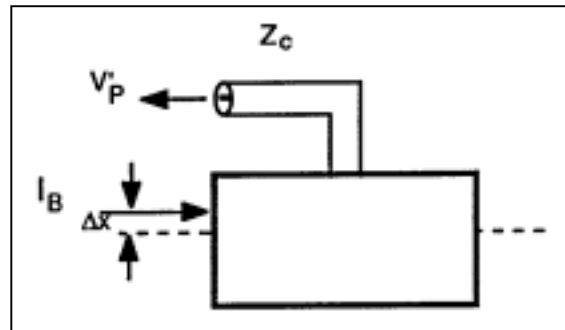
Longitudinal pickup



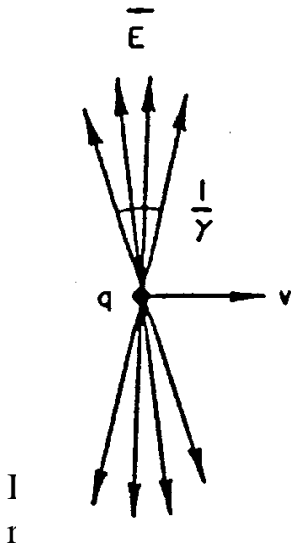
Transverse kicker



Transverse pickup



The wall current, or image current, generated by the beam is found from Ampere's law applied to the TEM-like fields of the beam:



$$\oint \mathbf{H} \cdot d\mathbf{l} = \int_s \mathbf{J} \cdot d\mathbf{S} + \frac{\partial}{\partial t} \int_s \mathbf{D} \cdot d\mathbf{S}$$

or in differential form

$$\nabla \times \mathbf{H} = \mathbf{J} + \frac{\partial \mathbf{D}}{\partial t}$$

TEM-like fields generated by the beam are TEM-like.

$$E_r = \frac{q}{2\pi\epsilon r} \delta(z-ct)$$

$$B_\phi = \frac{q}{2\pi\epsilon cr} \delta(z-ct)$$

The second term on the right of the Maxwell equations is zero since the electric field must be normal to the inside surface of the conductor and hence perpendicular to the vector of the plane we take the surface integral over,  $d\mathbf{S}$ . Thus,

$$\nabla \times \mathbf{H} = \mathbf{J}_{\text{beam}}$$

$$\mathbf{E} = -c(\mathbf{z} \times \mathbf{B})$$

The image current must cancel the surface tangential magnetic field, the image current density is:

For parallel plates  $\mathbf{J}_{\text{image}} = \mathbf{n} \times \mathbf{H}_{\text{surface}}$  separated in the y-direction by  $b$ , and with a centered beam, we find the image current density

$$\frac{dI}{dx} = \frac{I_0}{2b} \frac{1}{\cosh \frac{\pi x}{b}}$$

Thus the image currents in a vacuum chamber with height much less than width is concentrated near the beam axis, above and below the beam.

## ***Pickup response functions***

A prime (') symbol is used to indicate excitation in the transverse mode.

### Transfer impedance:

Relates the pickup output voltage to the beam current. For the longitudinal case,  $Z_p$  is given by

$$Z_p = \frac{V_p}{I}$$

For transverse pickups, the transfer impedance relates the output voltage to the beam dipole moment. For a beam displacement of  $\Delta x$ , the relation is

$$Z'_p = \frac{V'_p}{I \Delta x}$$

## ***Kicker response functions***

### Kicker constant:

Relates the change in beam voltage to the kicker input voltage  $V_k$ :

$$K_{\text{long.}} = \frac{\Delta E}{V} = \frac{e}{V}$$

For transverse kickers, we need the transverse equivalent of the beam voltage. In the longitudinal case, we have the change in beam energy  $\Delta E$

$$\Delta E_{\text{long.}} = \beta c \Delta p_{\text{long.}} = e V_{\text{long.}}$$

and by analogy for the transverse case

$$\Delta E_{\text{trans.}} = \beta c \Delta p_{\text{trans.}} = e V_{\text{trans.}}$$

So the transverse kicker constant is:

$$K_{\text{trans.}} = \frac{\Delta p_{\text{trans.}} \beta c}{e V} = \frac{V_{\text{trans.}}}{V}$$

Using the Panofsky-Wenzel theorem for the mode in which the device is excited as a transverse kicker we find:

$$K_{\text{trans.}} = - \frac{1}{jk_b} \nabla_t K'_{\text{long.}}$$

### Shunt impedance

The shunt impedance is a very useful figure of merit, since it relates the beam voltage to the input power:

$$R_{\text{long.}} T^2 = \frac{V^2}{P_{\text{in}}}$$

The transverse shunt impedance:

$$R_{\text{trans.}} T^2 = \frac{|\Delta p_{\text{trans.}} \beta c|^2}{P_{\text{in}}}$$

Here we have explicitly incorporated the transit time factor T.

## Constant velocity approximations

$$\mathbf{F} = \frac{d\mathbf{p}}{dt}$$

using  $\Delta\mathbf{p} = \int_{t_a}^{t_b} \mathbf{F} dt$   $dt = dz/\beta c$ , then

$$\Delta\mathbf{p} \beta c = \int_a^b \mathbf{F} dz$$

$$\Delta p_{\text{long}} \beta c = \int_a^b F_{\text{long}} dz$$

$$\Delta E = \int_a^b \mathbf{F} \cdot d\mathbf{z} = \int_a^b F_{\text{long}} dz$$

then

$$\Delta E = \Delta p_{\text{long}} \beta c$$

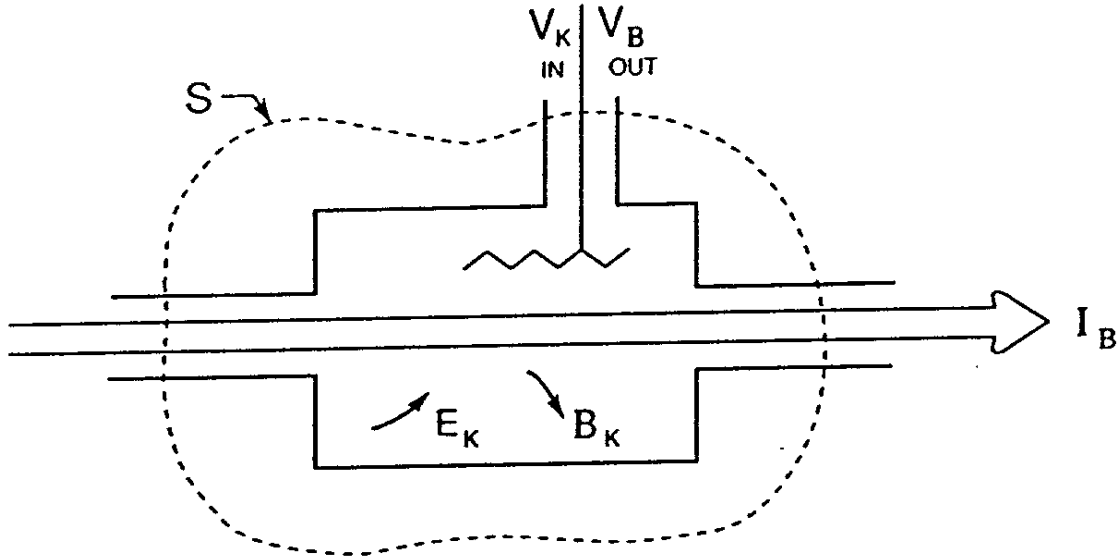
## *Reciprocity*

### Lorentz reciprocity theorem

The Lorentz reciprocity theorem relates the performance of an electrode structure as a pickup to its performance as a kicker.

The theorem applies to a volume  $V$  bounded by a surface  $S$ , which encloses the electrodes, feedthroughs, and field volume. We consider two distinct modes of excitation of the device, as a kicker (subscript  $k$ ) and as a pickup (subscript  $b$ ). We assume no energy sources within the volume, a signal cable of characteristic impedance  $Z_c$ , and wall fields and currents related by  $\mathbf{J} = \sigma \mathbf{E}$ .





Using phasor description of the complex fields and currents we have:

$$\oint_S (\mathbf{E}_k \times \mathbf{H}_b - \mathbf{E}_b \times \mathbf{H}_k) \cdot d\mathbf{S} = \int_V (\mathbf{E}_b \cdot \mathbf{J}_k - \mathbf{E}_k \cdot \mathbf{J}_b) dV$$

$$\oint_S (\mathbf{E}_k \times \mathbf{H}_b - \mathbf{E}_b \times \mathbf{H}_k) \cdot d\mathbf{S} = \int_V (\mathbf{E}_b \cdot \mathbf{J}_k - \mathbf{E}_k \cdot \mathbf{J}_b) dV$$

Beam-excited mode:

$\mathbf{J}_b$  comprises the beam current  $I_b$  plus any currents in the volume which are induced by the beam current

$V_b$  is the voltage at the cable output induced by the beam current

Kicker mode:

$\mathbf{J}_k$  comprises only those currents induced by the kicker voltage  $V_k$

- § Fields and currents induced by any beam present in the kicker are negligible compared the those produced by  $V_k$
- § Any beam current present would be negligibly influenced by fields induced by  $V_k$

The LHS of the equation reduces to

$$\oint_S (\mathbf{E}_k \times \mathbf{H}_b - \mathbf{E}_b \times \mathbf{H}_k) \cdot d\mathbf{S} = 2 \frac{V_k V_b}{Z_c}$$

and the RHS:

$$\int_V (\mathbf{E}_b \cdot \mathbf{J}_k - \mathbf{E}_k \cdot \mathbf{J}_b) dV = - \int_V (\mathbf{E}_k \cdot \mathbf{J}_b) dV$$

then

$$V_b = - \frac{Z_c}{2V_k} \int_V (\mathbf{E}_k \cdot \mathbf{J}_b) dV$$

### The beam voltage

The energy change is often expressed as the beam voltage:

$$V_b = \frac{\Delta U}{q} = \int_{a, t_a}^{b, t_b} \mathbf{E}(z, t) \cdot d\mathbf{z}$$

In phasor notation,  $E_z(z, t) = E_z(z) e^{j\omega z}$ , and with  $t = z/v$  we have:

$$V_b = \int_a^b E_z e^{jk_b z} dz$$

The exponential factor in the integrand results from expressing  $t$  in the time-dependent phasor as a function of position along the path. Both  $E$  and  $V$  will generally depend on the transverse coordinates.  $E$  will also generally depend on the longitudinal coordinate but  $V$  cannot.

## *Panofsky-Wenzel theorem*

If we differentiate the momentum kick experienced by a charge  $q$  with respect to time, we obtain

$$\frac{\partial \Delta \mathbf{p}}{\partial t} = q \int_{t_a}^{t_b} \left( \frac{\partial \mathbf{E}}{\partial t} dt + \frac{\partial(\mathbf{v} \times \mathbf{B})}{\partial t} dt \right)$$

$$\frac{\partial \Delta \mathbf{p}}{\partial t} = q \int_{t_a}^{t_b} \left( \frac{\partial \mathbf{E}}{\partial t} dt + \mathbf{v} \times \frac{\partial \mathbf{B}}{\partial t} dt + \mathbf{B} \times \frac{\partial \mathbf{v}}{\partial t} dt \right)$$

For relativistic particles, of constant velocity

$$d\mathbf{z} = \mathbf{v} dt$$

we have

$$\frac{\partial \Delta \mathbf{p}}{\partial t} = q \int_{t_a}^{t_b} \frac{\partial \mathbf{E}}{\partial t} dt + \int_a^b d\mathbf{z} \times \frac{\partial \mathbf{B}}{\partial t} dt$$

Using Maxwell's equation

$$\frac{\partial \mathbf{B}}{\partial t} = -\nabla \times \mathbf{E}$$

and the identity

$$d\mathbf{z} \times \nabla \times \mathbf{E} = \nabla(d\mathbf{z} \cdot \mathbf{E}) - (d\mathbf{z} \cdot \nabla)\mathbf{E} = \nabla(d\mathbf{z} \cdot \mathbf{E}) - \frac{\partial \mathbf{E}}{\partial z} dz$$

then we find

$$\frac{\partial \Delta \mathbf{p}}{\partial t} = q \int_{t_a}^{t_b} \frac{\partial \mathbf{E}}{\partial t} dt - \int_a^b \left( \nabla(d\mathbf{z} \cdot \mathbf{E}) - \frac{\partial \mathbf{E}}{\partial z} dz \right)$$

$$\frac{\partial \Delta \mathbf{p}}{\partial t} = q \int_a^b \left( \nabla(d\mathbf{z} \cdot \mathbf{E}) + 2d\mathbf{E} \right)$$

The transverse components are

$$\frac{\partial}{\partial t} (\Delta \mathbf{p}_\perp) = q \int_a^b \left[ -\nabla_\perp(d\mathbf{z} \cdot \mathbf{E}) + 2d\mathbf{E}_\perp \right]$$

and noting that

$$\Delta E = q \int_a^b \mathbf{dz} \cdot \mathbf{E}$$

we find

$$\frac{\partial}{\partial t} (\Delta \mathbf{p}_\perp) = -\nabla_\perp (\Delta E) + 2q[\mathbf{E}_\perp(b) - \mathbf{E}_\perp(a)]$$

The bracketed term we choose to extend over the region that the entry and exit fields  $\mathbf{E}_\perp(a)$ ,  $\mathbf{E}_\perp(b)$ , are zero. Then for fields with sinusoidal time variation we have the *Panofsky-Wenzel* theorem:

$$\frac{\omega \Delta \mathbf{p}_\perp}{q} = -\frac{1}{q} \nabla_\perp (\Delta E) = -\nabla_\perp V$$

This theorem tells us that the transverse kick can be described purely in terms of the longitudinal electric field. There must be a longitudinal electric field component in order to produce a transverse momentum change in a particle traveling through a structure. The frequency dependence shows that the higher the frequency at which the deflecting fields are encountered, the less of a kick they impart.

### ***Relations between pickup and kicker characteristics***

#### Longitudinal:

Using our result from the Lorentz reciprocity theorem

$$V_b = -\frac{Z_c}{2V_k} \int_v (\mathbf{E}_k \cdot \mathbf{J}_b) dV$$

in the longitudinal transfer impedance gives:

$$Z_b = -\frac{Z_c}{2V_k I_b} \int_v (\mathbf{E}_k \cdot \mathbf{J}_b) dV$$

For a beam moving in the positive z-direction with velocity  $\beta c$ , the z-dependence is  $e^{-jkz}$ , and we write

$$\int_{\text{beam area}} (\mathbf{E}_k \cdot \mathbf{J}_b) dx dy = \mathbf{E}_k \cdot \mathbf{I}_b e^{-jkz}$$

and

$$Z_p = -\frac{Z_c}{2} \int_{\text{beam path}} \frac{e^{-jkz}}{V_k} \mathbf{E}_k \cdot d\mathbf{z}$$

We can see that the integral differs from the definition of the longitudinal kicker constant only by the sense of direction in beam motion. This leads to an important result for electrode systems that exhibit directional behavior (such as striplines):

*The direction in which the beam passes when the device operates as a pickup must be opposite that which it does when the device acts as a kicker.*

and

$$Z_p = \frac{Z_c}{2} K_{\text{long.}}$$

| <u>Longitudinal</u>   | <u>Transverse</u>   |
|---|---|
| <u>Kickers</u>  |   |
| $V = K_{\parallel} V_K$   | $\Delta p_{\perp} \beta c / e = K_{\perp} V_K$                  |
| $K_{\perp} = -\frac{1}{jk} \nabla_{\perp} K'_{\parallel}$   |   |
| $P_K \equiv  V ^2 / 2R_{\parallel} T^2$   | $P'_K \equiv  \Delta p_{\perp} \beta c / e ^2 / 2R_{\perp} T^2$ |
| $R_{\parallel} T^2 = Z_c  K_{\parallel} ^2$   | $R_{\perp} T^2 = Z_c  K_{\perp} ^2$                             |
| <u>Relations Between Pickups and Kickers</u>  |   |
| $Z_p = \frac{1}{2} Z_c K_{\parallel}$   | $Z'_p = -\frac{1}{2} jk Z_c K_{\perp}$                          |
| $Z_p = \sqrt{Z_c R_{\parallel} T^2} / 2$  | $Z'_p = k_B \sqrt{Z_c R_{\perp} T^2} / 2$                       |
| <u>Pickups</u>  |   |
| $Z_p \equiv V_p / I_B$  | $Z'_p \equiv V'_p / I_B \Delta x$                               |
| $P_p = \langle I_B^2 \rangle R_{\parallel} T^2 / 4$   | $P'_p = \langle I_B^2 x^2 \rangle k_B^2 R_{\perp} T^2 / 4$      |
| <p><sup>a</sup>As noted in Appendix 1, some authors define the transverse beam voltage as simply <math>c\Delta p_{\perp}</math>, omitting the factor of <math>\beta</math>. Using this convention, one would simply need to replace all the <math>k_B</math> appearing in the above formulas by the free-space wave-number <math>k = \omega/c</math>. The effect of this change will be to re-define the transverse kicker constant and shunt impedance, but to leave the calculated physical quantities of input power and transverse momentum kick unchanged.</p> |   |

## Green's reciprocity theorem

Green's reciprocity theorem relates charges and fields in two different modes of excitation. It describes a reciprocity relation for electrostatics problems, but is also applicable to electromagnetic excitation.

Assume a set of  $n$  conductors under two distinct modes of excitation:

Mode 1: Electrodes have charges and are at potentials

$$Q_i^1 \quad V^1$$

Mode 2: Electrodes have charges and are at potentials

$$Q_i^2 \quad V^2$$

$$\sum^n Q_i^1 V_i^2 = \sum^n Q_i^2 V_i^1$$

The application is in calculating the coverage factor  $g$  which represents the fraction of the image current an electrode intercepts.

For an array of  $n$  electrodes, connected to ground so that charges may flow, what is the fraction of charge  $Q_i^b$  on electrode  $i$  due to a charge  $Q^b$  at a point P within the array?

§ With  $Q^b$  at P, ground all but the  $i^{\text{th}}$  electrode. Assume the distribution of the  $Q_i^b$  remains the same (*pickup mode*)

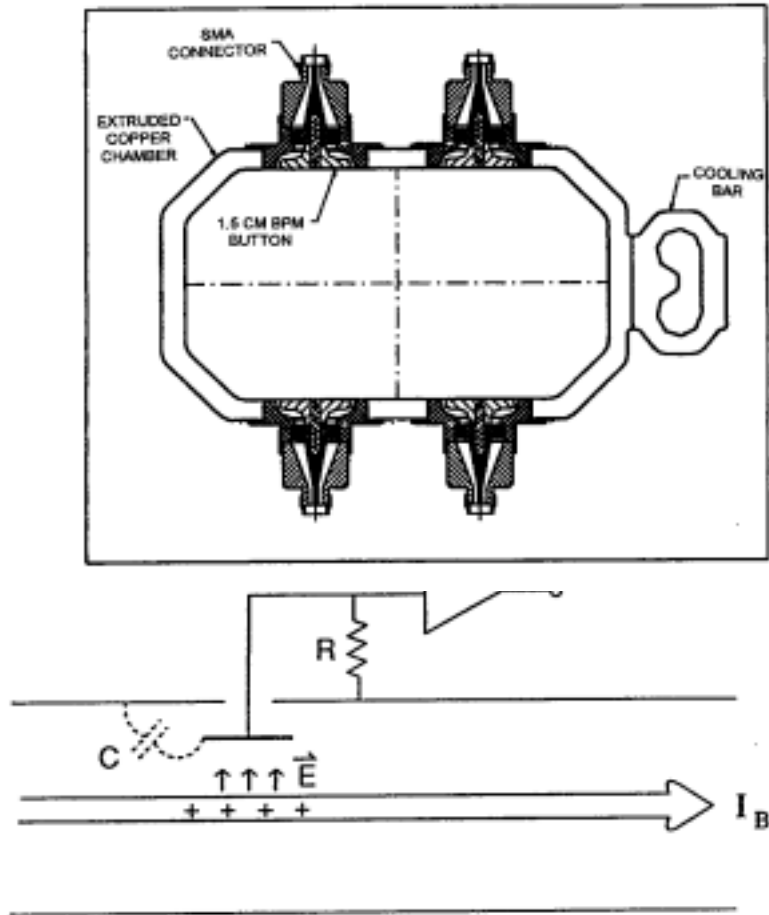
§ Place a voltage  $V^k$  on the  $i^{\text{th}}$  electrode, and ground the remaining electrodes. Then the voltage at P is  $V_i^k$  (*kicker mode*)

$$\frac{-Q_i^b}{Q^b} = \frac{V^k}{V_i^k} = g_i$$

## Types of Pickups

### Capacitive button pickups

Capacitive plates at the beampipe walls allow sampling of the beam-induced image currents. Since the small button essentially behaves as a capacitance, it cannot act as a matched load and has limited utility as a kicker.



The image charge on a plate of effective length  $l$  is

$$q = - \frac{g l I_b}{\beta c}$$
$$I_c = \frac{\partial q}{\partial t} = j \omega q$$

The charging current is

And the current flows through the series combination of  $C$  and  $R$ , resulting in a voltage across  $R$



$$V = -j\omega q \frac{R}{1 + j\omega RC} = jI_b g \frac{\omega l}{\beta c} \frac{R}{1 + j\omega RC}$$

Then we find the transfer impedance:

$$Z_p = \frac{V_p}{I_b} = jglk_b \frac{R}{1 + j\omega RC}$$

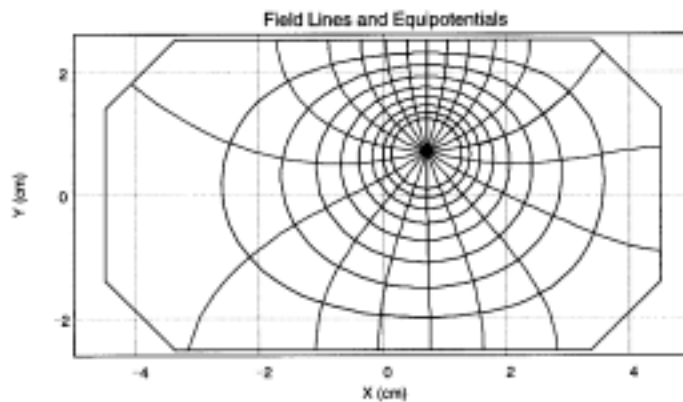
At high frequencies ( $\omega RC \gg 1$ ), this becomes

$$Z_p \rightarrow \frac{gl}{\beta c C}$$

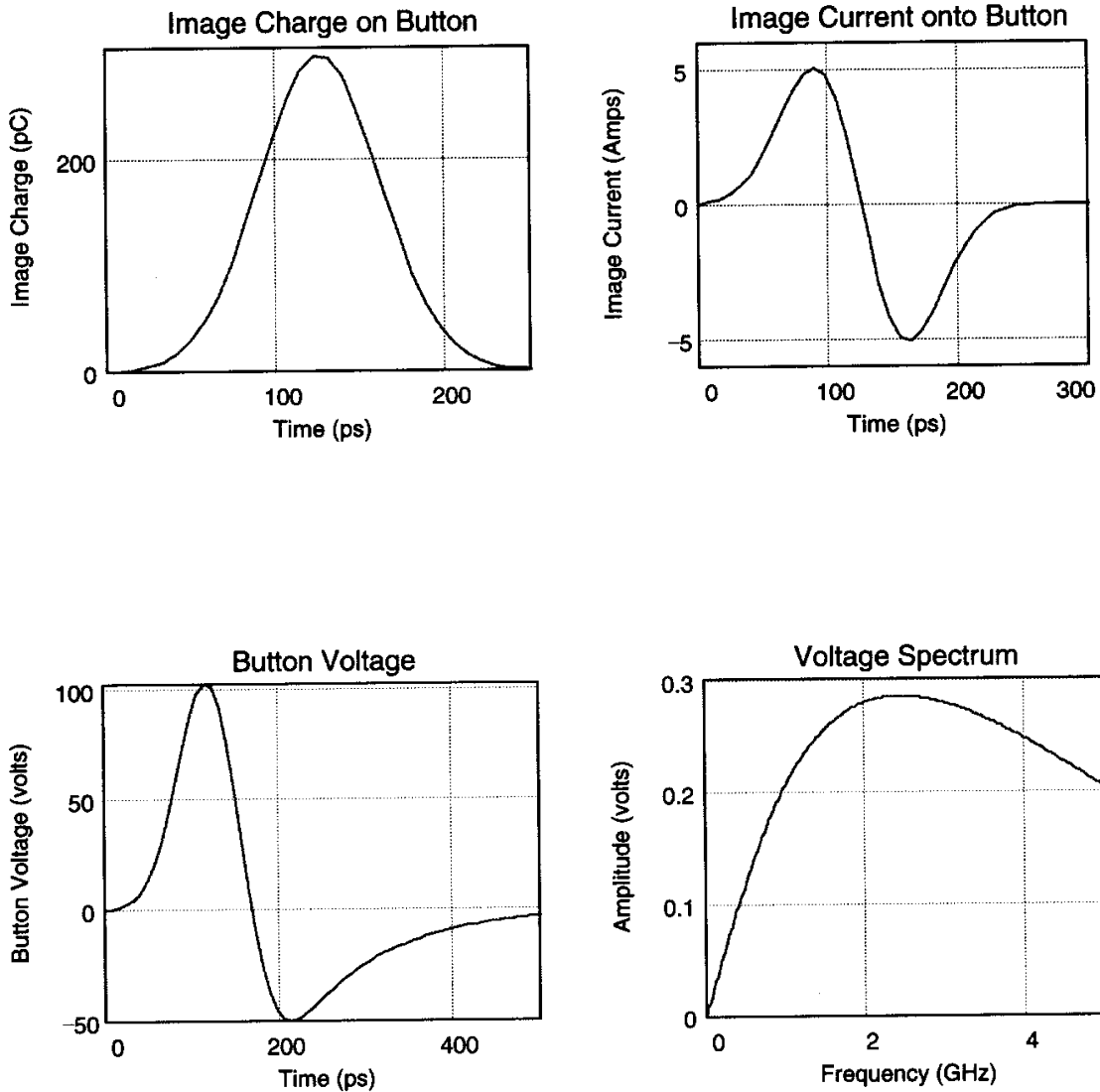
For an electrode of area  $A$  at distance  $a$  from the beam, we can approximate  $gl$  by  $A/2\pi a$ , giving:

$$Z_p \rightarrow \frac{A}{2\pi a \beta c C}$$

Beam position may be derived from the ratio of voltage generated on each of four buttons located in the vacuum chamber.



The following example is for a button of radius 7.5mm, beampipe radius 4.4 cm, bunch charge  $8 \times 10^8$  electrons, Gaussian bunch  $s = 1$  cm, bunch rate 238 MHz,  $50 \Omega$  coaxial output (PEP-II).

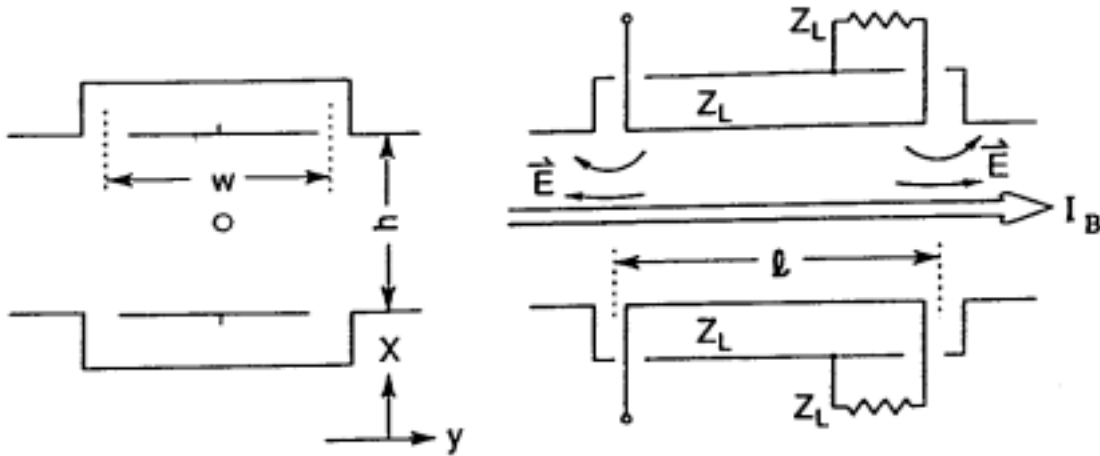


### Stripline electrodes

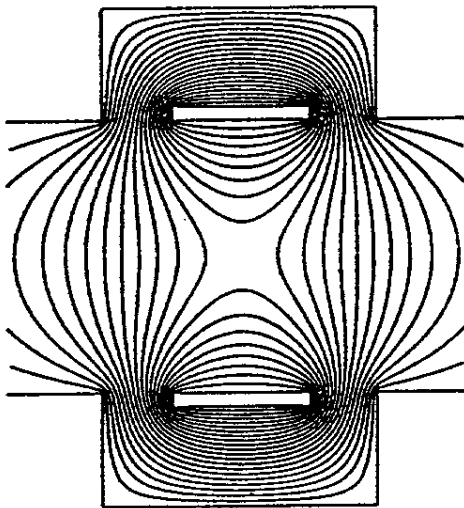
A stripline electrode is a TEM mode transmission line with the ground plane formed by the vacuum chamber wall. We generally match the impedance of

the stripline to the connecting cable characteristic impedance in the mode of operation (which will in general be a different characteristic impedance for transverse operation than longitudinal).

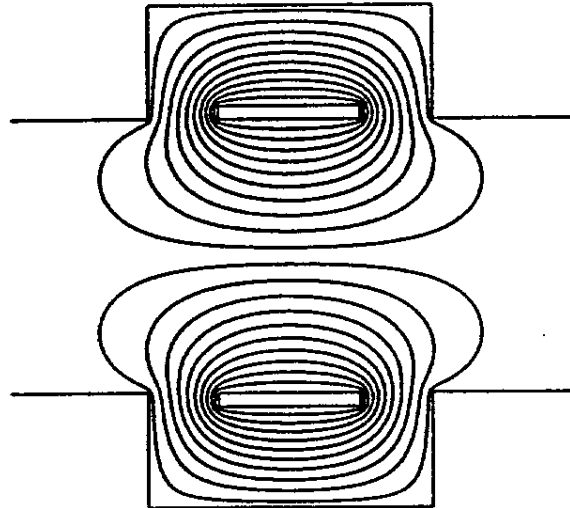
Schematic of striplines in pickup mode



Sum mode



Difference mode



When the beam reaches the upstream end of the electrode, it repels charges into the output line and along the stripline. With the stripline matched into the output line, a signal  $V$  is induced in the output line and the stripline

The signal propagates along light, and arrives at the

$$V = \int g i_b(t) Z_L \text{ the stripline at the speed of downstream end at time } l/c$$

later. Also at time  $l/c$  later, the beam arrives at the downstream gap and induces *negative* pulses in the output line and stripline. The stripline pulse then propagates in the upstream direction. The output in time domain at the upstream end of a stripline is:

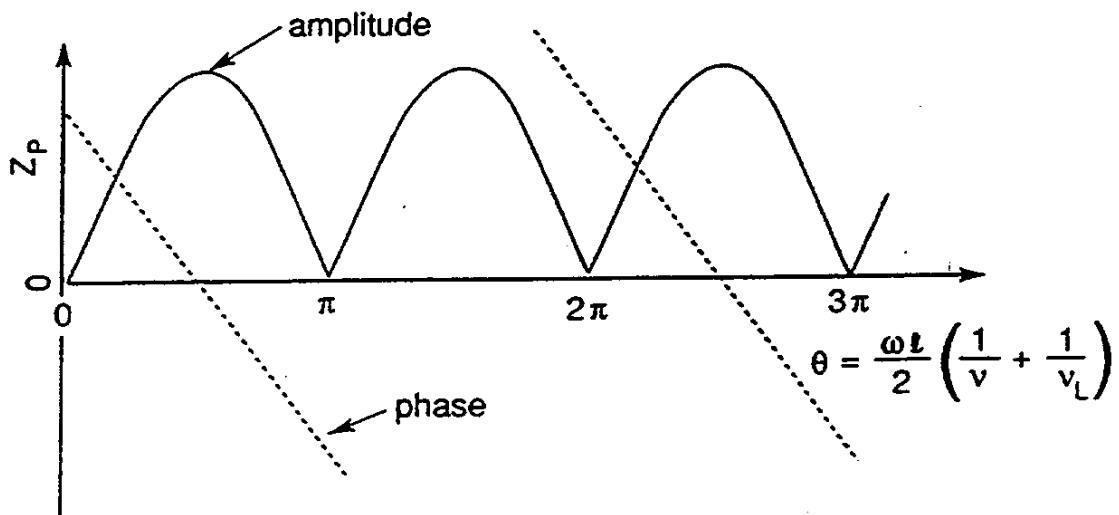
In the frequency domain, the output is

$$V_p = \frac{g}{2} I_b Z_L (1 - e^{-j\omega l}) = g I_b Z_L e^{j(\frac{\pi}{2} - k_0 l)} \text{sinc}_0 l$$

so that the transfer impedance is

$$Z_p = g Z_L e^{j(\frac{\pi}{2} - k_0 l)} \text{sinc}_0 l$$

The single-plate coverage factor  $g$  is transverse-position sensitive. If we sum the output of the two plates, the resulting longitudinal signal is to first order independent of transverse position



In the transverse case

$$Z'_p = Z_1 \underline{g}_{\text{trans.}} e^{j\left(\frac{\pi}{2} - k_0 l\right)} \text{sinc}_0 l$$

## Kicker behavior

In the gaps at the ends of the stripline, at the beampipe radius  $h/2$ , and if the gap is short ( $T=1$ ), then

$$\int_{z-\frac{\Delta z}{2}}^{z+\frac{\Delta z}{2}} E_z e^{jkz} dz = V_k e^{jkz}$$

Integrating along the stripline incorporating the gaps, we find

$$V_b(h/2) = V_k (1 - e^{-j2kl}) = 2 V_k e^{j(\frac{\pi}{2} - kl)} \sin kl$$

We use Green's reciprocity theorem to get the beam voltage at the beam location ( $y=0$ ), using the coverage factor  $g$ :

$$V_b(y=0) = g(0)V(y=h/2)$$

Then

$$V_b(y=0) = 2g V_k e^{j(\frac{\pi}{2} - kl)} \sin kl$$

the kicker constant is

$$K = 2g e^{j(\frac{\pi}{2} - kl)} \sin kl$$

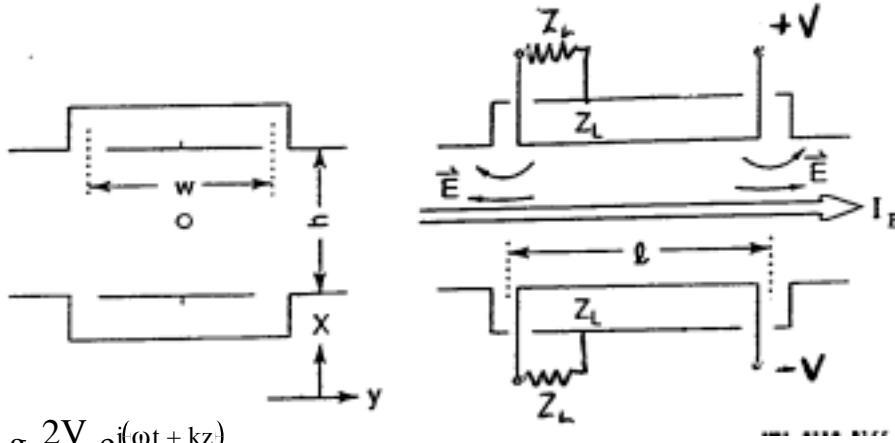
the transfer impedance is, (note that  $Z_c = Z_1$  here)

$$K = Z_1 g e^{j(\frac{\pi}{2} - kl)} \sin kl$$

and the shunt impedance is:

$$R_{\text{long}}.T^2 = 2Z_1 g^2 \sin^2 kl$$

## Transverse kicker behavior



$$E_{\text{trans.}} = g \frac{2V}{h} e^{j(\omega t + kz)}$$

$$E = c B$$

$$\text{Beam } z = \beta c t$$

$$F(t) = e (E_{\text{trans.}} + \beta c B_{\text{trans.}})$$

$$F(t) = e g \frac{2V}{h} (1 + \beta) e^{j(\omega t + k \beta c t)}$$

$$V_{\text{trans.}} = \frac{\Delta p_{\text{trans.}} c}{e} = \int_{-\frac{1}{\beta c}}^0 \frac{c}{e} F(t) dt = c g \frac{2V}{h} (1 + \beta) \int_{-\frac{1}{\beta c}}^0 e^{j(1 + \beta) \omega t} dt$$

$$V_{\text{trans.}} = c g \frac{2V}{h} \frac{1}{j\omega} \left( 1 - e^{-j \frac{1 + \beta}{\beta} k l} \right)$$

$$V_{\text{trans.}} = 2 g \frac{V}{h} e^{-j \frac{1 + \beta}{2\beta} k l} 2 \sin \left( \frac{1 + \beta}{2\beta} k l \right)$$

$$V_{\text{trans.}} = 4 g \frac{V}{h} e^{-j\Theta} \sin\Theta \quad K_{\text{trans.}} = \frac{V_{\text{trans.}}}{V_{\text{input}}} = \frac{\frac{1 + \beta}{2\beta} k l = \Theta}{\sqrt{2 \frac{R}{Z}} V} = \sqrt{2 \frac{Z_L}{R}} 2 g \frac{1}{h k} e^{-j\Theta} \sin\Theta$$

Power P

$$P = \frac{|V_{\text{trans.}}|^2}{2 R} = 2 \frac{V^2}{2 Z}$$

$$R_{\text{trans.}} = \frac{Z_L}{2} \left( \frac{V_{\text{trans.}}}{Z_L} \right)^2 = 2 Z_L \left( \frac{2 g \sin \Theta}{\omega} \right)^2$$

